

Fragmentation of the Giant Pairing Vibration induced
by many-body processes

or...

Where has the Giant Pairing Vibration gone?

F. Barranco

University of Sevilla

E. Vigezzi

INFN Milano

G. Potel

LLNL(formerly)/(Now)Univ. of Sevilla



PID2020-114687GB-100

Pairing Vibrations around Closed Shell Nuclei

1.D.2

Nuclear Physics **80** (1966) 289–313; © North-Holland Publishing Co., Amsterdam

Not to be reproduced by photoprint or microfilm without written permission from the publisher

PAIRING VIBRATIONS

D. R. BÈS†

NORDITA, Copenhagen

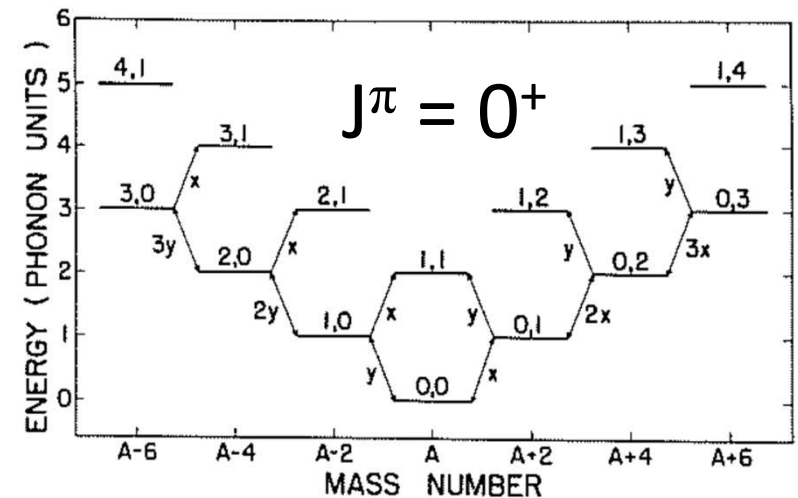
and

R. A. BROGLIA

Facultad de Ciencias Exactas y Naturales, Buenos Aires

Received 30 September 1965

Abstract: We study the properties of the collective states (pairing vibrations) which are associated with fields changing the numbers of particles. In particular, we discuss which processes may be enhanced by the coherence in the pairing-vibration state.



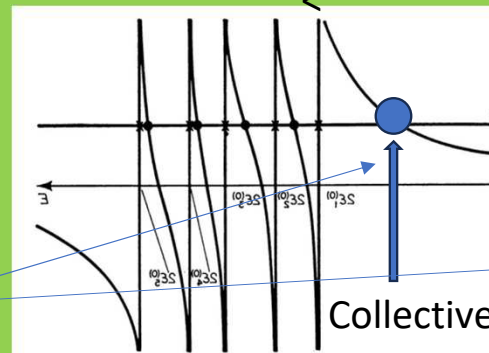
Schematic monopole pairing hamiltonian

$$H = \sum_v \varepsilon_v^{(0)} a_v^\dagger a_v - G \sum_{\mu, \nu > 0} a_\mu^\dagger a_\mu^\dagger a_\nu a_\nu$$

Two neutron separation energy
get augmented (diminished)

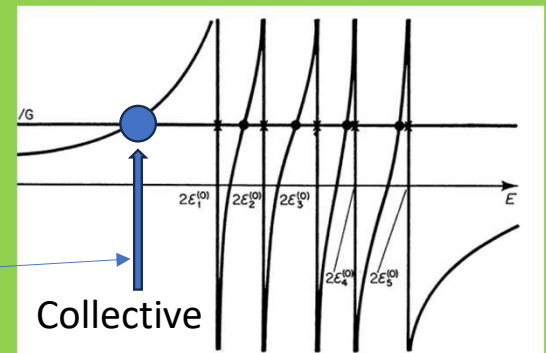
Pair removal mode

$$|\alpha\rangle = A_\alpha^\dagger |0\rangle = \sum_{\nu > 0} X_\nu(\alpha) a_\nu^\dagger a_\nu^\dagger |0\rangle$$



Pair addition mode

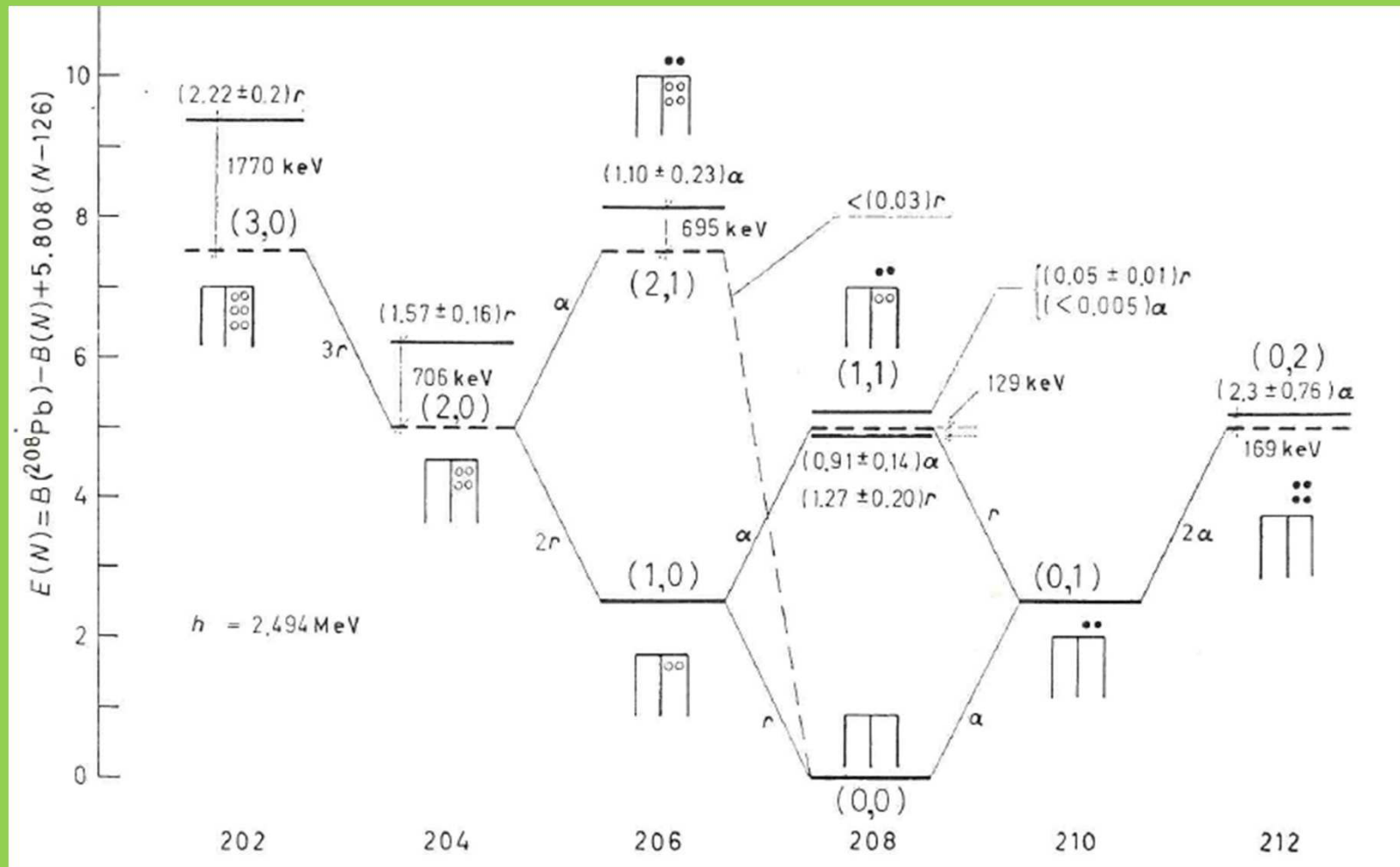
$$|\alpha\rangle = A_\alpha^\dagger |0\rangle = \sum_{\nu > 0} X_\nu(\alpha) a_\nu^\dagger a_\nu^\dagger |0\rangle$$



to II A. (11.11) notations and to notations in I.11 and

are 11.1. Graphical solution of the eigenvalue equation (11.31). All of

The Pairing Vibration seminal paper



For a general pairing force and including pairing GSC's:

The pp-RPA equations

$$|A+2, \tau\rangle = \left(\sum_{m < n} X_{mn}^{\tau} a_m^{\dagger} a_n^{\dagger} - \sum_{i < j} Y_{ij}^{\tau} a_j^{\dagger} a_i^{\dagger} \right) |A, 0\rangle$$

$$\begin{pmatrix} A & B \\ B^{\dagger} & C \end{pmatrix} \begin{pmatrix} R_p^{\tau, \lambda} \\ R_h^{\tau, \lambda} \end{pmatrix} = \begin{pmatrix} 1 & 0 \\ 0 & -1 \end{pmatrix} \begin{pmatrix} R_p^{\tau, \lambda} \\ R_h^{\tau, \lambda} \end{pmatrix} \cdot \hbar \Omega_{\tau, \lambda},$$

Pairing GSC's

NOT CRUCIAL

$$A_{mnm'n'} = \delta_{mm'} \delta_{nn'} (\epsilon_m + \epsilon_n) + \bar{v}_{mnm'n'},$$

$$C_{ijij'} = -\delta_{ii'} \delta_{jj'} (\epsilon_i + \epsilon_j) + \bar{v}_{ijij'},$$

$$B_{mnij} = -\bar{v}_{mnij},$$

$$(R_p^{\tau})_{mn} = X_{mn}^{\tau}, \quad (R_p^{\lambda})_{mn} = Y_{mn}^{\lambda},$$

$$(R_h^{\tau})_{ij} = Y_{ij}^{\tau}, \quad (R_h^{\lambda})_{ij} = X_{ij}^{\lambda}.$$

From The Nuclear Many Body Problem by Ring and Schuck

Giant Pairing Vibrations (GPV)

Volume 69B, number 2

PHYSICS LETTERS

1 August 1977

HIGH-LYING PAIRING RESONANCES*

R.A. BROGLIA

*The Niels Bohr Institute, University of Copenhagen, DK-2100 Copenhagen Ø, Denmark¹
State University of New York, Department of Physics, Stony Brook, New York 11794, USA*

and

D.R. BES²

NORDITA, DK-2100 Copenhagen Ø, Denmark

Received 1 April 1977

Pairing vibrations based on the excitation of pairs of particles and holes across major shells are predicted at an excitation energy of about $70/A^{1/3}$ MeV and carrying a cross section which is 20%–100% the ground state cross section.

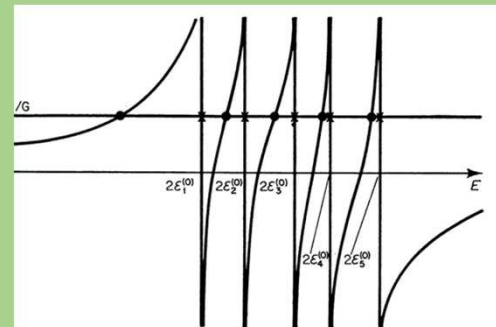
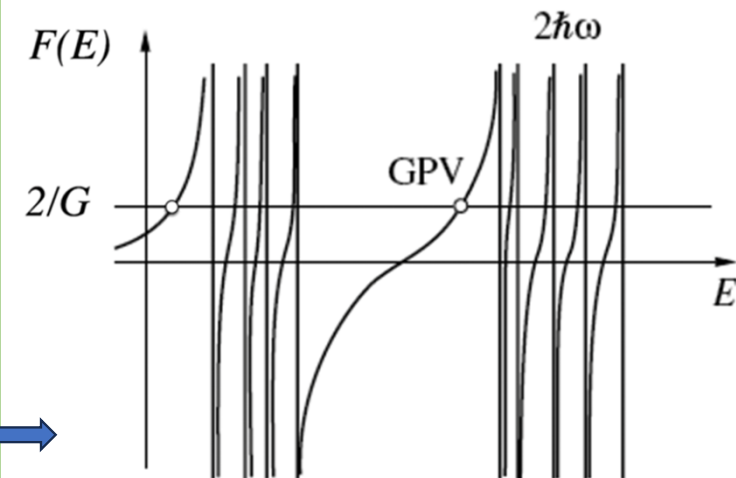


Figure 11.1. Graphical solution of the eigenvalue equation (11.31). All of

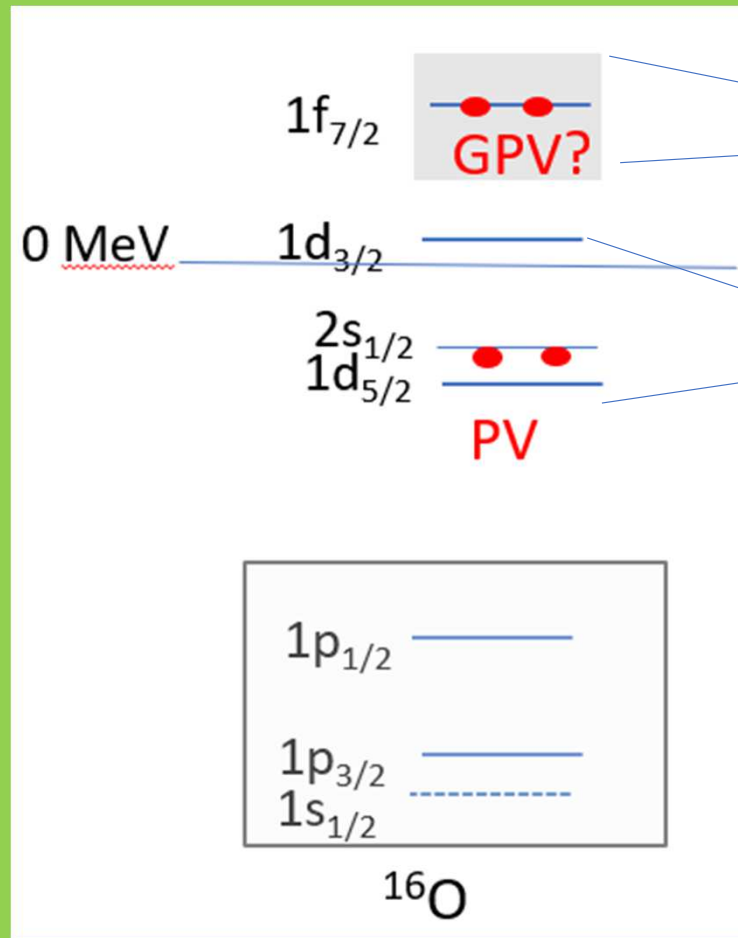
EXTENSION



$$\hbar\omega_{GPV} \sim 2\hbar\omega_0 - \Omega G \sim \frac{65 \text{ MeV}}{A^{1/3}}$$

The Pairing Vibrations; An interesting example: 16-O

$A \rightarrow A+2$; for example $^{16}\text{O} \rightarrow ^{18}\text{O}$



Pairing Interaction \rightarrow Coherent mix
 \rightarrow Collectivity \rightarrow Cooper pair like

Pairing Interaction \rightarrow Coherent mix
 \rightarrow Collectivity \rightarrow Cooper pair like

Pair Addition mode
produced in two neutron
transfer reactions:
 $A(t,p)A+2$ for example

The Pairing Vibrations; a realistic pp-RPA for 16-O

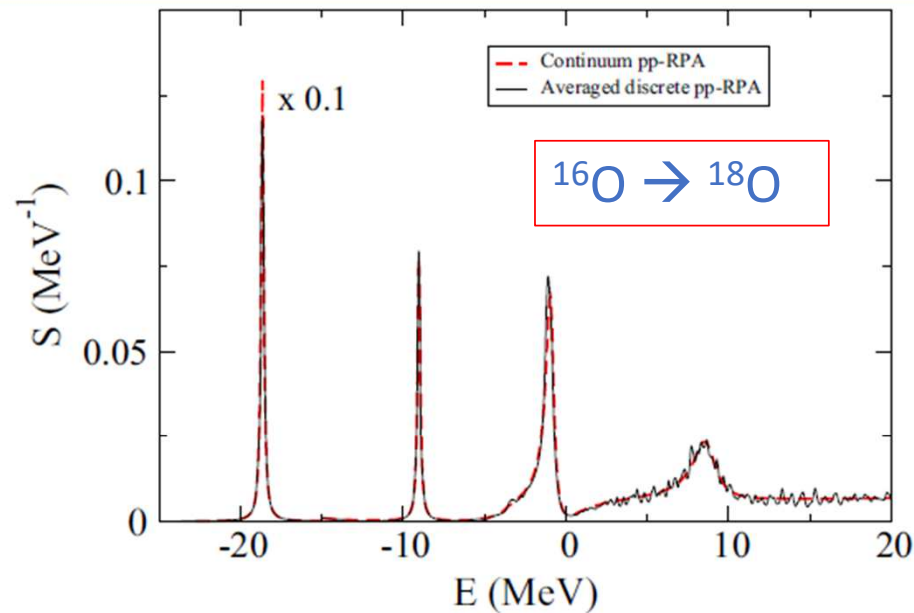
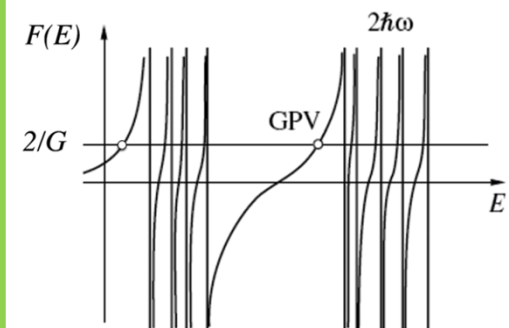
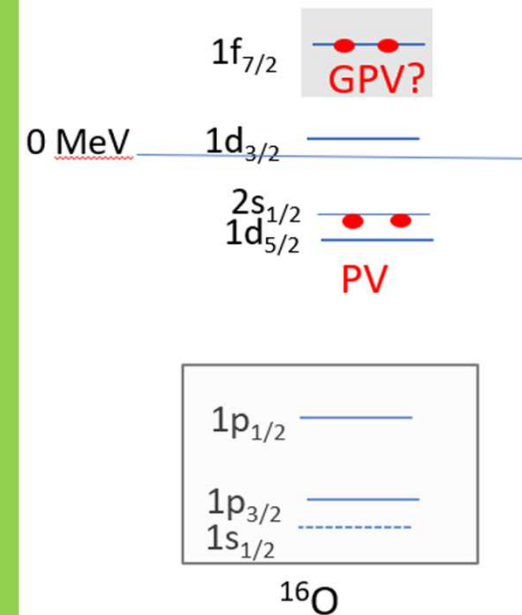


FIG. 1. The strength function calculated for ^{18}O with the continuum pp-RPA (M. Matsuo, private communication) is compared to our results obtained by averaging over several boxes and using a Lorentzian with FWHM = 0.2 MeV. In this

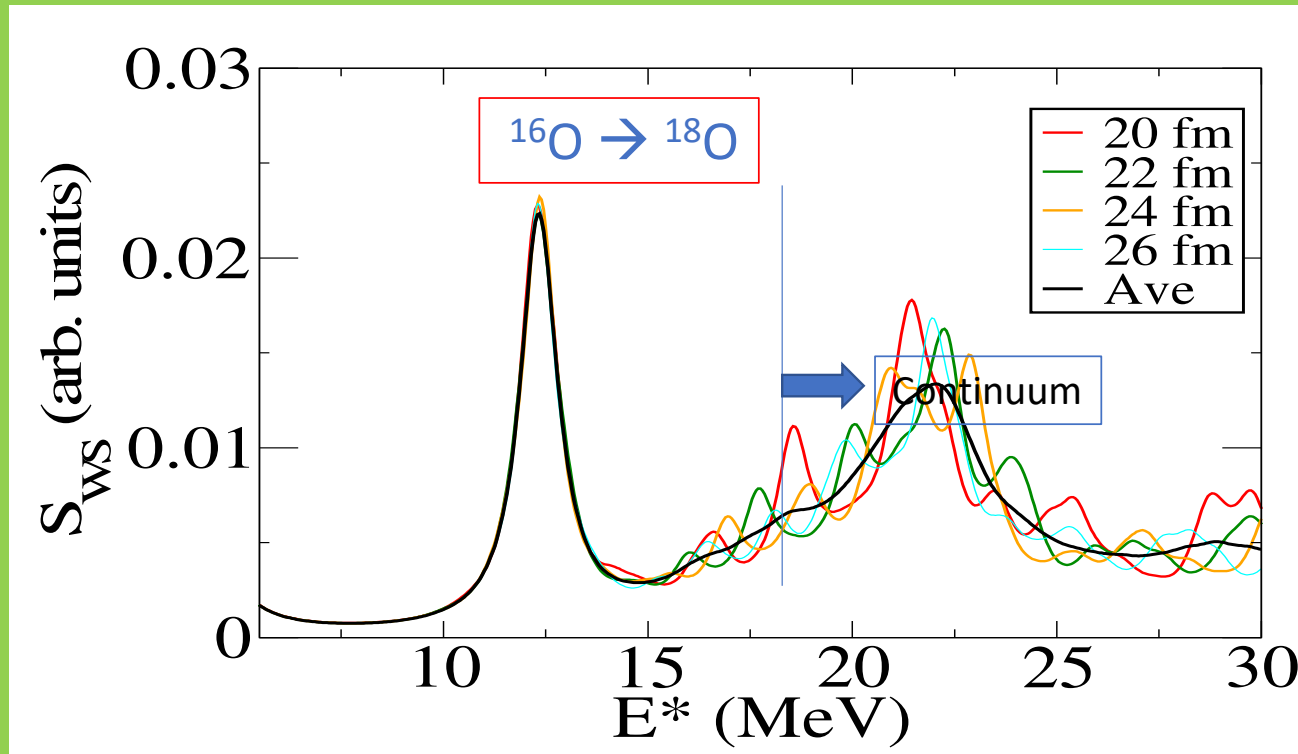
$$S_{WS}^i = \left(\sum_{nn'lj} [X_{nn'lj}^i + Y_{nn'lj}^i] \int dr G(r) \psi_{nlj}(r) \psi_{n'lj}(r) \right)^2$$

$$G(r) \equiv (1 + \exp[(r - R_S)/a_S])^{-1}$$



$$\hbar\omega_{\text{GPV}} \sim 2\hbar\omega_0 - \Omega G \sim \frac{65 \text{ MeV}}{A^{1/3}}$$

Treating continuum: pp-RPA using BOX boundary conditions



pp-RPA with the
Gogny(pairing)
force.

Averaging details:
1.Box sampling
2.Small Gaussian
convolution.

$$S_{WS}^i = \sum_{nn'lj} [X_{nn'lj}^i + Y_{nn'lj}^i] \int dr G(r) \psi_{nlj}(r) \psi_{n'lj}(r).$$

$$G(r) \equiv (1 + \exp[(r - R_S)/a_S])$$

What about experiment ?

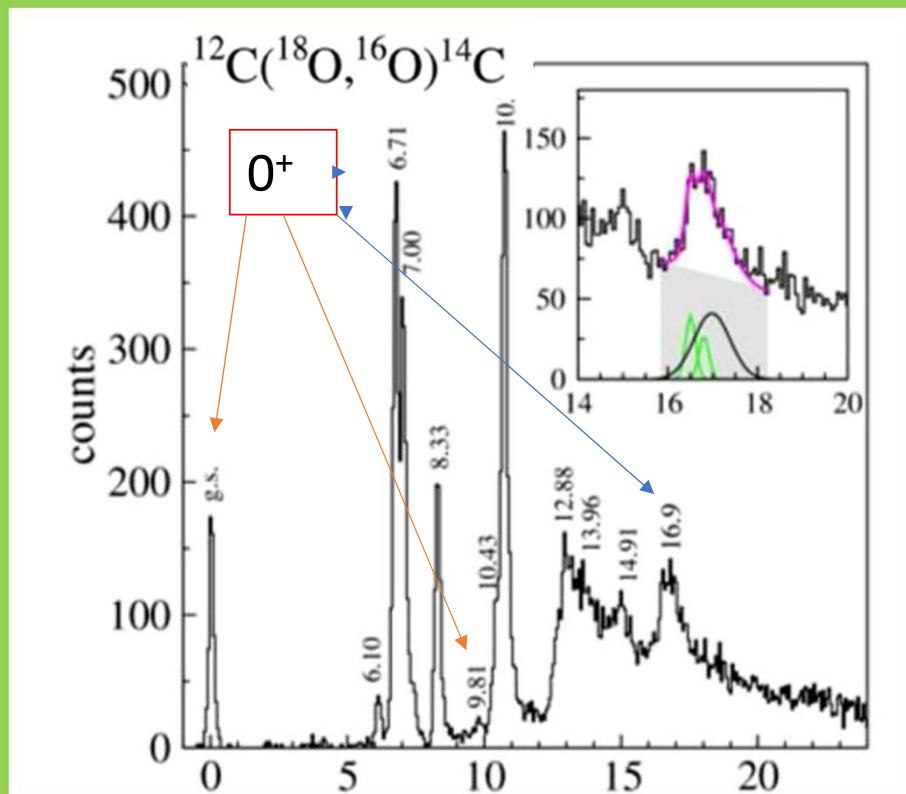
Several unsuccessful experimental searches have been carried out over the years , but...

recently a bump has been detected at $E^* \approx 16$ MeV in the reaction $^{12}\text{C}(^{18}\text{O}, ^{16}\text{O})^{14}\text{C}$ at $E_{\text{lab}} = 84$ and 275 MeV and interpreted as a signature of

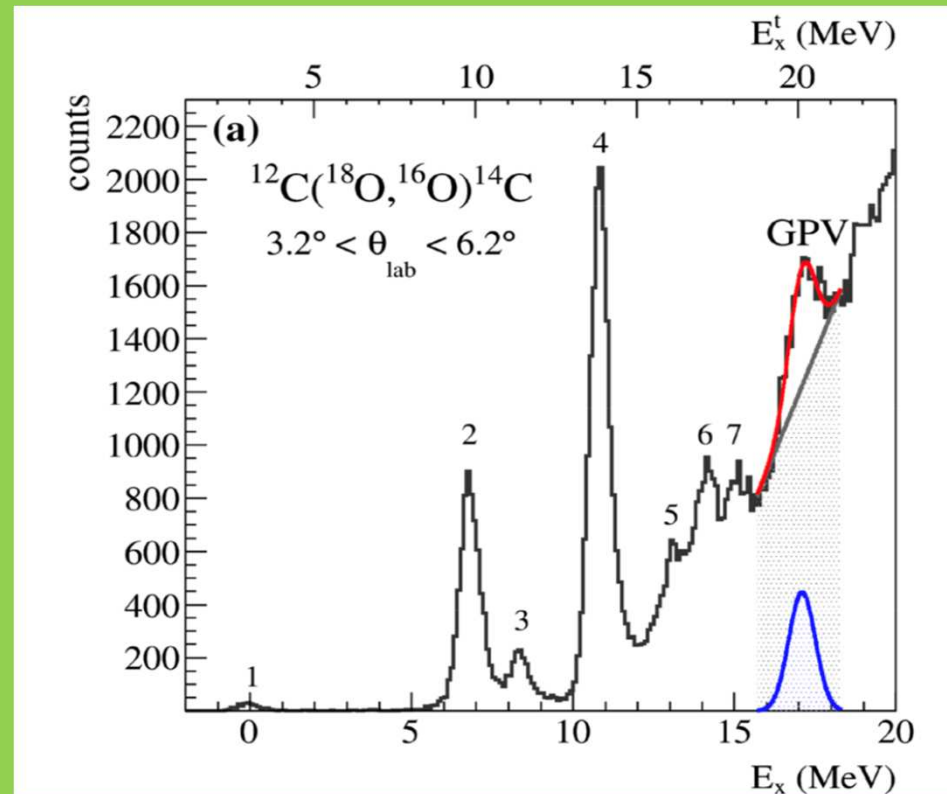
12-C GPV

12-C GPV

A bump has been detected at $E^* \approx 16$ MeV in the reaction $^{12}\text{C}(^{18}\text{O}, ^{16}\text{O})^{14}\text{C}$ at $E_{\text{lab}} = 84$ and 275 MeV and interpreted as a signature of GPV

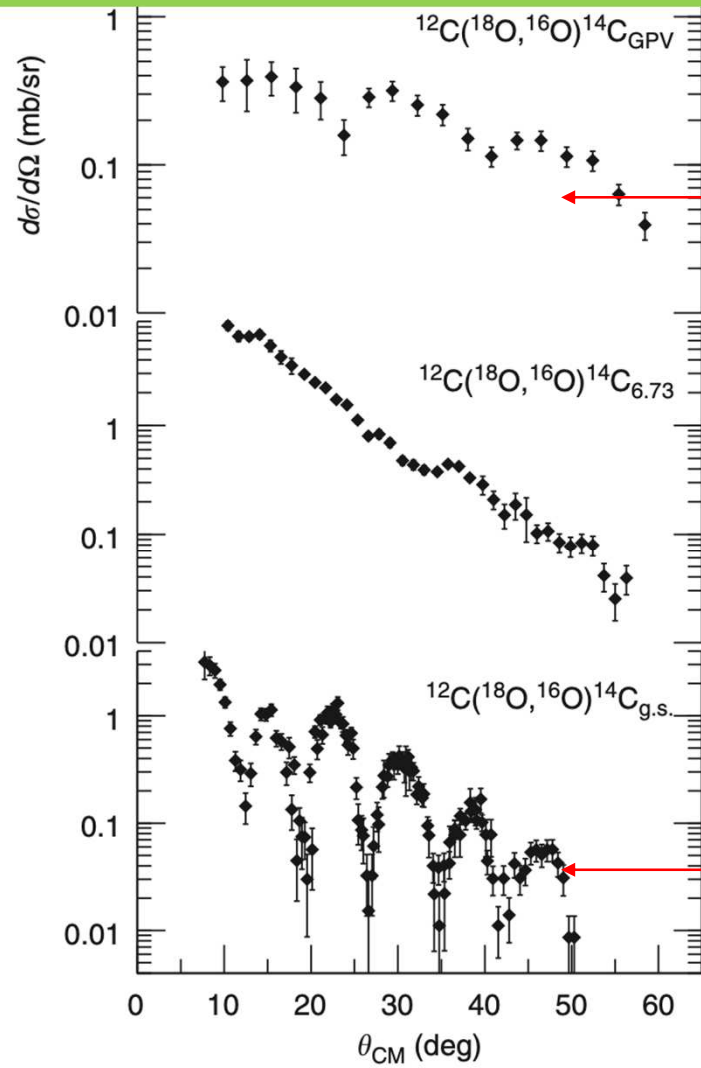


F. Cappuzzello et al., Nat. Comm. 6 (2015) 6743



F. Cappuzzello et al., Eur. Phys. J. A 57 (2021) 34

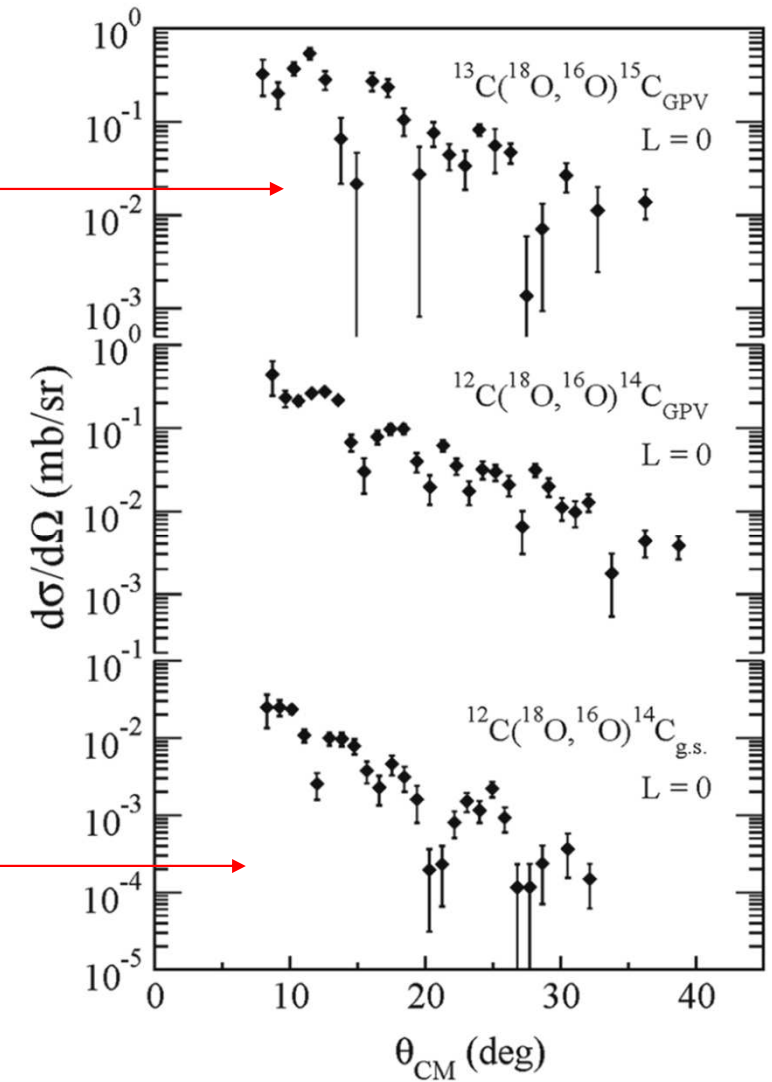
$E_{\text{lab}} = 84 \text{ MeV}$



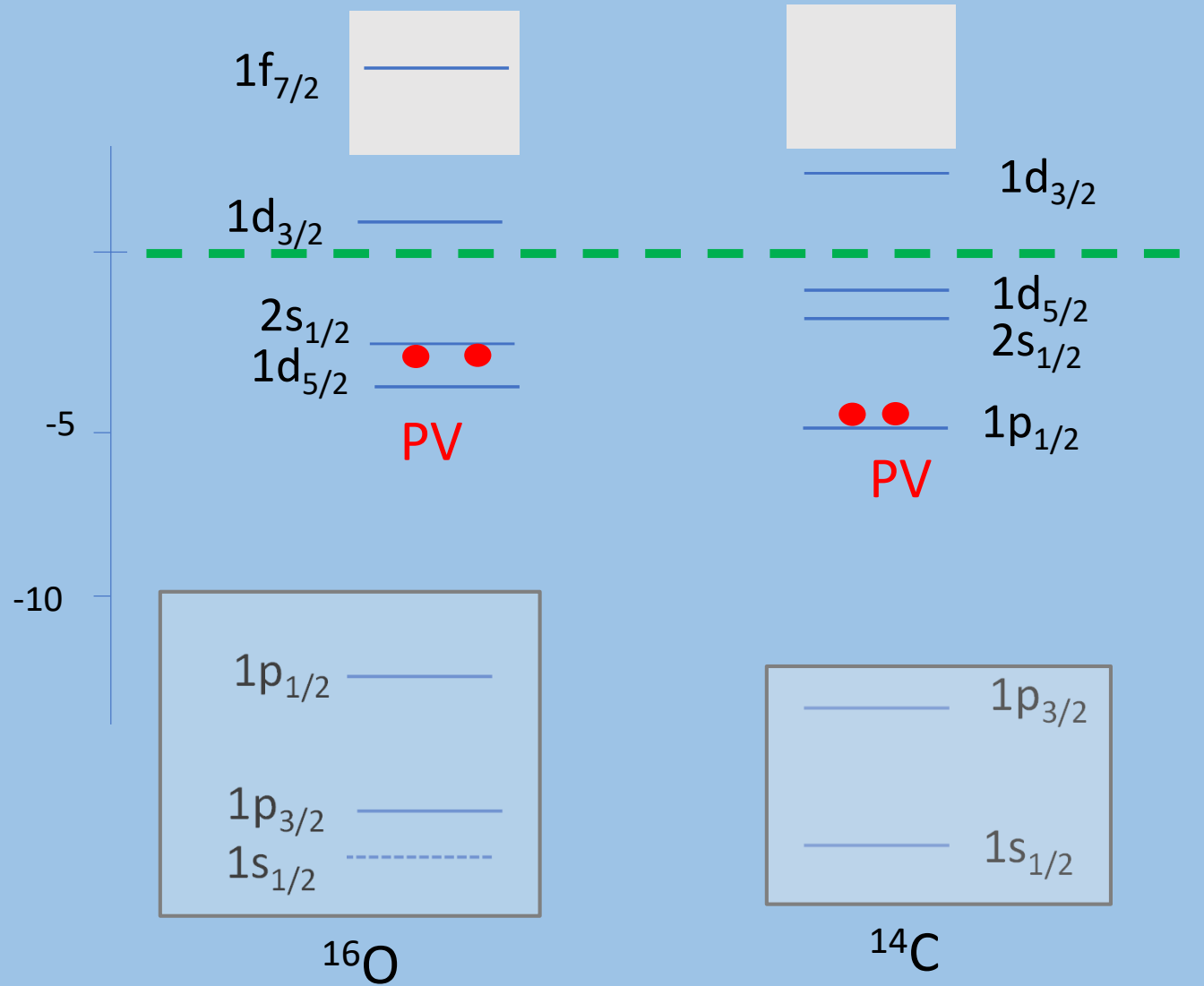
GPV?

gs.

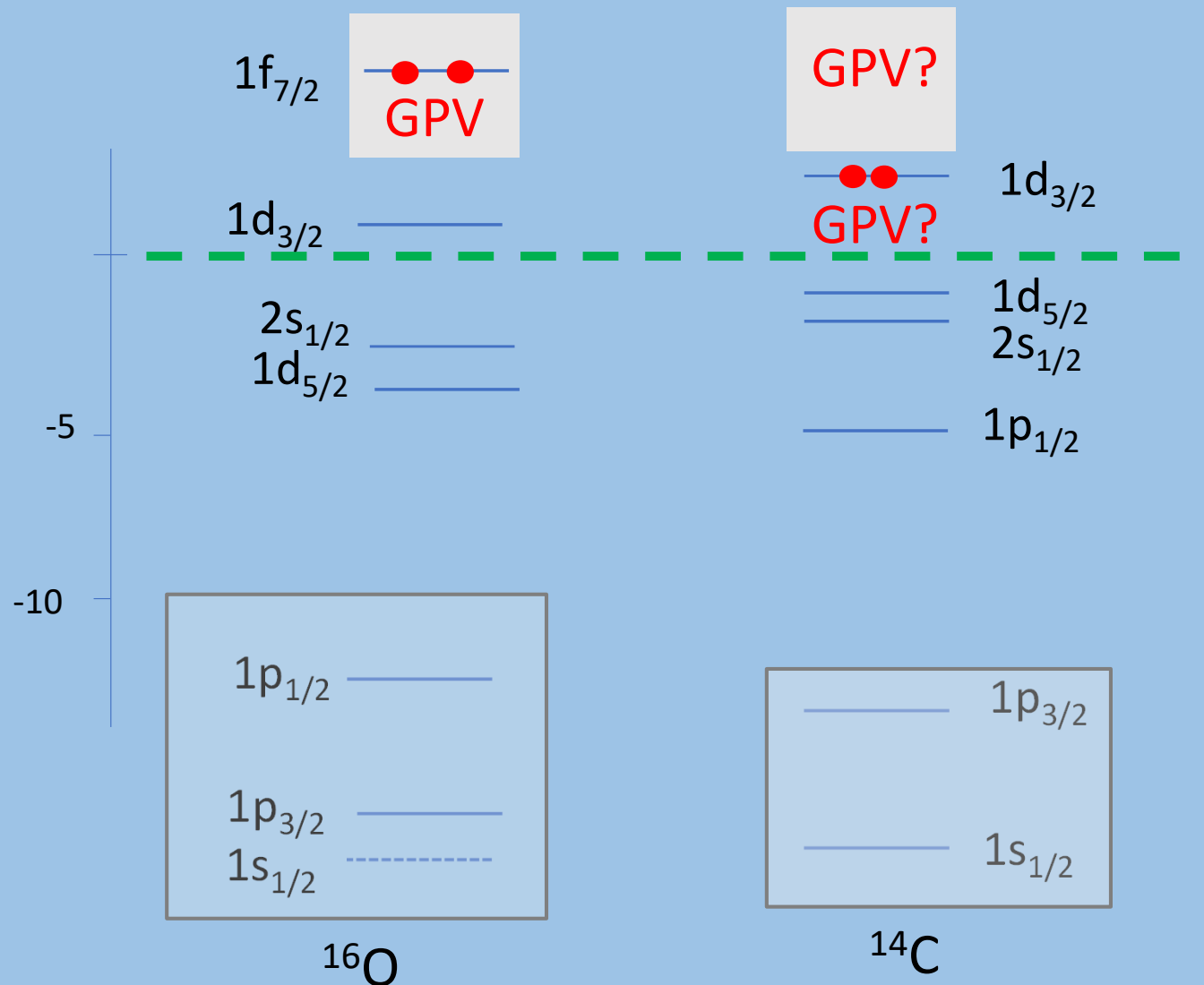
$E_{\text{lab}} = 275 \text{ MeV}$



GPV calculation challenges



GPV calculation challenges



1. In the GPV **both** neutrons lie in the continuum \rightarrow **discretization method via hard wall boundary**.

2. An accurate description of s-p levels is crucial \rightarrow **Many-body effects** \rightarrow Particle Vibration Coupling (PVC)

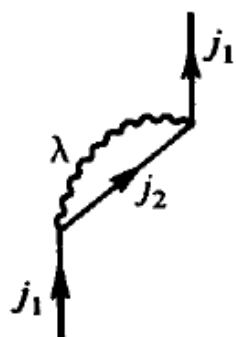
3. Realistic pairing interaction to be used in the continuum is needed (Gogny, DDDI, V-14,...) + **Induced Interaction** \rightarrow **Many-body effects** \rightarrow Particle Vibration Coupling (PVC)

4. Incorporate all this in the pp-RPA eq.'s

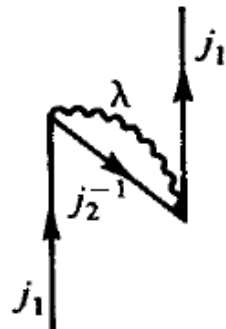
Position of the Single Particle Levels

PVC: Self-energy due to coupling surface vibrations

Polarization



Correlation (inhibition)



$\lambda^\pi: 2^+$ most relevant

Part of the S-P strength goes to the intermediate state \rightarrow Fragmentation

PVC vertex

$$\Sigma(j_1) = \begin{cases} \frac{h^2(j_1, j_2 \lambda)}{\varepsilon(j_1) - \varepsilon(j_2) - \hbar\omega_\lambda} & \varepsilon(j_2) > \varepsilon_F \\ -\frac{h^2(j_1, j_2 \lambda)}{\varepsilon(j_2) - \varepsilon(j_1) - \hbar\omega_\lambda} & \varepsilon(j_2) < \varepsilon_F \end{cases}$$

Experimental Collective
Quadrupole States properties

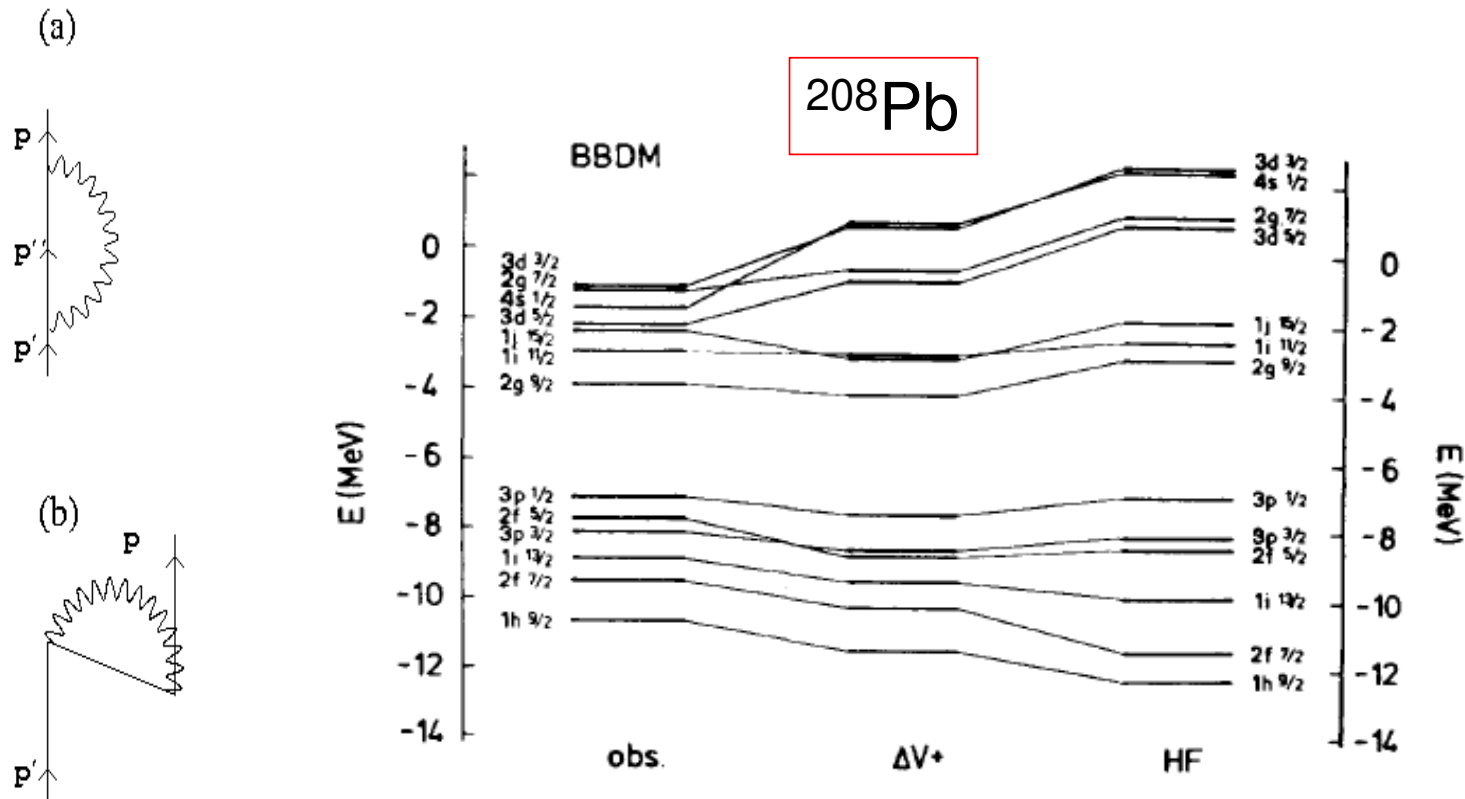
$$h(j_1, j_2 \lambda) \equiv \langle j_2, n_\lambda = 1; I = j_1, M = m_1 | H' | j_1 m_1 \rangle$$

$$= (-1)^{j_1 + j_2} (2j_1 + 1)^{-1/2} (2\lambda + 1)^{-1/2} \langle j_2 || k_\lambda Y_\lambda || j_1 \rangle \langle n_\lambda = 1 || \alpha_\lambda || n_\lambda = 0 \rangle$$

General expression

Bohr-Mottelson VPM

SELF ENERGY RENORMALIZATION OF SINGLE-PARTICLE STATES: CLOSED SHELL A CLASSICAL REFERENCE



C. Mahaux, P.F. Bortignon, R.A. Broglia, C.H. Dasso and Mahaux, Phys. Rep.(1985)1

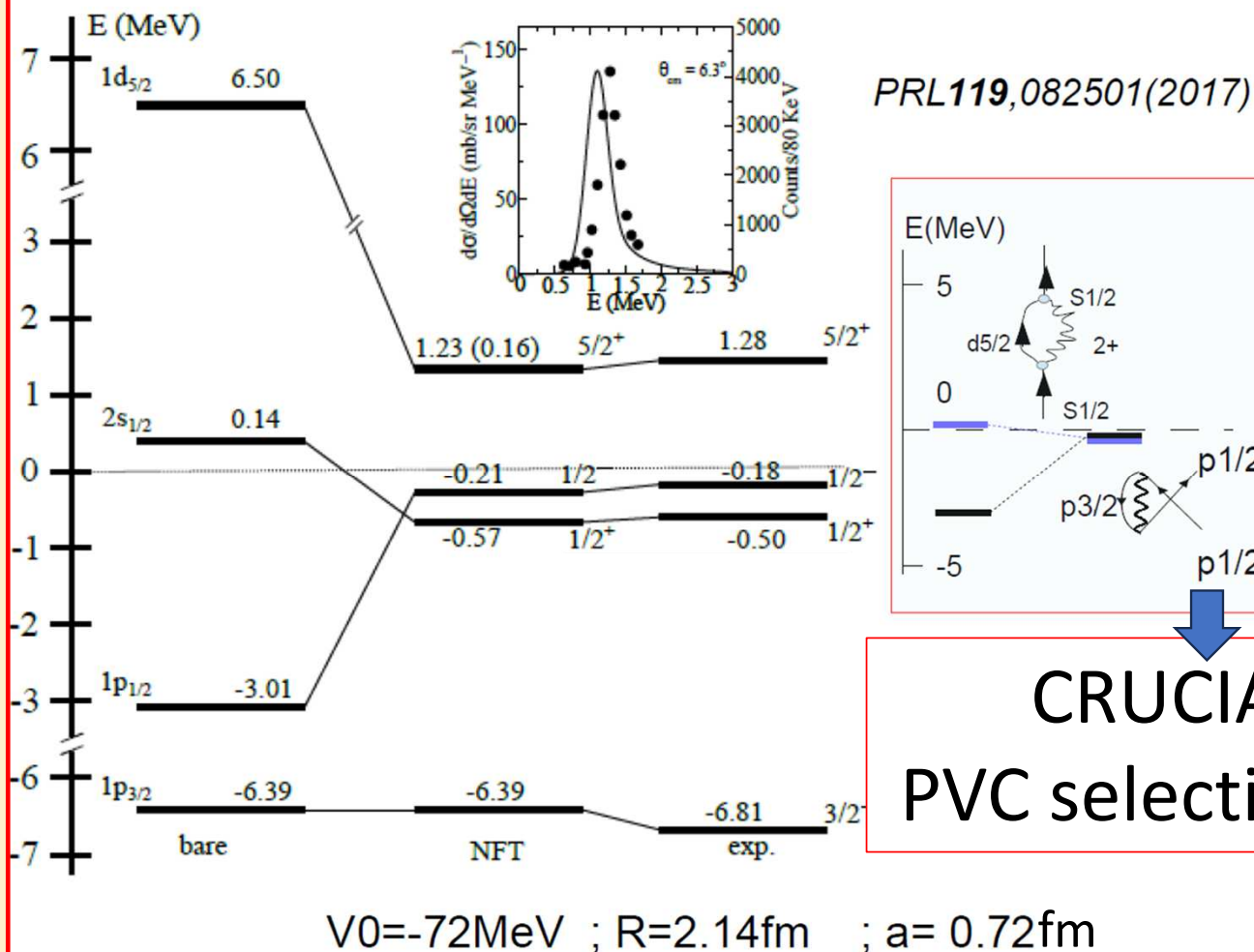
Position of the Single Particle Levels and PVC: Self-energy and Bare Mean Field in ^{11}Be

The parity inversion problem in ^{11}Be

No mean field (WS, Skyrme, Gogny, spherical, deformed...) gives the Inversion of the energy order of the $j=1/2$ states.

We have solved the problem by including the PVC effects (**polarization and correlation**)

The “bare” mean field is an output of our calculation



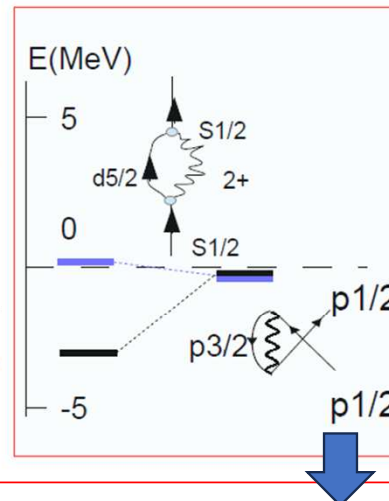
Other observables:

Spectroscopic factors in one-neutron transfer,

Population of 2^+ in $^{11}\text{Be}(p,d)^{10}\text{Be}$ reaction.

Nuclear radii isotope shift

...

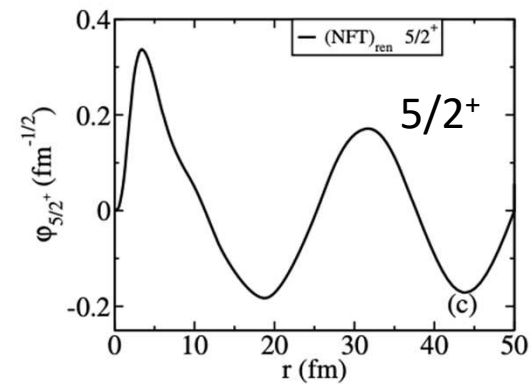
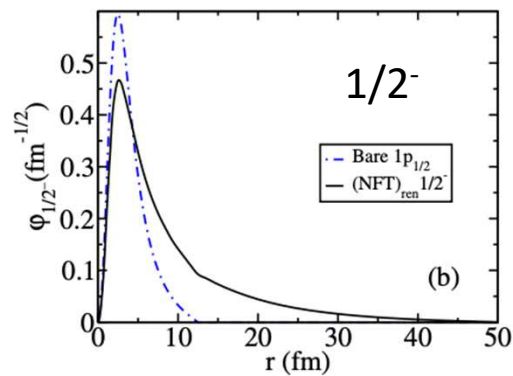
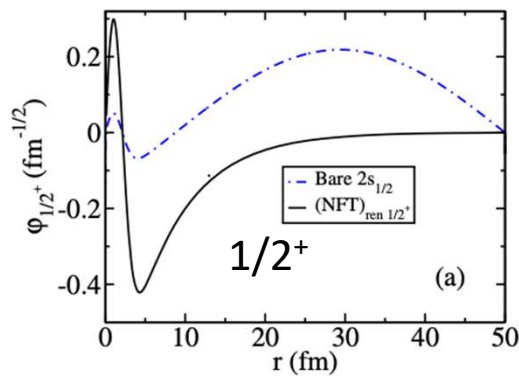


CRUCIAL!!!
PVC selection rules

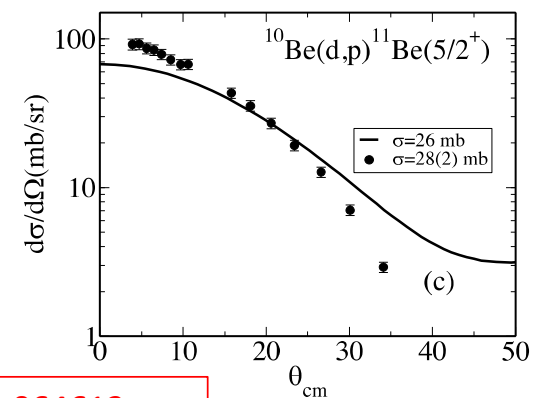
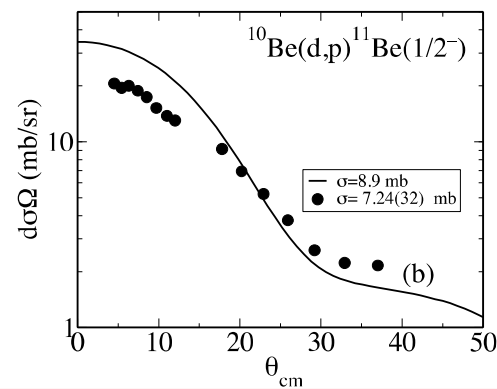
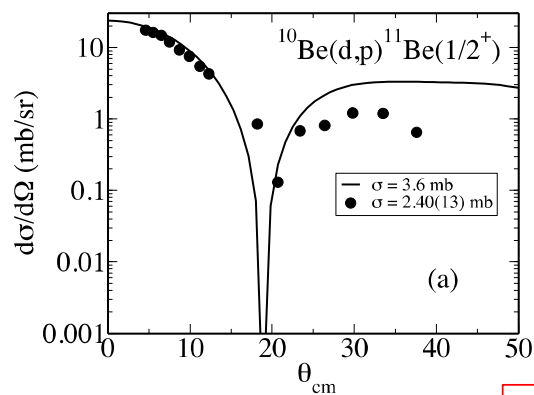
$^{10}\text{Be}(d,p)^{11}\text{Be}$ at $E_d = 21.4$ MeV

Test of the single-particle component of the many-body wave function

Form factors



Cross sections



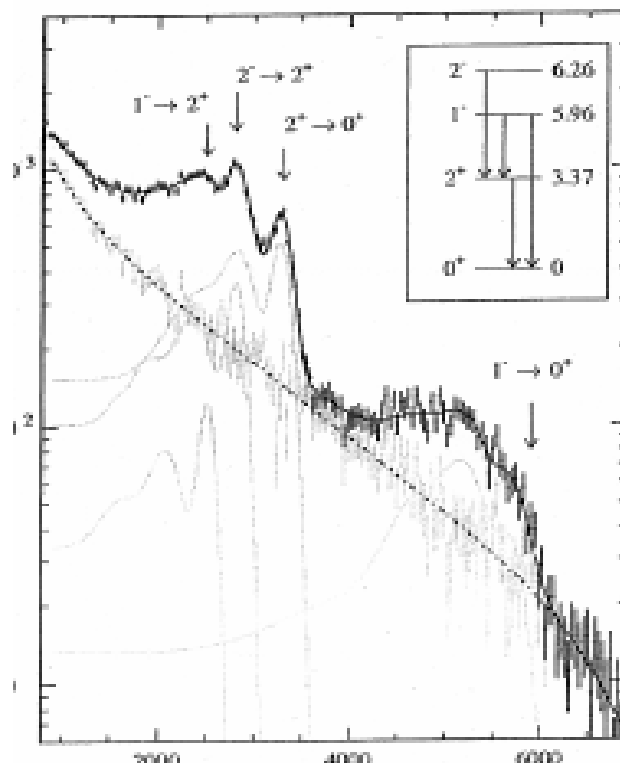
Data: K.T. Schmitt et al., PRC88 (2012) 064612

... experiments demonstrated that the core dynamics plays an important role...

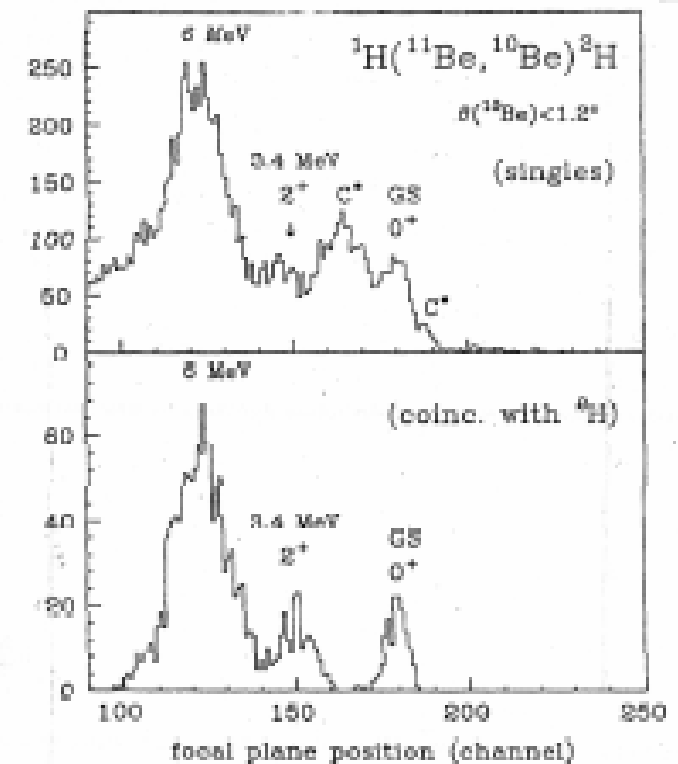
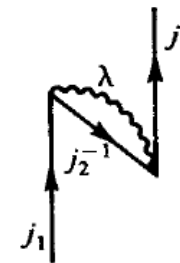
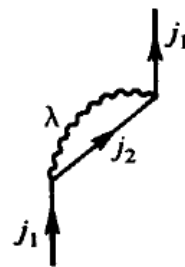
The admixture of $d_{5/2} \times 2^+$ configuration in the $1/2^+$ g.s. of ^{11}Be is about 15%

$p(^{11}\text{Be}, ^{10}\text{Be})d$

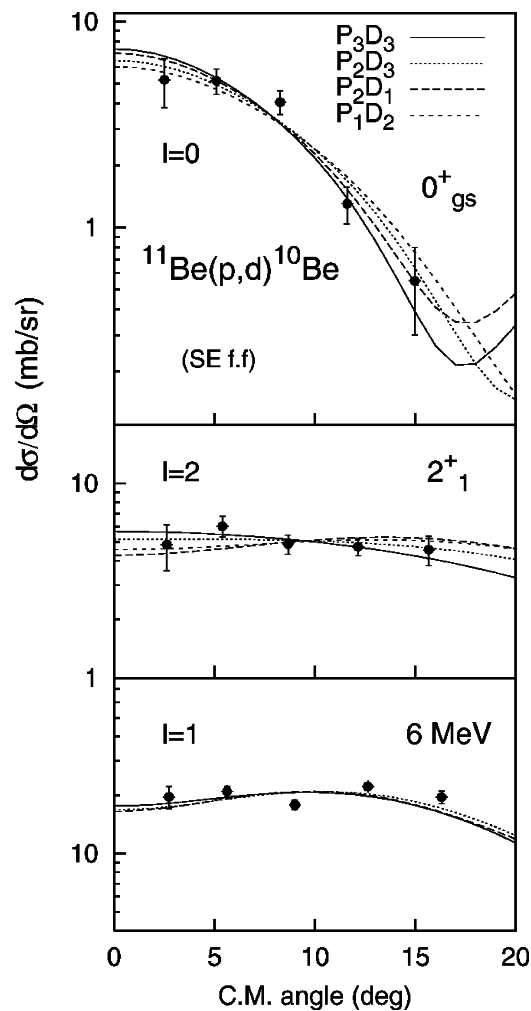
$9\text{Be}(^{11}\text{Be}, ^{10}\text{Be}+\gamma)X$



T. Aumann et al. PRL 84 (2000) 35



S. Fortier et al. Phys. Lett. B461 (1999)22
J.S. Winfield et al., Nucl.Phys. A683 (2001)48



A careful analysis of transfer reactions is needed to estimate phonon admixtures in the wavefunctions

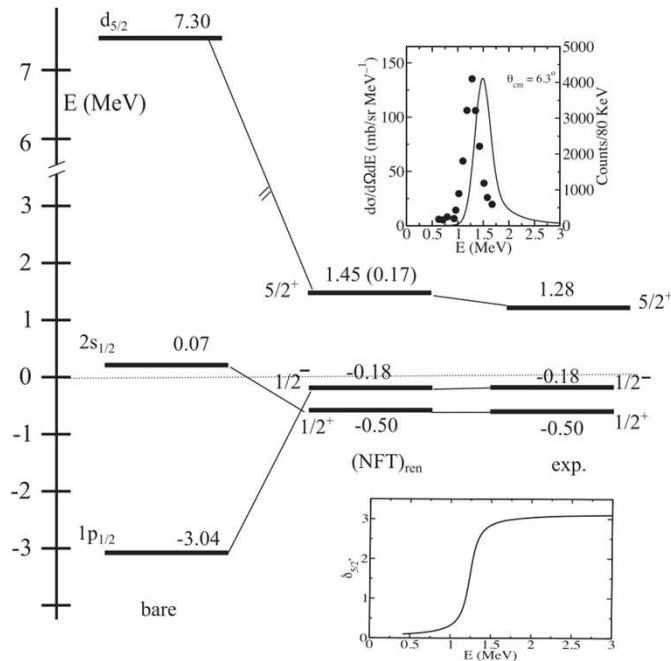
$$|^{11}\text{Be}_{\text{gs}}\rangle = \alpha |^{10}\text{Be}(0^+) \otimes 2s\rangle + \beta |^{10}\text{Be}(2^+) \otimes 1d\rangle$$

Good agreement with 2+ cross sections is obtained in DWBA with $\beta^2 = 0.17$ considering the coupling effects on the transfer form factor; using β as a simple spectroscopic factor one finds $\beta^2 = 0.28$

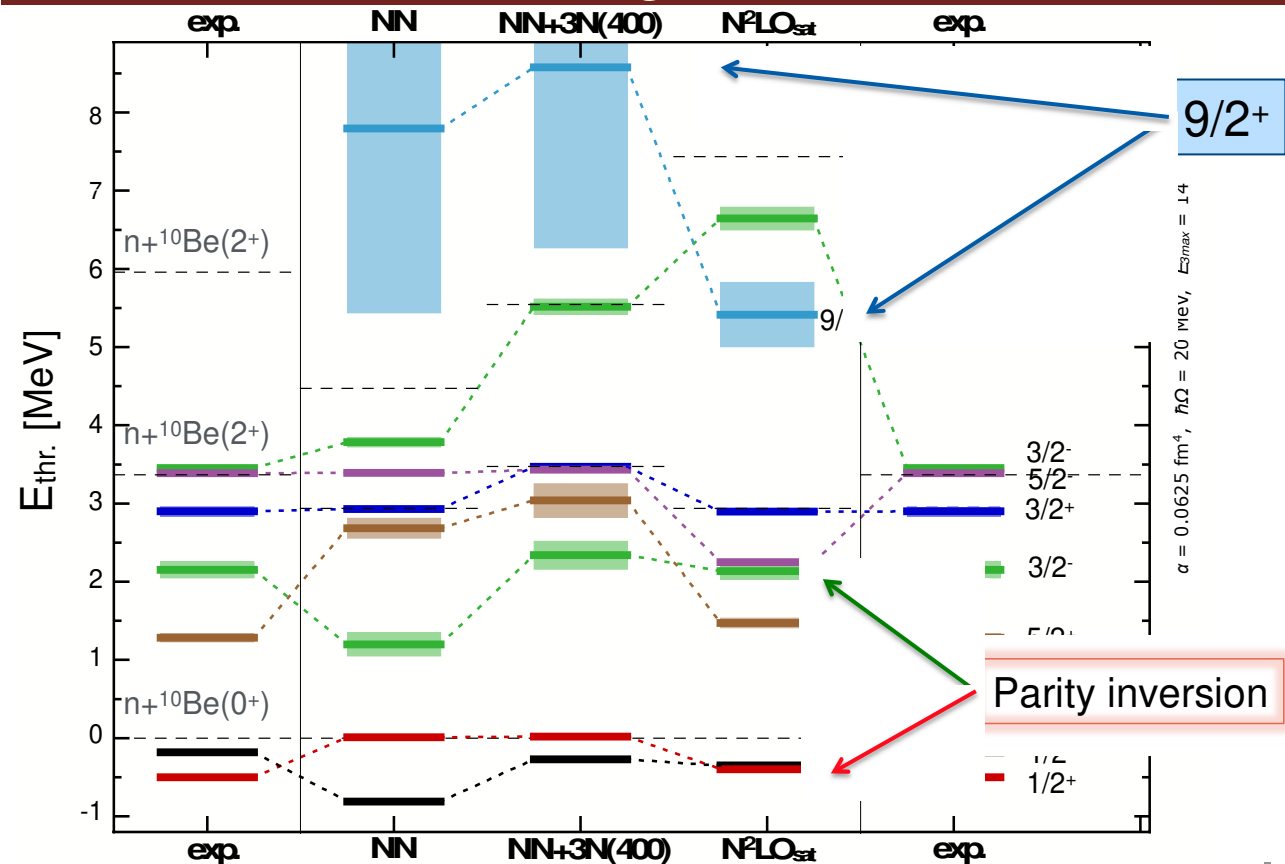
J.S. Winfield et al.,
Nucl.Phys. A683 (2001)48

The critical description of the experimental results from complementary approaches can be of great interest

PVC



Ab Initio

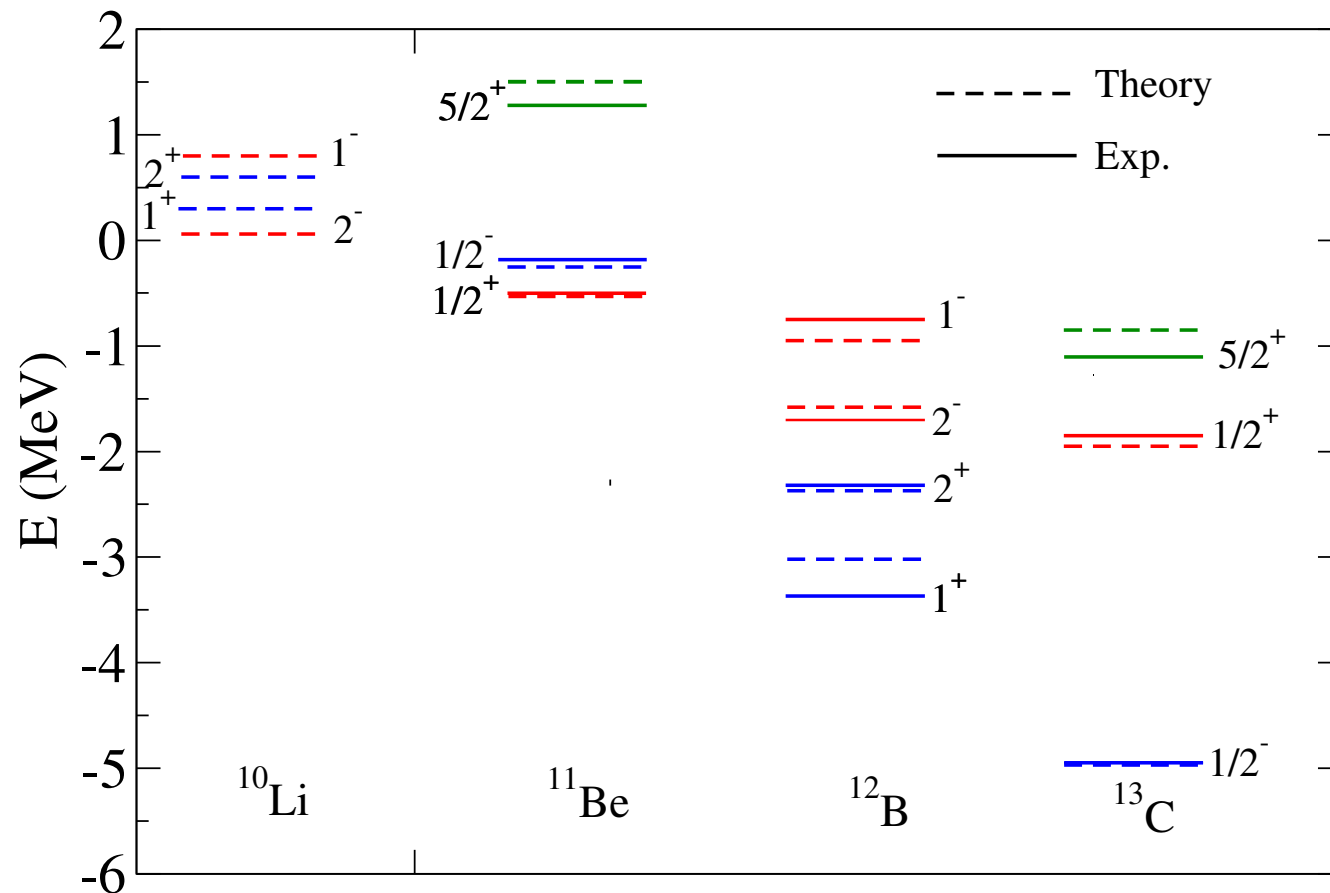


A. Calci, P. Navratil, R. Roth, J. Dohet-Eraly, S. Quaglioni, G. Hupin, PRL 117, 242501 (2016)

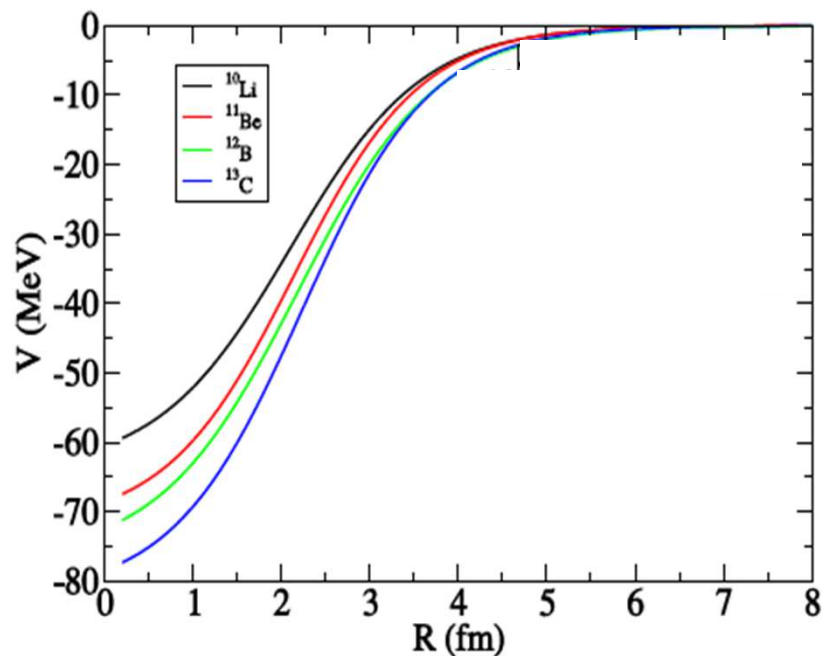
Calci, Navratil, Roth, Dohet-Eraly, Hupin, PRL117, 24250 1 (2016)

Position of the Single Particle Levels and PVC: Self-energy

Many-body states in N=7 isotones arising from quadrupole coupling with single-particle states calculated using mean-field potentials



Position of the Single Particle Levels and PVC: Self-energy



These potentials were determined by a consistent fit to data considering the PVC renormalization effects.

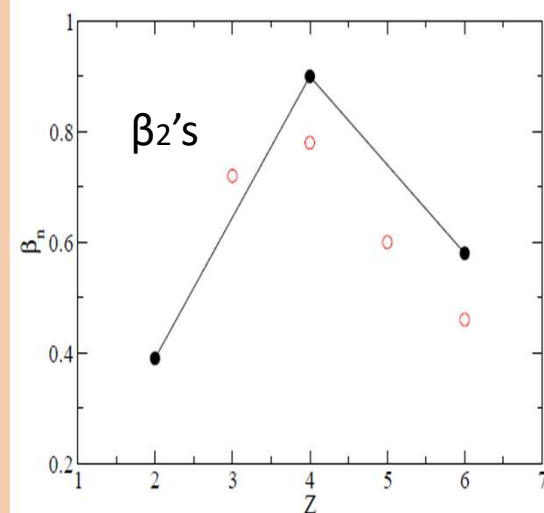
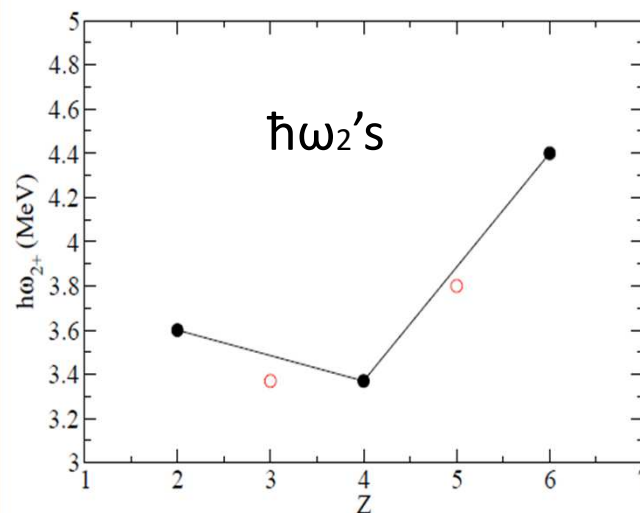
Simple parametrization:

$$V_{\text{WS}} = -82 + 54(N-Z)/A \text{ MeV}$$

$$a = 0.75 \text{ fm}; R_{\text{WS}} = 0.99A^{1/3} \text{ fm}$$

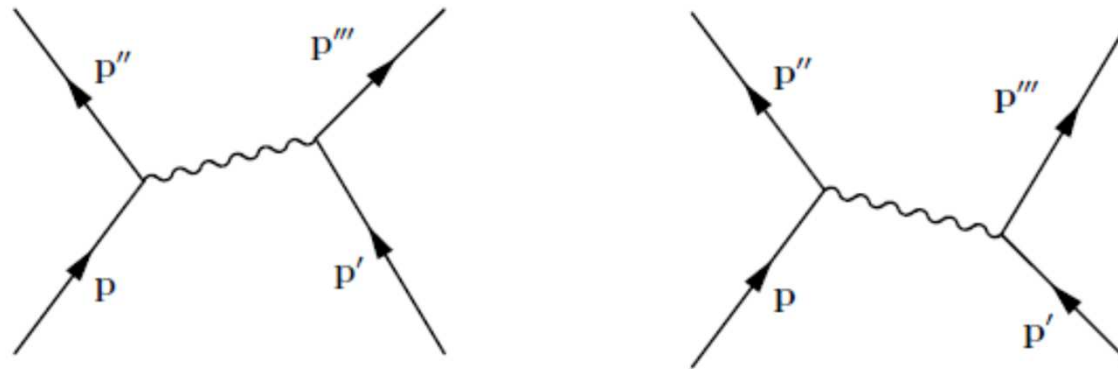
$$V_{\text{LS}} = 0.0082V_{\text{WS}}$$

Bare mean field potential for $N=7$ isotones



Extended Role of Vibrations in the PV and GPV:
The Phonon Exchange

Induced Interaction, V^{ind}



$$V_{pp'p''p'''}^{\text{ind}} = \sum_{\lambda\nu} \left[\frac{h_{pp''\lambda\nu} h_{p'''p'\lambda\nu}}{E - (\epsilon_{p''}^{\text{emp}} + \epsilon_{p'}^{\text{emp}} + \hbar\omega_{\lambda\nu})} + \frac{h_{p''p\lambda\nu} h_{p'p'''\lambda\nu}}{E - (\epsilon_p^{\text{emp}} + \epsilon_{p'''}^{\text{emp}} + \hbar\omega_{\lambda\nu})} \right]$$

Present in every nucleus!!

As a consequence: any pairing $V^{\text{eff}}(p,p';p'',p''')$ must leave room to V^{ind}

For a general pairing force and including pairing GSC's:

The pp-RPA equations

$$\begin{pmatrix} A & B \\ B^+ & C \end{pmatrix} \begin{pmatrix} R_p^{\tau, \lambda} \\ R_h^{\tau, \lambda} \end{pmatrix} = \begin{pmatrix} 1 & 0 \\ 0 & -1 \end{pmatrix} \begin{pmatrix} R_p^{\tau, \lambda} \\ R_h^{\tau, \lambda} \end{pmatrix} \cdot \hbar \Omega_{\tau, \lambda},$$

$$A_{mm'm'n'} = \delta_{mm'} \delta_{nn'} (\epsilon_m + \epsilon_n) + \bar{v}_{mm'm'n'},$$

$$(R_p^\tau)_{mn} = X_{mn}^\tau, \quad (R_p^\lambda)_{mn} = Y_{mn}^\lambda,$$

$$C_{ij i' j'} = -\delta_{ii'} \delta_{jj'} (\epsilon_i + \epsilon_j) + \bar{v}_{ij i' j'},$$

$$(R_h^\tau)_{ij} = Y_{ij}^\tau, \quad (R_h^\lambda)_{ij} = X_{ij}^\lambda.$$

$$B_{mnij} = -\bar{v}_{mnij},$$

From The Nuclear Many Body Problem by Ring and Schuck

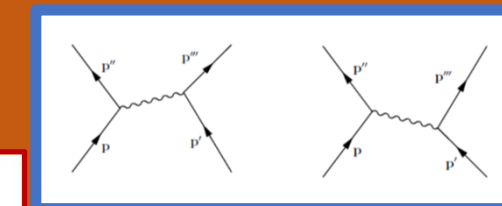
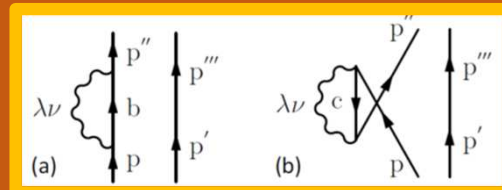
pp-RPA and PVC (E-dependent!!)

$$\begin{pmatrix} A_{pp'p''p'''} & B_{pp'h''h'''} \\ -B_{p''p'''hh'} & -A_{hh'h''h'''} \end{pmatrix} \begin{pmatrix} X_{p''p'''} \\ Y_{h''h'''} \end{pmatrix} = E \begin{pmatrix} X_{pp'} \\ Y_{hh'} \end{pmatrix}$$

Incorporating Self-energy and Induced Interaction

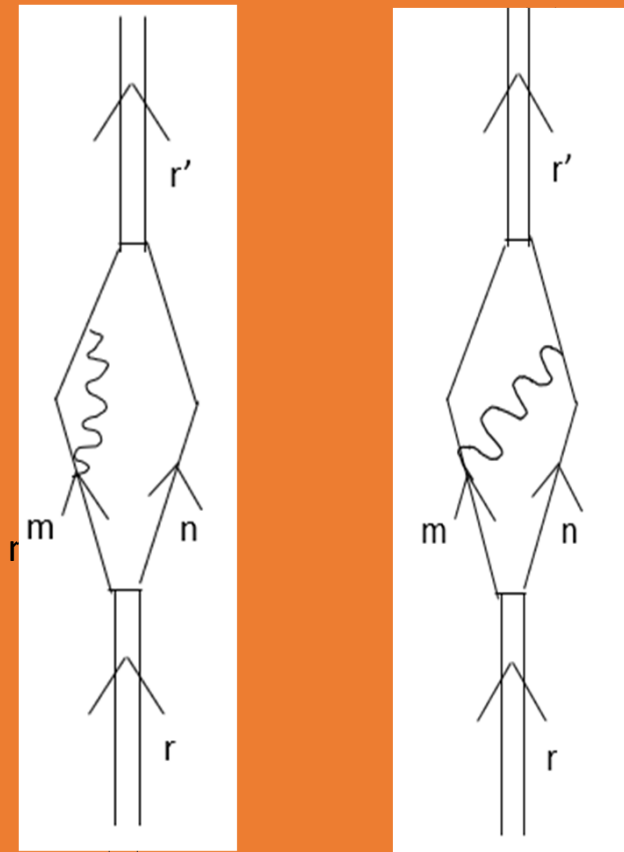
$$A_{pp'p''p'''} = [(\epsilon_p + \epsilon_{p'}) + \Sigma_{pp''(p')}(E)\delta_{p'p'''} + \Sigma_{p'p'''(p)}(E)\delta_{pp''} + V_{pp'p''p'''}^{bare} + V_{pp'p''p'''}^{ind}(E) + Exch(p, p')] N_{pp'p''p'''}]$$

$$B_{pp'hh'} = [V_{pp'hh'}^{bare} + V_{pp'hh'}^{ind}(E) + Exch(p, p')] N_{pp'p''p'''}]$$



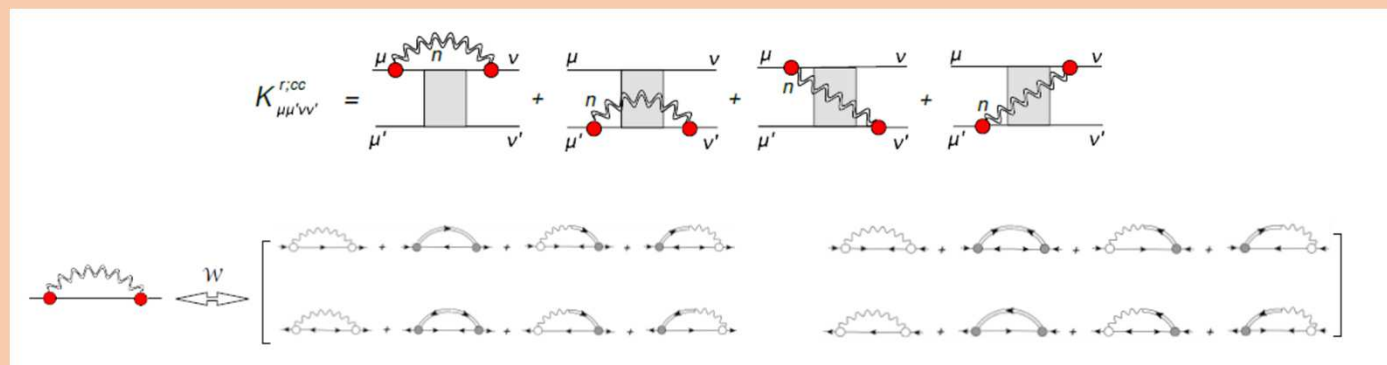
pp-RPA and PVC (E-dependent!!)

Technical note: This extension of pp-RPA can be treated included perturbatively or in a second diagonalisation. Using Feynman diagrams...

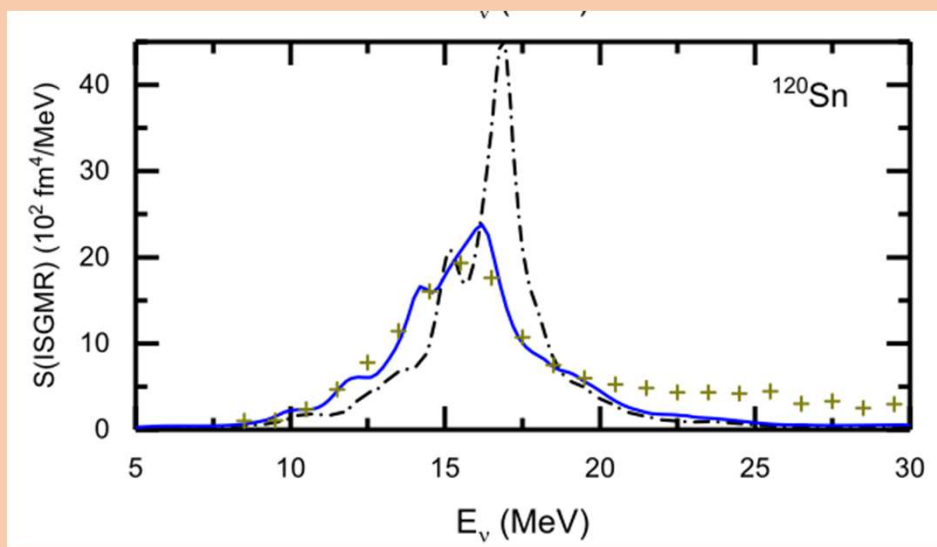


“Similar” theoretical schemes

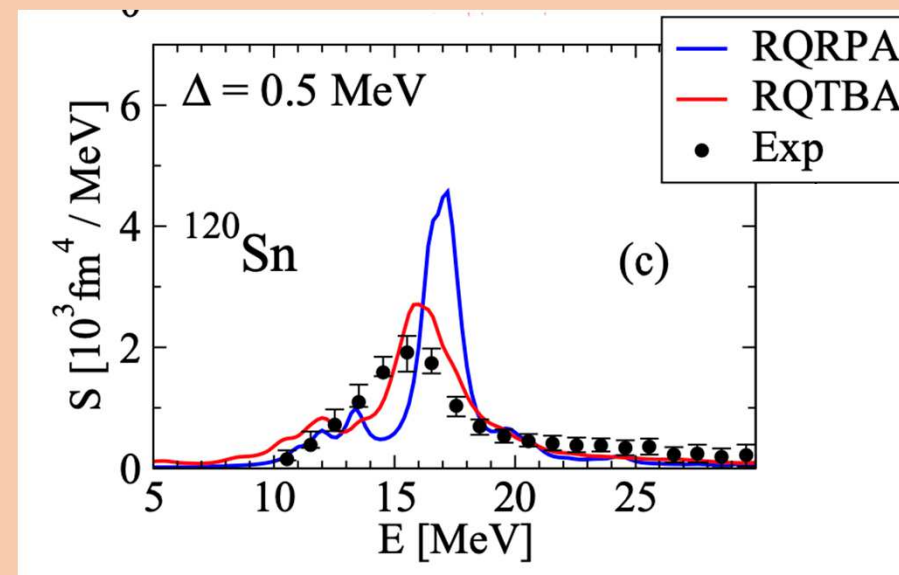
E. Litvinova and Y. Zhang
(arXiv 2208.07843v1)



Particle-vibration coupling on top of self-consistent density functional calculations has been mostly applied to heavy nuclei near closed shells. It provides a successful reproduction of the width of giant resonance modes



Z.Z. Li, Y.F. Niu, G. Colò. PRL 131 (2023) 082501



E. Litvinova, PRC 107 (2023) L041302

pp-RPA and PVC (E-dependent!!)

MIXED components: $|pp'-2+(Surf_vibration)>_0+$

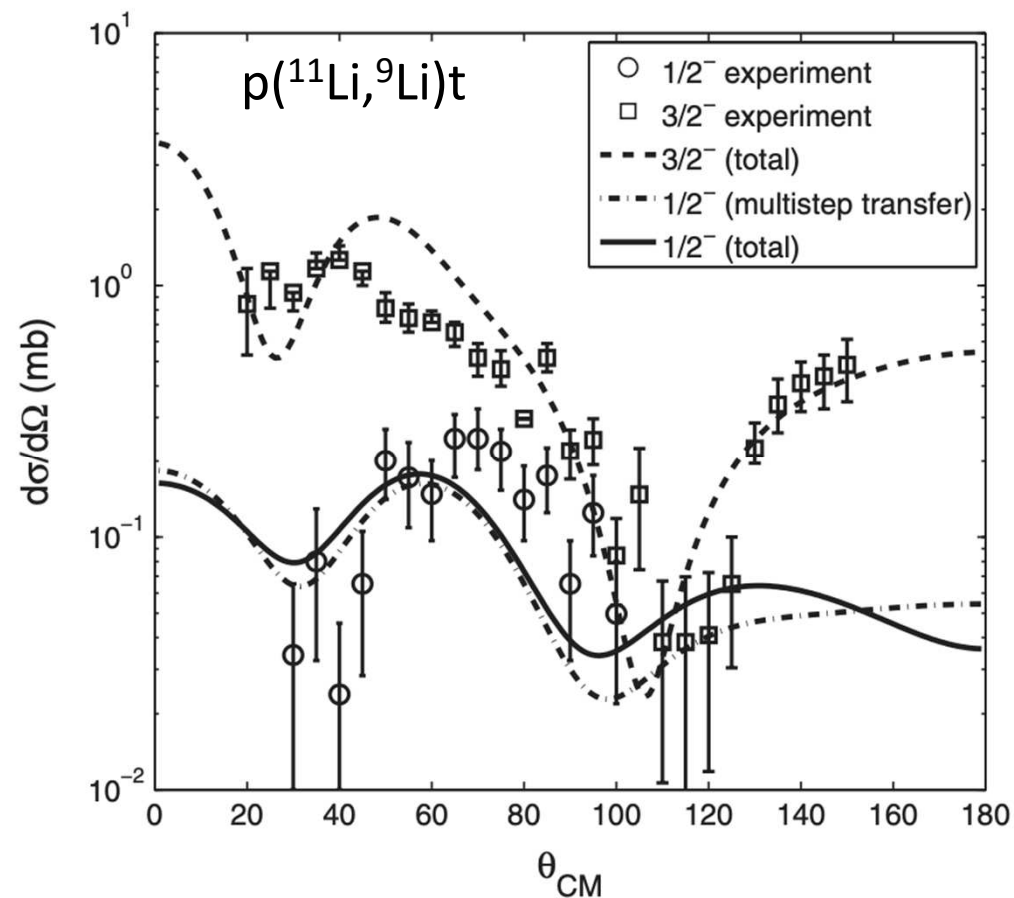
Technical note II:

The self-energy and the induced interaction are energy-dependent, thus it is possible to reconstruct the amplitudes of the resulting $0+$ states on the intermediate $2p-1$ phonon configurations, so that they can be written:

$$|0_n^+> = \sum_{pp'} (X_{pp'}(n) |pp'(0^+)> + Y_{hh'}(n) |hh'(0^+)>) + \sum_{pp'\nu} R_{pp'\nu}(n) |pp'(2^+)\nu(2^+)>$$

Can also be obtained by diagonalizing an energy independent matrix in the extended basis including them.

Role of phononic components in direct reactions



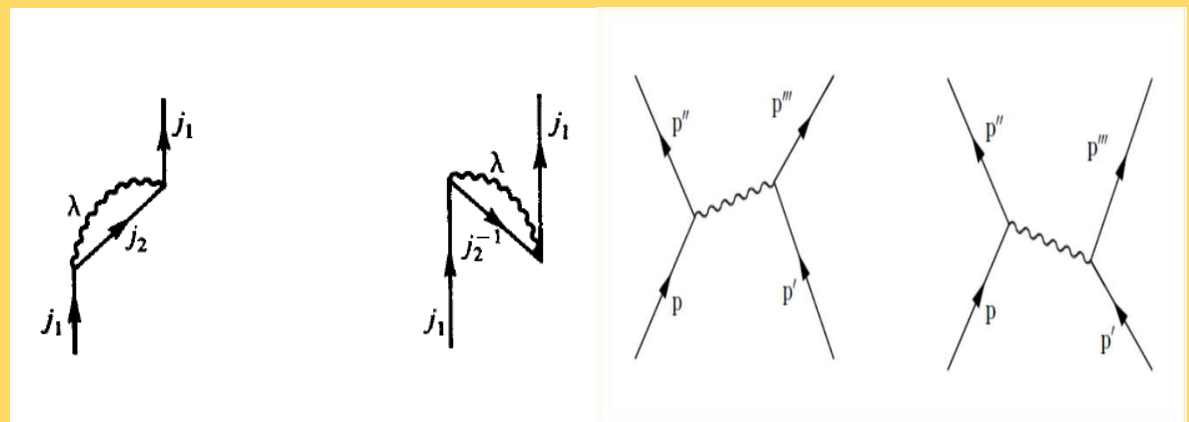
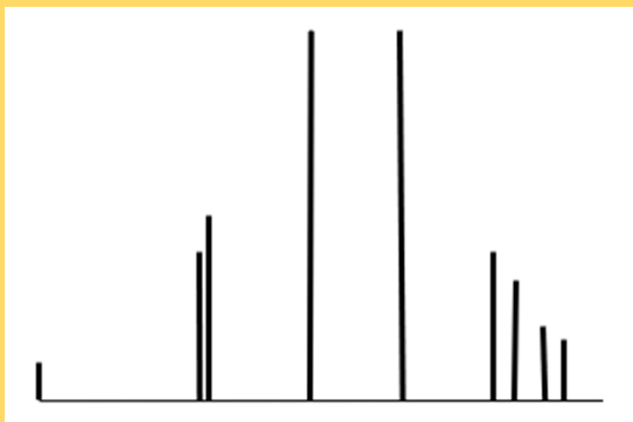
Theor.: G. Potel et al, PRL 105 (2010) 172502

Exp.: Tanihata et al. PRL192502(2008)

Summarizing: Pairing correlations , Decay width to the continuum and PVC effects

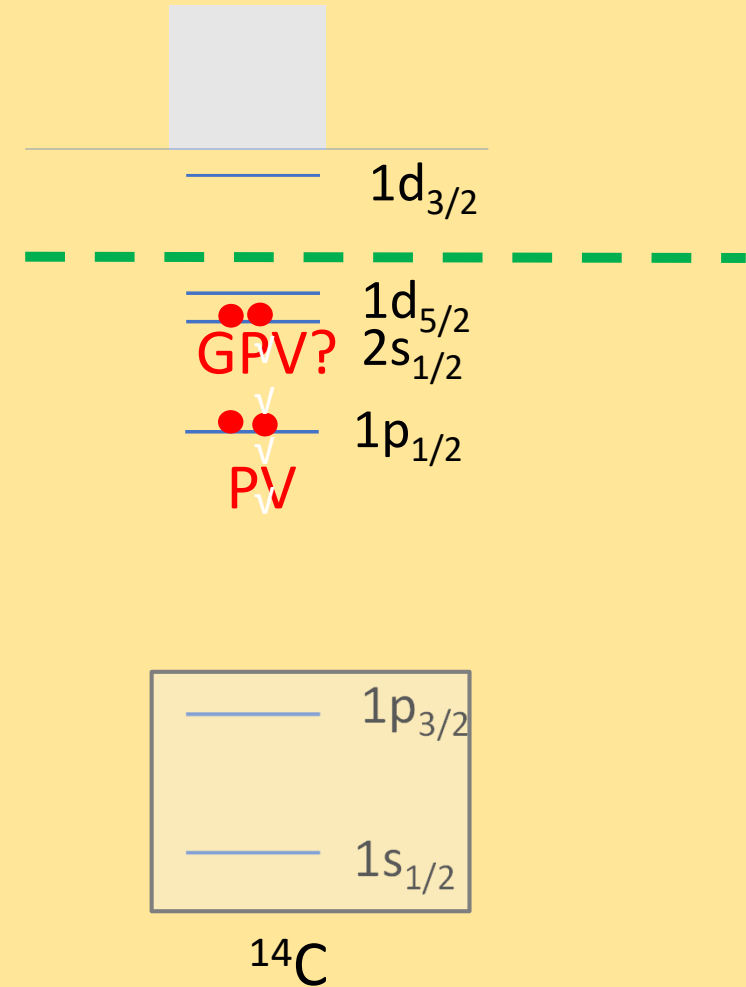
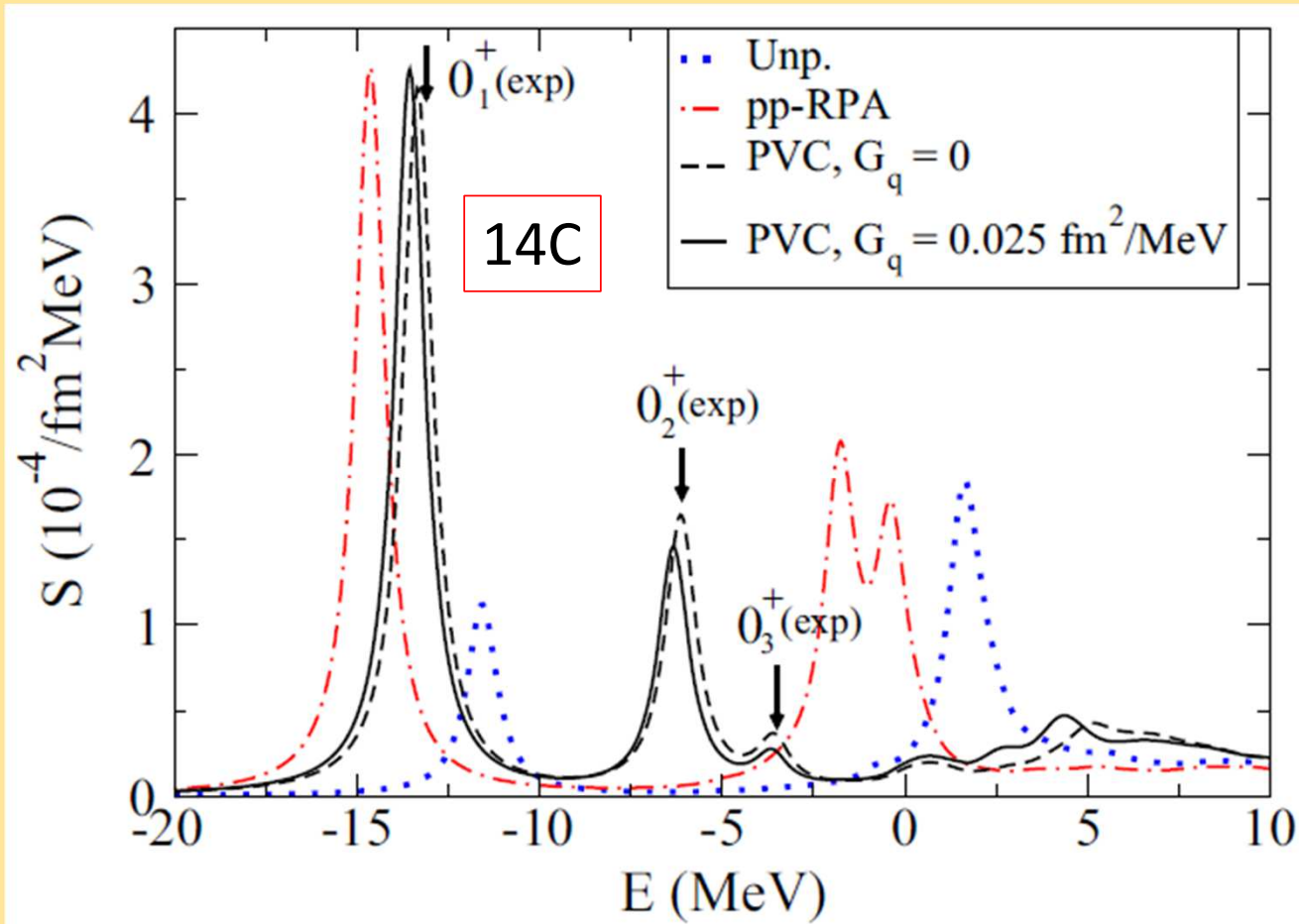
$$\underline{X}_{mn}(r) = \text{diagram with lines } m, n, r$$

$$\underline{Y}_{ij}(r) = \text{diagram with lines } i, j, r$$

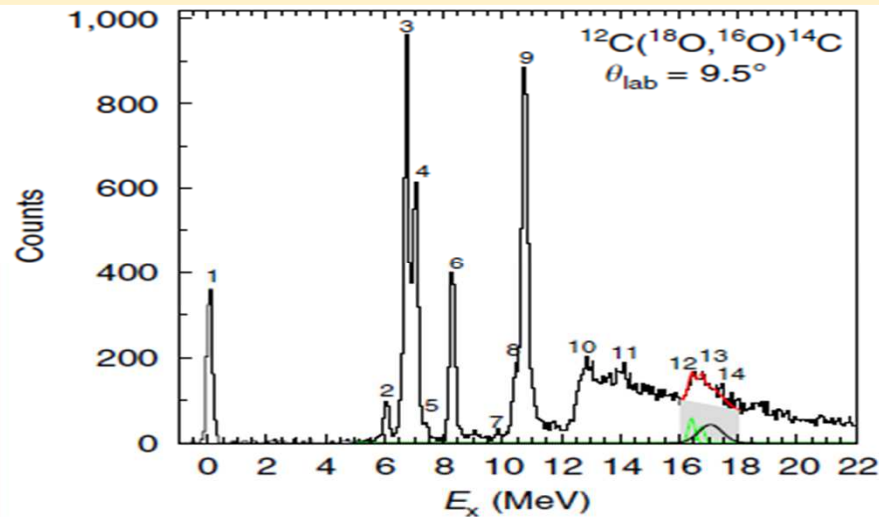
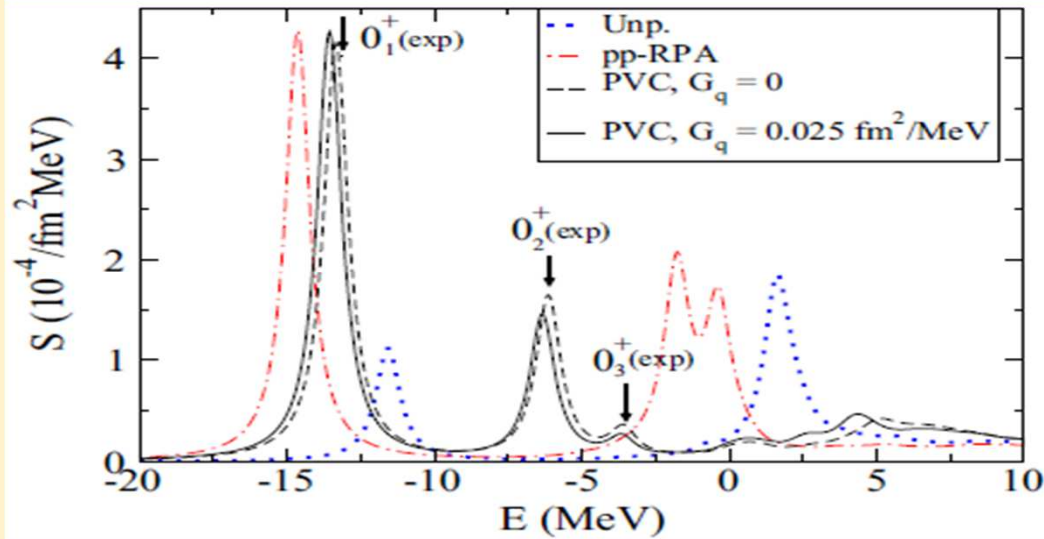


12C PV and GPV

pp-RPA and PVC



14C



PHYSICAL REVIEW LETTERS VOL..XX, 000000 (XXXX)

Fragmentation of the Giant Pairing Vibration in ^{14}C Induced by Many-Body Processes

F. Barranco¹, G. Potel^{1,2} and E. Vigezzi³

¹Departamento de Física Aplicada III, Escuela Técnica Superior de Ingeniería, Universidad de Sevilla, Camino de los Descubrimientos, Sevilla, Spain

²Lawrence Livermore National Laboratory, Livermore, California, USA

³INFN Sezione di Milano, Via Celoria 16, I-20133 Milano, Italy

(Received 23 February 2024; revised 4 June 2024; accepted 13 December 2024)

$$S_{WS}^i = \sum_{nn'l_j} [X_{nn'l_j}^i + Y_{nn'l_j}^i] \int dr G(r) \psi_{nl_j}(r) \psi_{n'l_j}(r).$$

$$G(r) \equiv (1 + \exp[(r - R_S)/a_S])$$



ARTICLE

Received 28 Dec 2014 | Accepted 24 Feb 2015 | Published 27 Mar 2015

DOI: 10.1038/ncomms7743

OPEN

Signatures of the Giant Pairing Vibration in the ^{14}C and ^{15}C atomic nuclei

F. Cappuzzello^{1,2}, D. Carbone², M. Cavallaro², M. Bondi^{1,2}, C. Agodi², F. Azaiez³, A. Bonaccorso⁴, A. Cunsolo², L. Fortunato^{5,6}, A. Foti^{1,7}, S. Franchoo³, E. Khan³, R. Linares⁸, J. Lubian⁸, J.A. Scarpaci⁹ & A. Vitturi^{5,6}

pp-RPA and PVC

$$|0_n^+\rangle = \sum_{pp'} (X_{pp'}(n) |pp'(0^+)\rangle + Y_{hh'}(n) |hh'(0^+)\rangle) + \sum_{pp'\nu} R_{pp'\nu}(n) |pp'(2^+)\nu(2^+)\rangle$$

| | $E_{gs} = -13.09 \text{ MeV}$ $R_{1^+}^{2^+} = 0.130$ | | | $E_{0_2^+} = -5.96 \text{ MeV}$ $R_{1^+}^{2^+} = 0.382$ | | | $E_{0_3^+} = -3.47 \text{ MeV}$ $R_{1^+}^{2^+} = 0.348$ | |
|-----------|--|-------------|--|--|-------------|--|--|-------------|
| l_j | $X_{l_j}^2$ | $Y_{l_j}^2$ | | $X_{l_j}^2$ | $Y_{l_j}^2$ | | $X_{l_j}^2$ | $Y_{l_j}^2$ |
| $s_{1/2}$ | 0.006 | 0.003 | | 0.283 | - | | 0.376 | - |
| $p_{1/2}$ | 0.833 | - | | 0.050 | - | | 0.043 | - |
| $p_{3/2}$ | - | 0.002 | | 0.001 | - | | - | - |
| $d_{3/2}$ | 0.003 | - | | 0.005 | - | | - | - |
| $d_{5/2}$ | 0.046 | - | | 0.327 | - | | 0.256 | - |

Table 4: Main 0-phonon components of the wavefunctions of the ground state and of the two lowest excited 0^+ states calculated with a constant effective mass, $m_{eff} = m_{red} = 0.92m$ ($R_{box} = 28 \text{ fm}$).

| | $R_{l_j l' j'}^{2^+}$ | | | | | | |
|-----------------|-----------------------|-----------|-----------|-----------|-----------|-----------|-----------|
| $l_j / l'_{j'}$ | $s_{1/2}$ | $p_{1/2}$ | $p_{3/2}$ | $d_{3/2}$ | $d_{5/2}$ | $f_{5/2}$ | $f_{7/2}$ |
| $s_{1/2}$ | - | - | - | - | 0.003 | - | - |
| $p_{1/2}$ | - | - | 0.105 | - | - | 0.0146 | - |
| $p_{3/2}$ | - | 0.105 | - | 0.004 | - | - | - |
| $d_{3/2}$ | - | - | 0.004 | - | - | - | - |
| $d_{5/2}$ | 0.003 | - | - | - | 0.005 | - | - |
| $f_{5/2}$ | - | 0.0146 | - | - | - | - | - |
| $f_{7/2}$ | - | - | - | - | - | - | - |

pp-RPA and PVC

Xpp' and cumulative Rpp'2+ amplitudes for $^{12}\text{C} + 2n$ (0+;GPV)

| | $E=6.87$ $R_{box}=20$ $R^{2+}_1 = 0.623$ | $E=6.91$ $R_{box}=22$ $R^{2+}_1 = 0.729$ | $E=7.14$ $R_{box}=24$ $R^{2+}_1 = 0.728$ | $E=6.96$ $R_{box}=26$ $R^{2+}_1 = 0.613$ | $E=7.11$ $R_{box}=28$ $R^{2+}_1 = 0.785$ |
|-----------|---|---|---|---|---|
| l_j | $X_{l_j}^2$ | $X_{l_j}^2$ | $X_{l_j}^2$ | $X_{l_j}^2$ | $X_{l_j}^2$ |
| $s_{1/2}$ | 0.06 | 0.041 | 0.03 | 0.04 | 0.012 |
| $p_{1/2}$ | 0.112 | 0.004 | 0.001 | 0.005 | 0.012 |
| $p_{3/2}$ | 0.029 | 0.003 | 0.056 | 0.005 | 0.05 |
| $d_{3/2}$ | 0.006 | 0.019 | 0.007 | 0.003 | 0.007 |
| $d_{5/2}$ | 0.154 | 0.195 | 0.179 | 0.279 | 0.111 |
| $f_{5/2}$ | - | - | - | - | - |
| $f_{7/2}$ | - | - | - | - | - |

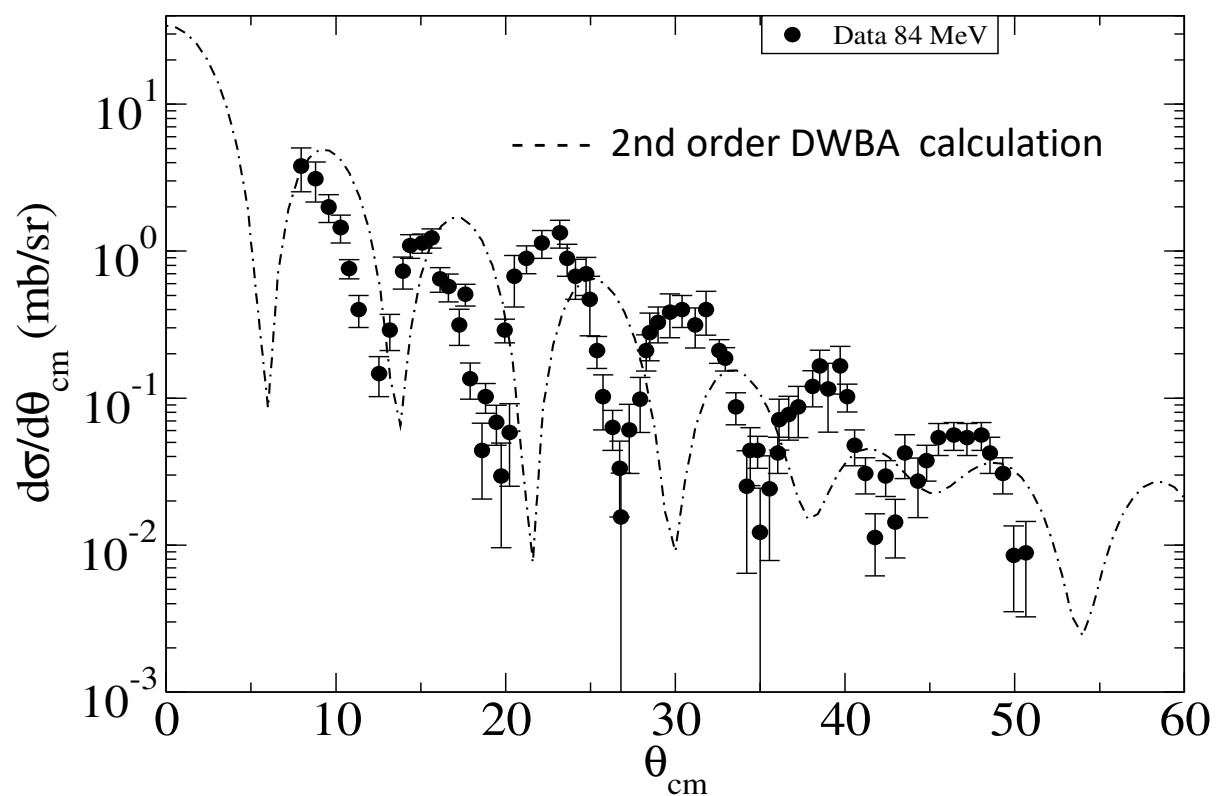
Table 23: Main 0-phonon components of the wavefunctions of the excited state of ^{14}C carrying the largest S_{dUdr} strength around $E = 7$ MeV for a series of boxes ($R_{box} = 20$ -28 fm).

Note: About 70% on the phononic side!!

$$|0^+_n\rangle = \sum_{pp'} (X_{pp'}(n) |pp'(0^+)\rangle + Y_{hh'}(n) |hh'(0^+)\rangle) + \sum_{pp'\nu} R_{pp'\nu}(n) |pp'(2^+)\nu(2^+)\rangle$$

EXTENDED pp-RPA RESULTS

$^{12}\text{C}(^{18}\text{O}, ^{16}\text{O})^{14}\text{C}(\text{gs})$ at $E_{\text{lab}} = 84 \text{ MeV}$



EXTENDED pp-RPA RESULTS

$^{132}\text{Sn} \pm 2n$

Application to médium and heavy nuclei: many more s-p levels

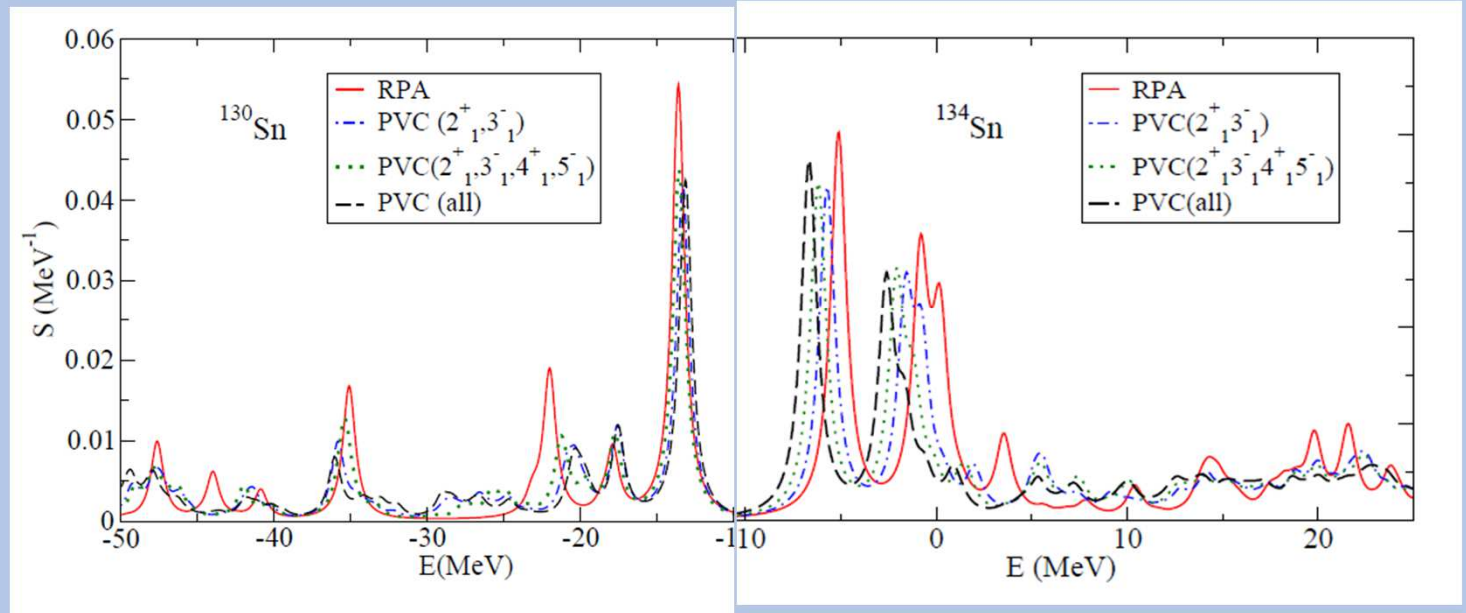
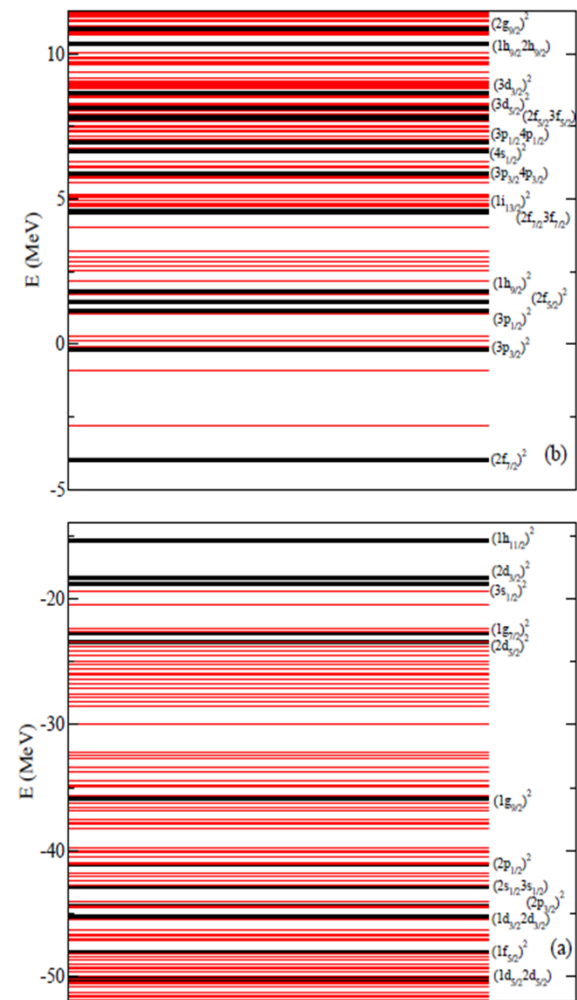


Figure 1. (a) The energies of the hh' -pairs in ^{132}Sn up to -50 MeV are shown by black thick lines. These states are embedded among the $hh' \lambda$ states (thin red lines), arising from the coupling to the lowest $2_1^+, 3_1^-, 4_1^+, 5_1^-$ vibrations. (b) The same, for the pp' -pairs with energies up to 11 MeV embedded among $pp' \lambda$ states, calculated in a box of radius $R_{\text{box}} = 14$ fm.

EXTENDED pp-RPA RESULTS

$^{132}\text{Sn} + 2n$

Application to médium and heavy nuclei: much more s-p levels

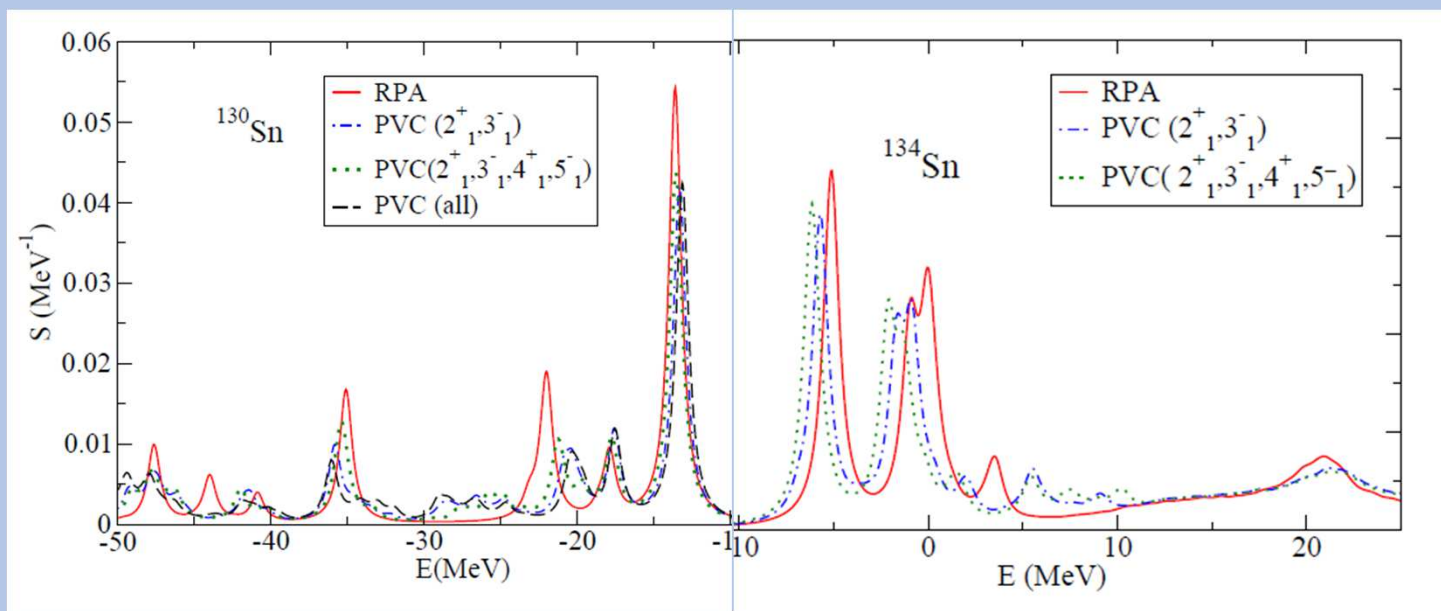
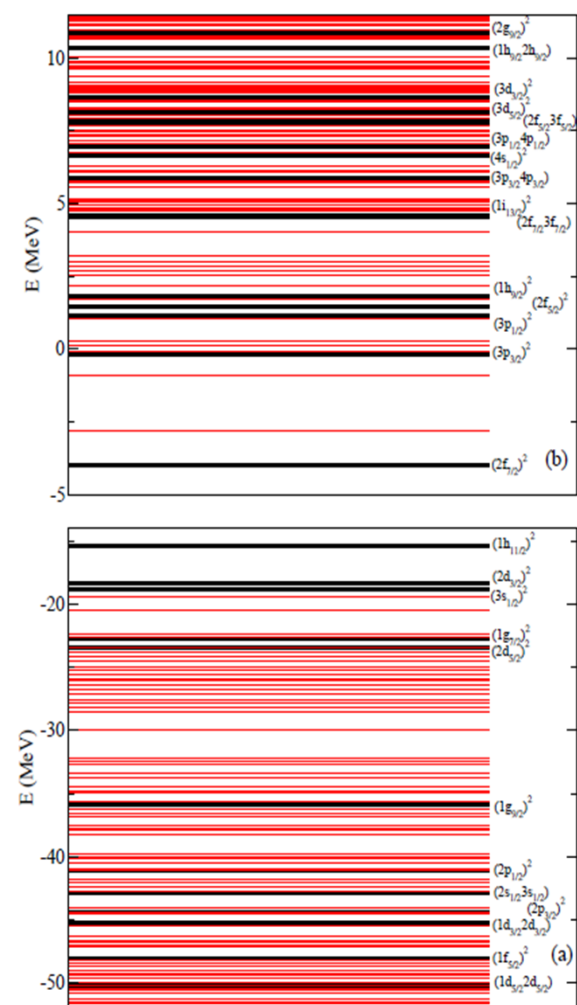
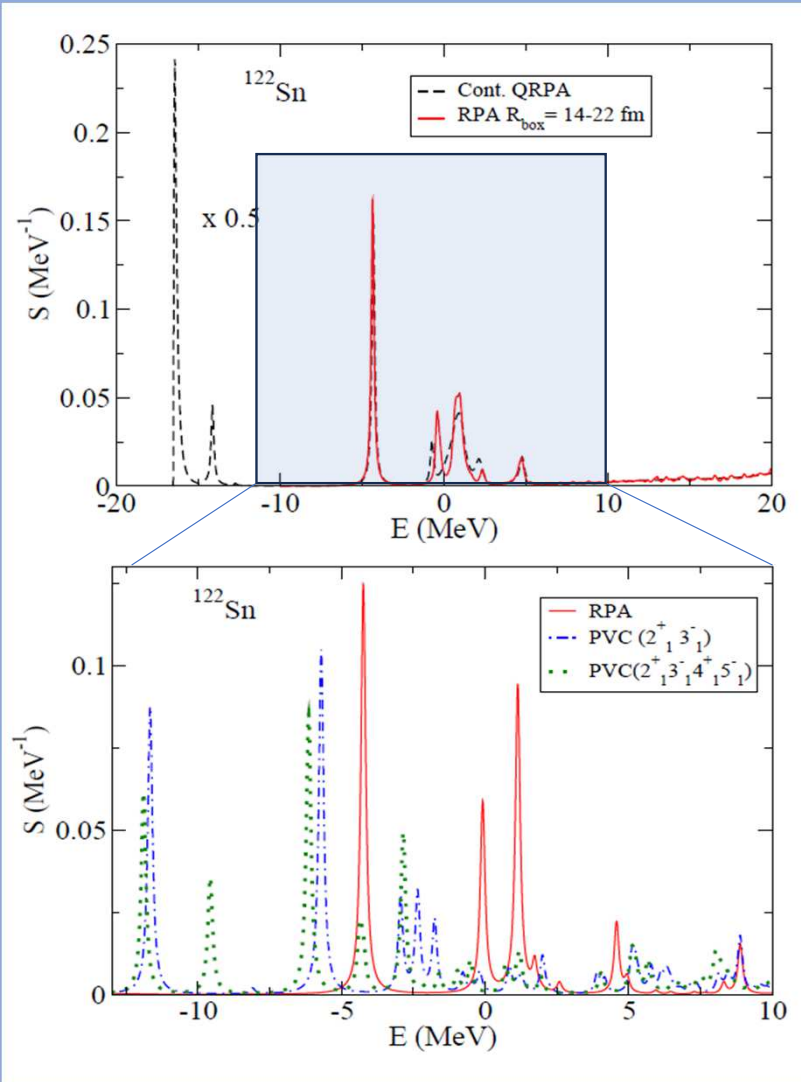
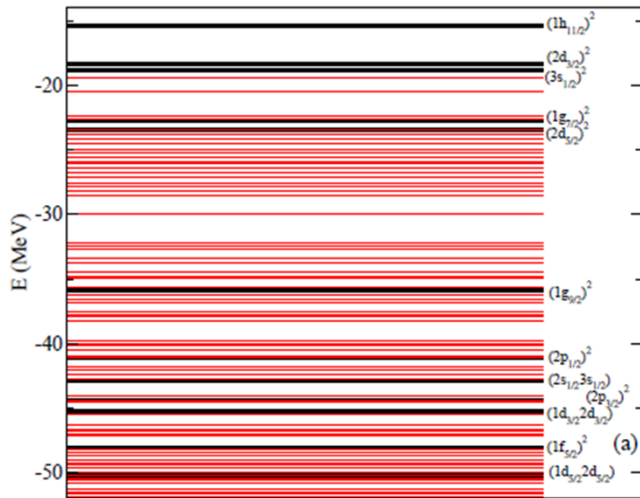
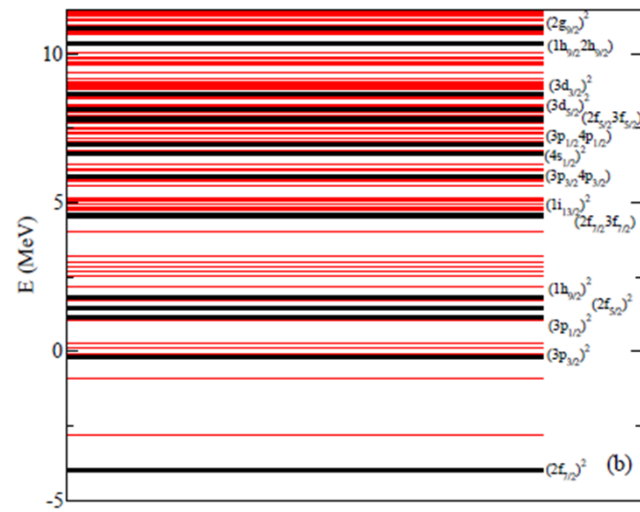


Figure 1. (a) The energies of the hh' -pairs in ^{132}Sn up to -50 MeV are shown by black thick lines. These states are embedded among the $hh' \lambda$ states (thin red lines), arising from the coupling to the lowest $2^+_1, 3^-_1, 4^+_1, 5^-_1$ vibrations. (b) The same, for the pp' -pairs with energies up to 11 MeV embedded among $pp' \lambda$ states, calculated in a box of radius $R_{box} = 14$ fm.

EXTENDED pp-RPA RESULTS

Application to médium and heavy nuclei: much more s-p levels

120Sn + 2n



CONCLUSIONS

We have computed the 2n-transfer strength to populate 0+ states in the continuum of ^{14}C and made the first steps to compute the absolute cross section of the reaction $^{12}\text{C}(^{18}\text{O}, ^{16}\text{O})^{14}\text{C}$. The theoretical model is based on particle-particle RPA extended to include many-body effects of the coupling to collective quadrupole vibrations, in keeping with previous calculations of weakly-bound systems.

The aim is to compare our results with the bump and the associated angular distribution revealed in the excitation spectrum and attributed to the Giant Pairing Vibration.

In general it is found that many body effects significantly modify the energy position, line shape and associated strength of the GPV

CONCLUSIONS

We have computed the 2n-transfer strength to populate 0+ states in the continuum of ^{14}C and made the first steps to compute the absolute cross section of the reaction $^{12}\text{C}(^{18}\text{O}, ^{16}\text{O})^{14}\text{C}$. The theoretical model is based on particle-particle RPA extended to include many-body effects of the coupling to collective quadrupole vibrations, in keeping with previous calculations of weakly-bound systems.

The aim is to compare our results with the bump and the associated angular distribution revealed in the excitation spectrum and attributed to the Giant Pairing Vibration.

In general it is found that many body effects significantly modify the energy position, line shape and associated strength of the GPV (High-Lying Pairing Resonances)

HIGH-LYING PAIRING RESONANCES★

R.A. BROGLIA

*The Niels Bohr Institute, University of Copenhagen, DK-2100 Copenhagen Ø, Denmark¹
State University of New York, Department of Physics, Stony Brook, New York 11794, USA*

and

D.R. BES²

NORDITA, DK-2100 Copenhagen Ø, Denmark

Additional material

Pairing Rotations (Superfluid systems) and PVC

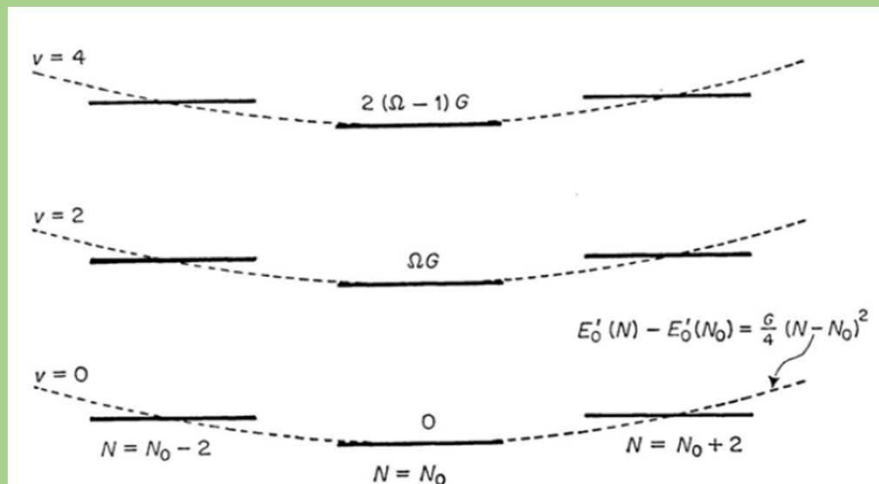


Figure 11.2. Exact energy spectrum for the Hamiltonian $H' = H - \lambda(N - N_0)$.

BCS theory

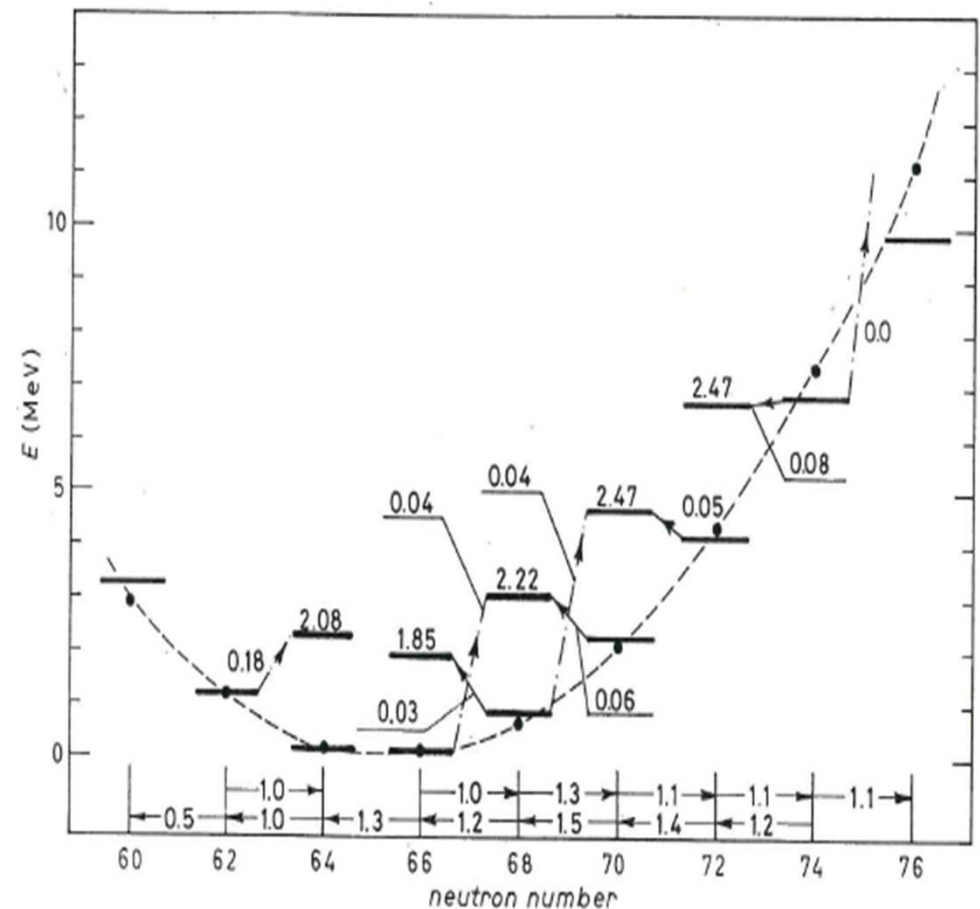
$$|> = \prod_{v>0} (u_v + v_v a_v^\dagger a_{-v}^\dagger) |0>$$

$$u_v^2 = \frac{1}{2} \left\{ 1 + \frac{\epsilon_v - \lambda}{[(\epsilon_v - \lambda)^2 + \Delta^2]^{\frac{1}{2}}} \right\}$$

$$v_v^2 = \frac{1}{2} \left\{ 1 - \frac{\epsilon_v - \lambda}{[(\epsilon_v - \lambda)^2 + \Delta^2]^{\frac{1}{2}}} \right\}$$

$$\frac{G}{2} \sum_{v>0} \frac{1}{[(\epsilon_v - \lambda)^2 + \Delta^2]^{\frac{1}{2}}} = 1$$

$$\sum_{v>0} \left\{ 1 - \frac{\epsilon_v - \lambda}{[(\epsilon_v - \lambda)^2 + \Delta^2]^{\frac{1}{2}}} \right\} = N$$

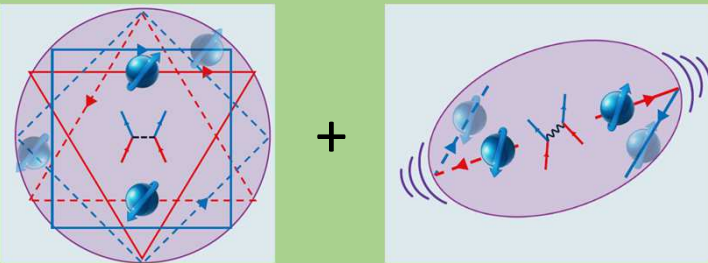


Pairing Rotations and PVC

$$\tilde{\Delta}_{a(n)} = -Z_{a(n)} \sum_{b,m} V_{\text{eff}}[a(n)b(m)] N_{b(m)} \frac{\tilde{\Delta}_{b(m)}}{2\tilde{E}_{b(m)}}.$$

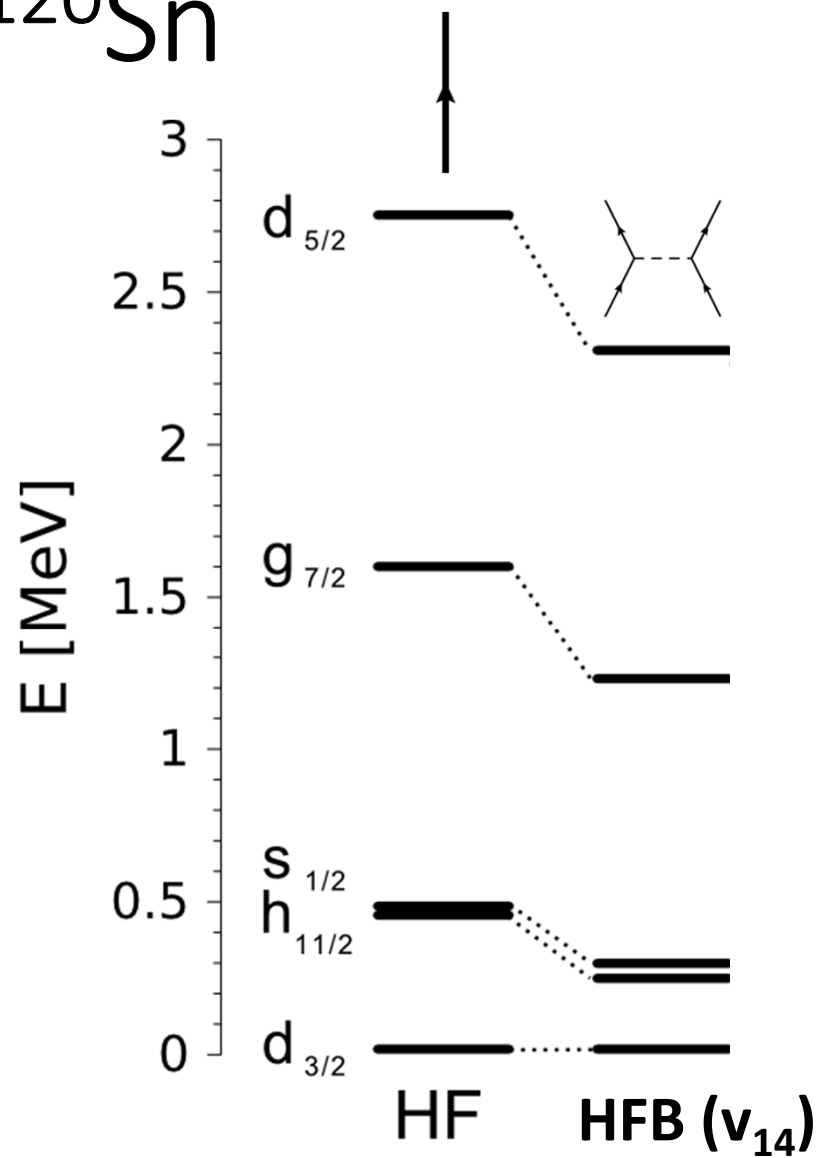
$$\tilde{E}_{a(n)} = \sqrt{(\tilde{\epsilon}_{a(n)} - \epsilon_F)^2 + \tilde{\Delta}_{a(n)}^2}$$

$V_{\text{eff}} =$



$$\Delta = \frac{G}{2} \sum_{\nu > 0} \frac{\Delta}{[(\epsilon_{\nu} - \lambda)^2 + \Delta^2]^{\frac{1}{2}}}$$

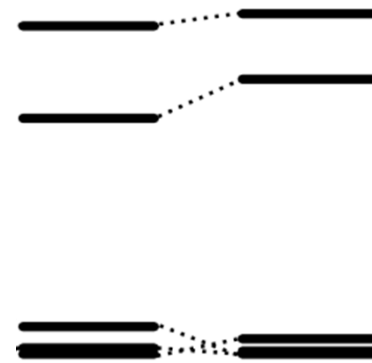
^{120}Sn



excitation spectrum

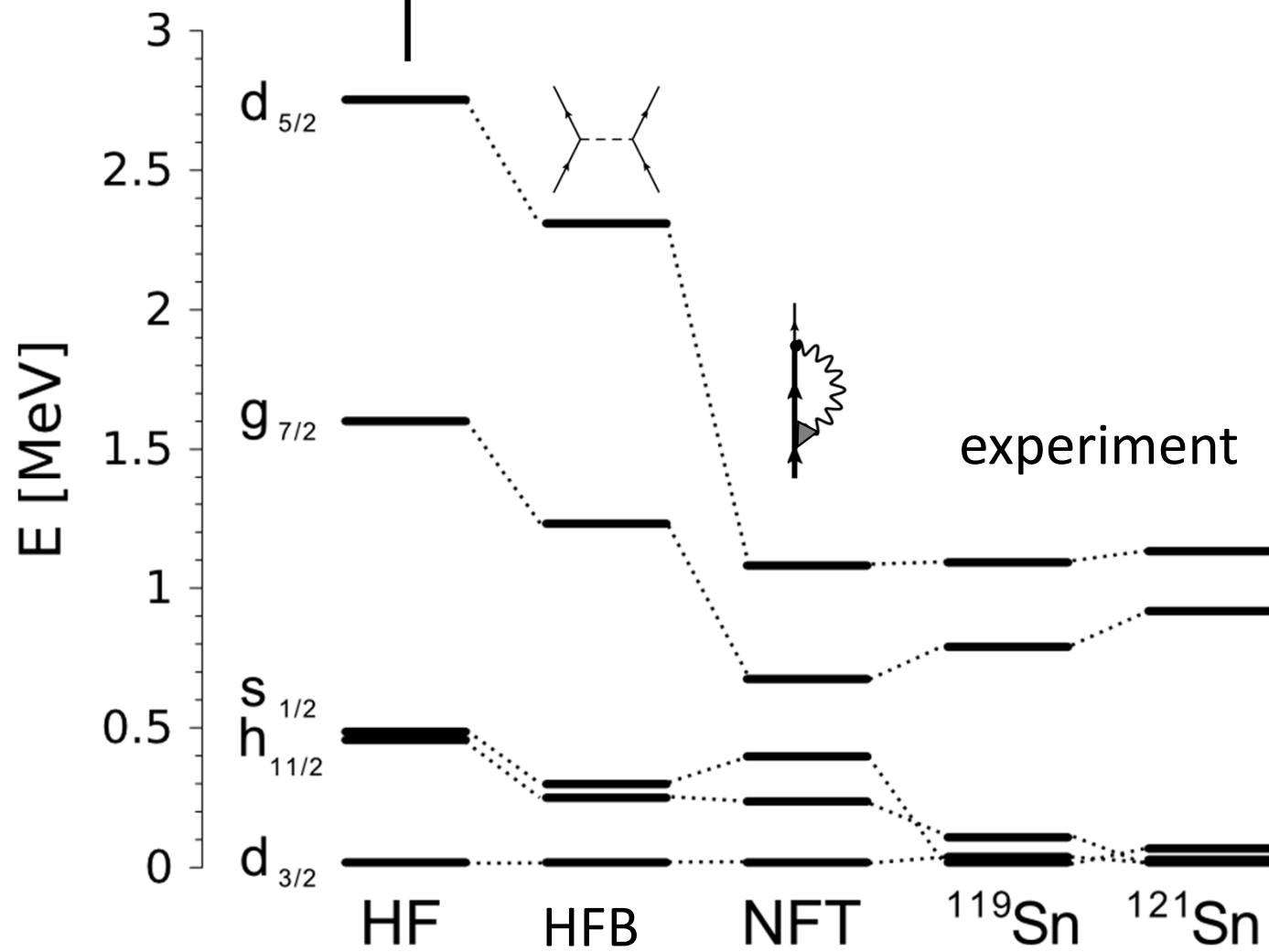
experiment

^{119}Sn ^{121}Sn

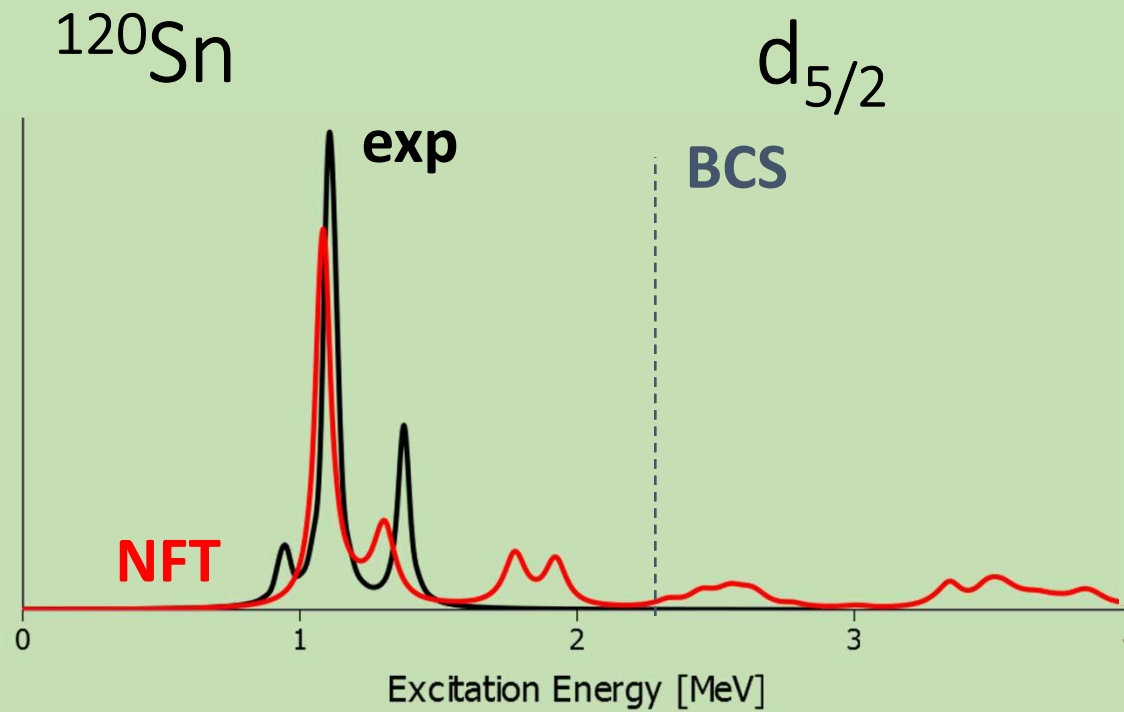


^{120}Sn

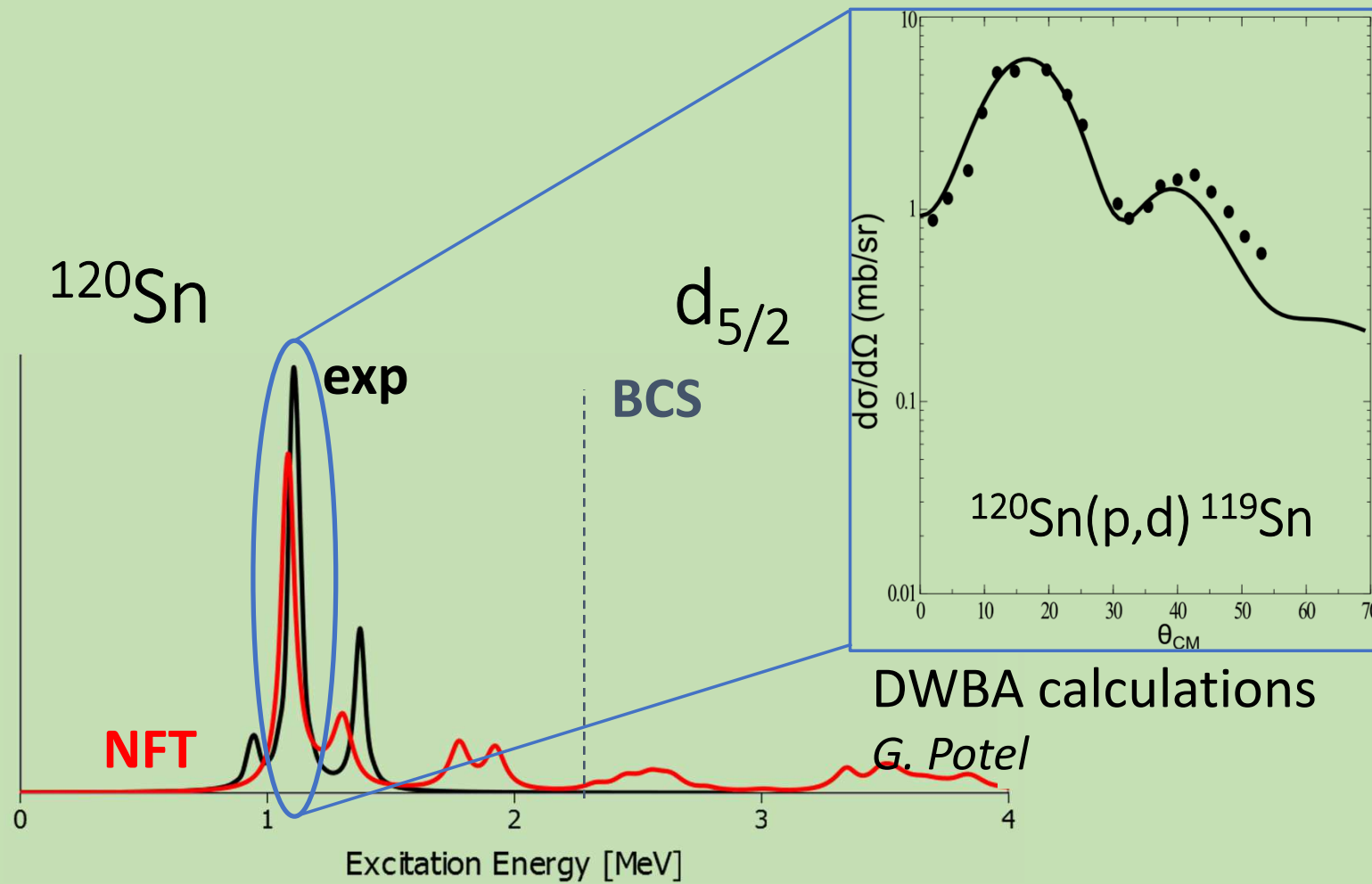
excitation spectrum



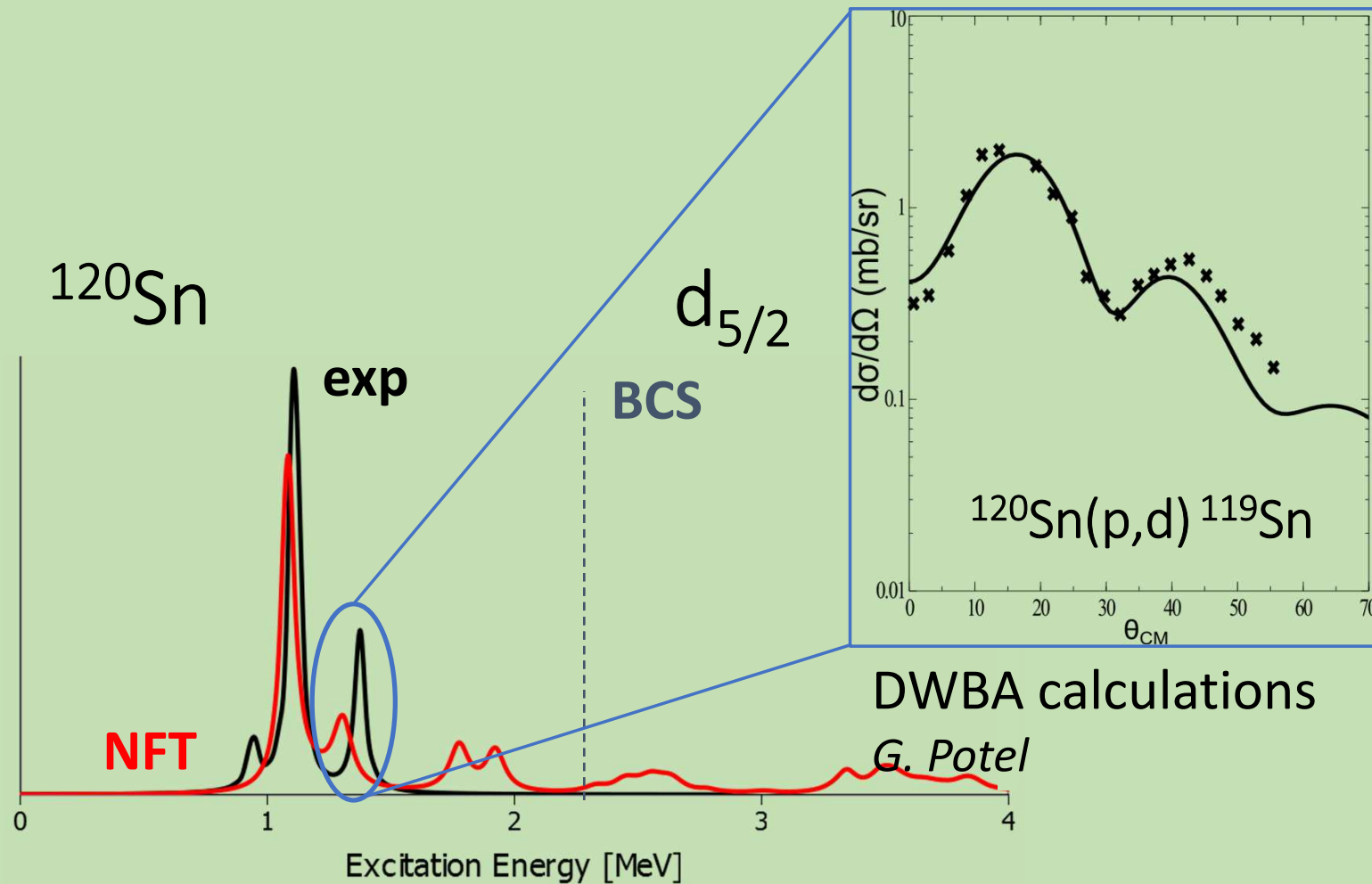
Quasiparticle strength can now be compared with experiment

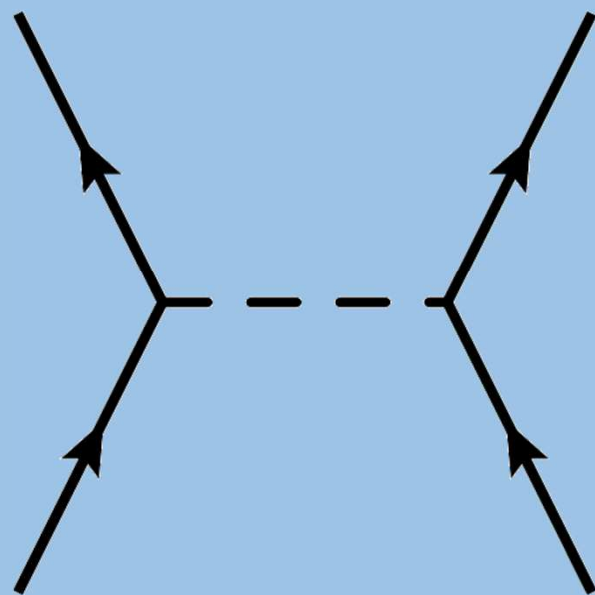


Quasiparticle strength can now be compared with experiment

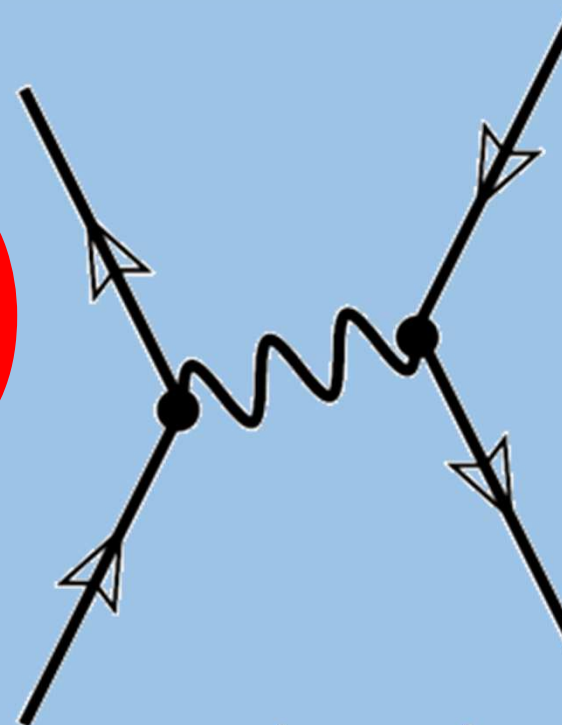
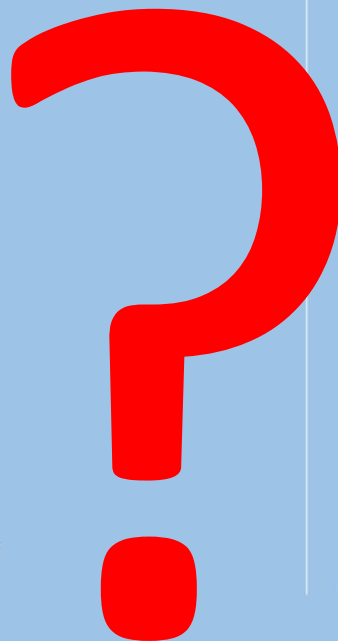


Quasiparticle strength can now be compared with experiment





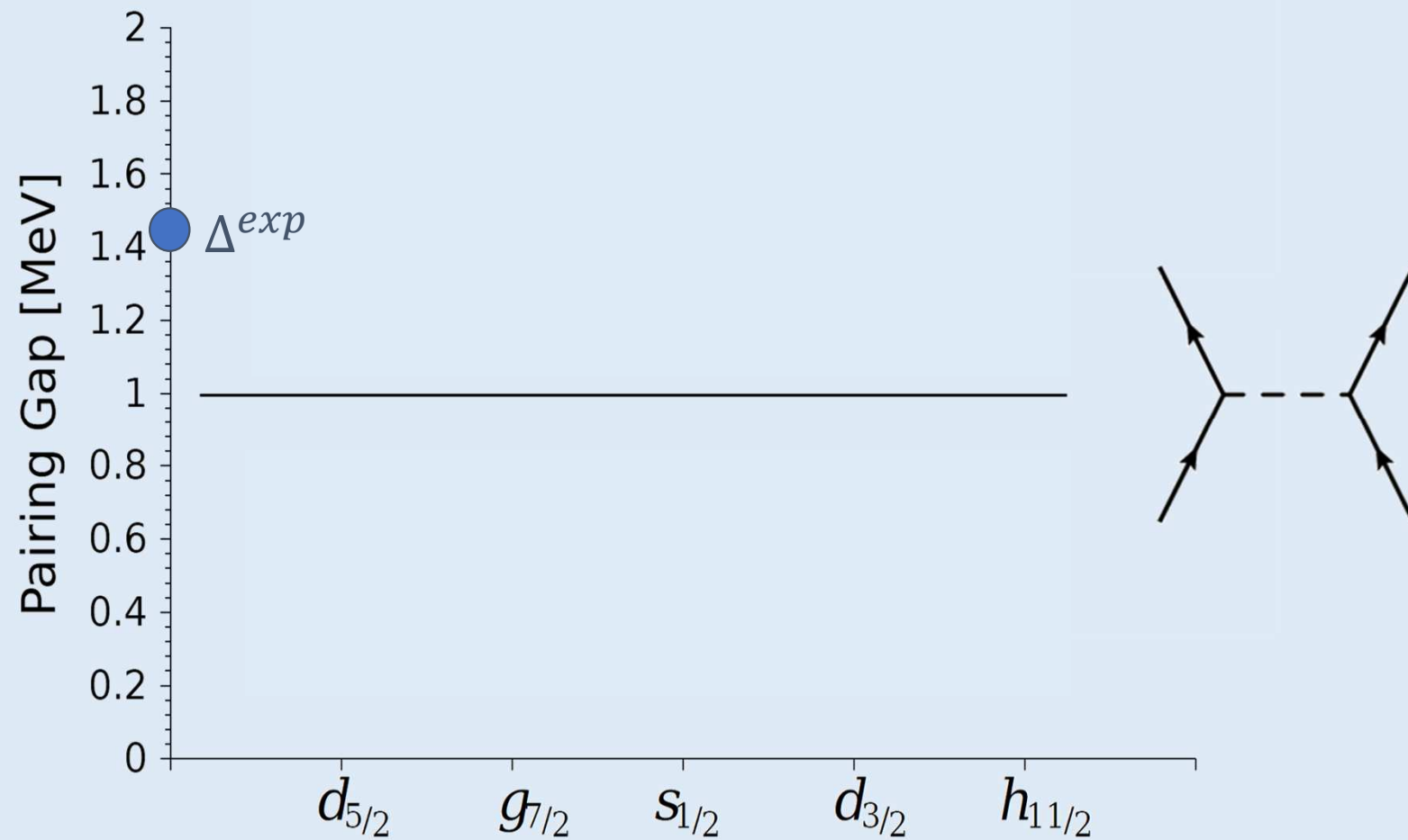
Bare
Nucleon-Nucleon
Interaction



Induced
Interaction

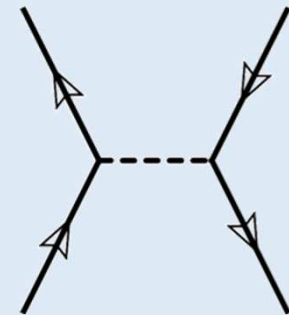
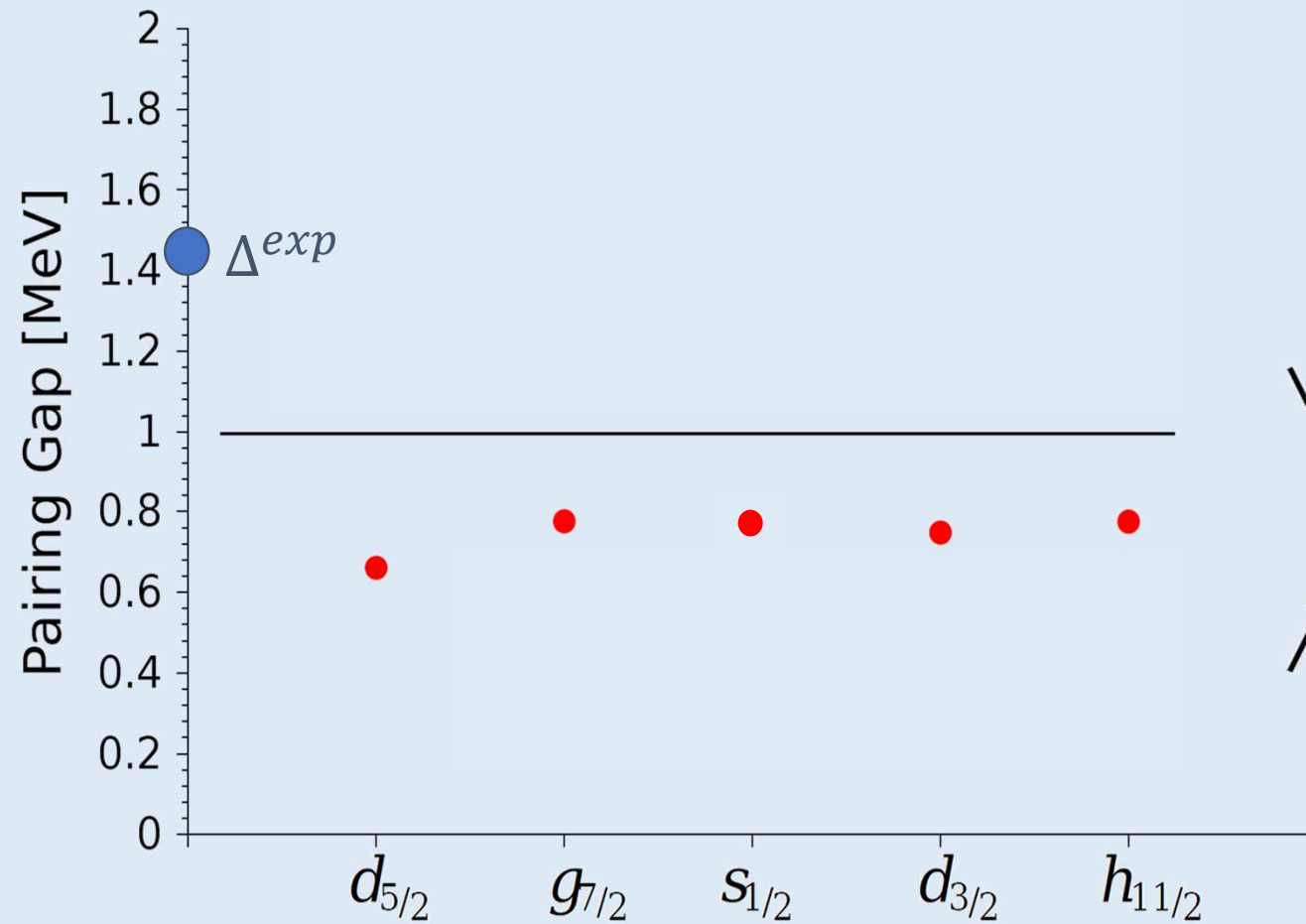
— Bare - BCS

We start from a **bare**
 v_{14} pairing interaction...



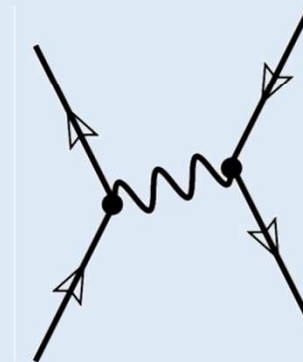
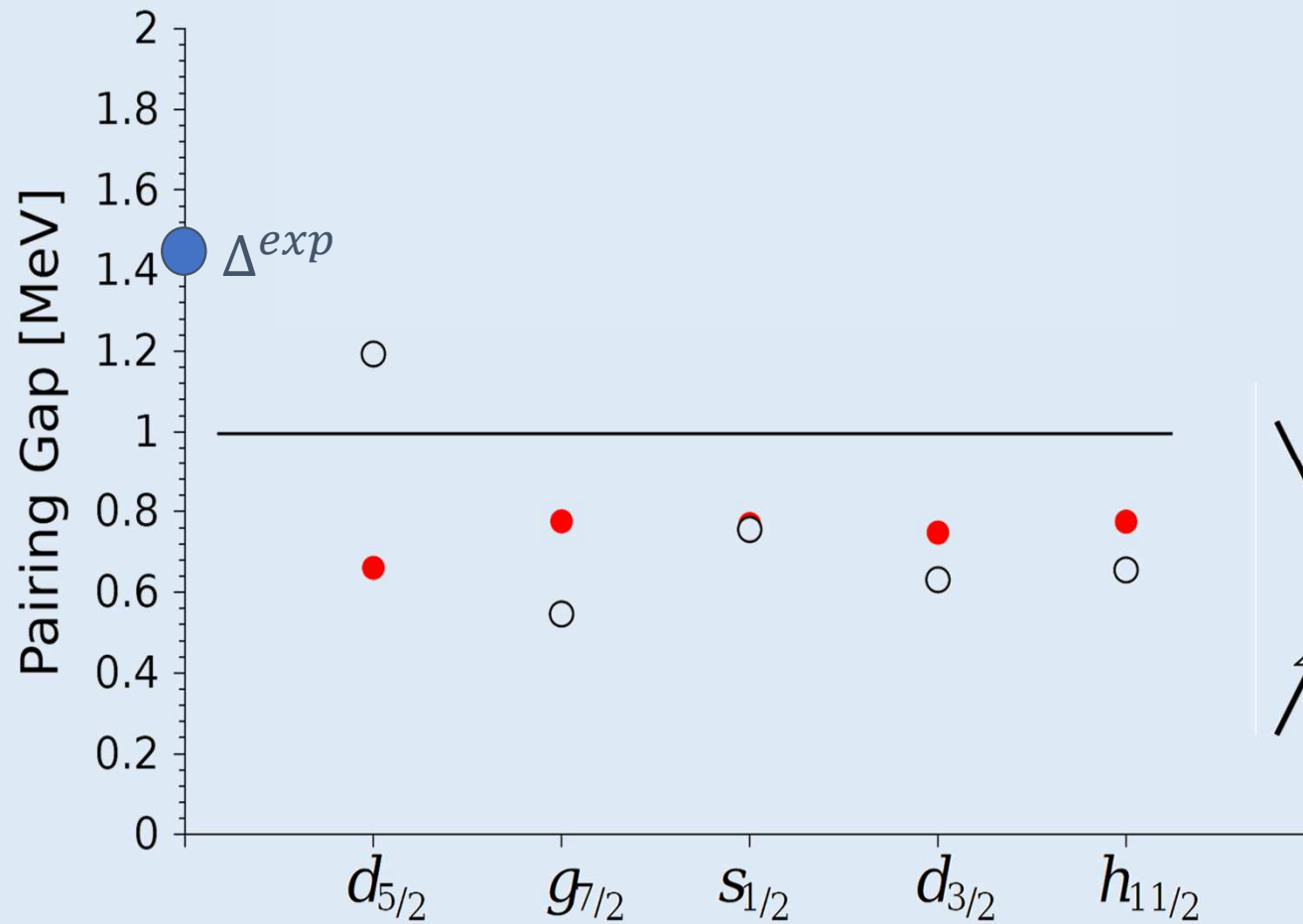
- Bare - BCS
- Bare – renorm.

...that get **renormalized**
by Self Energy processes...



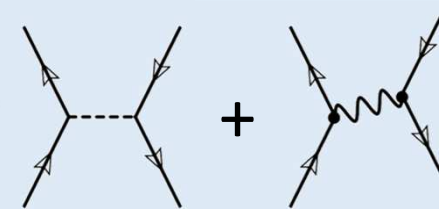
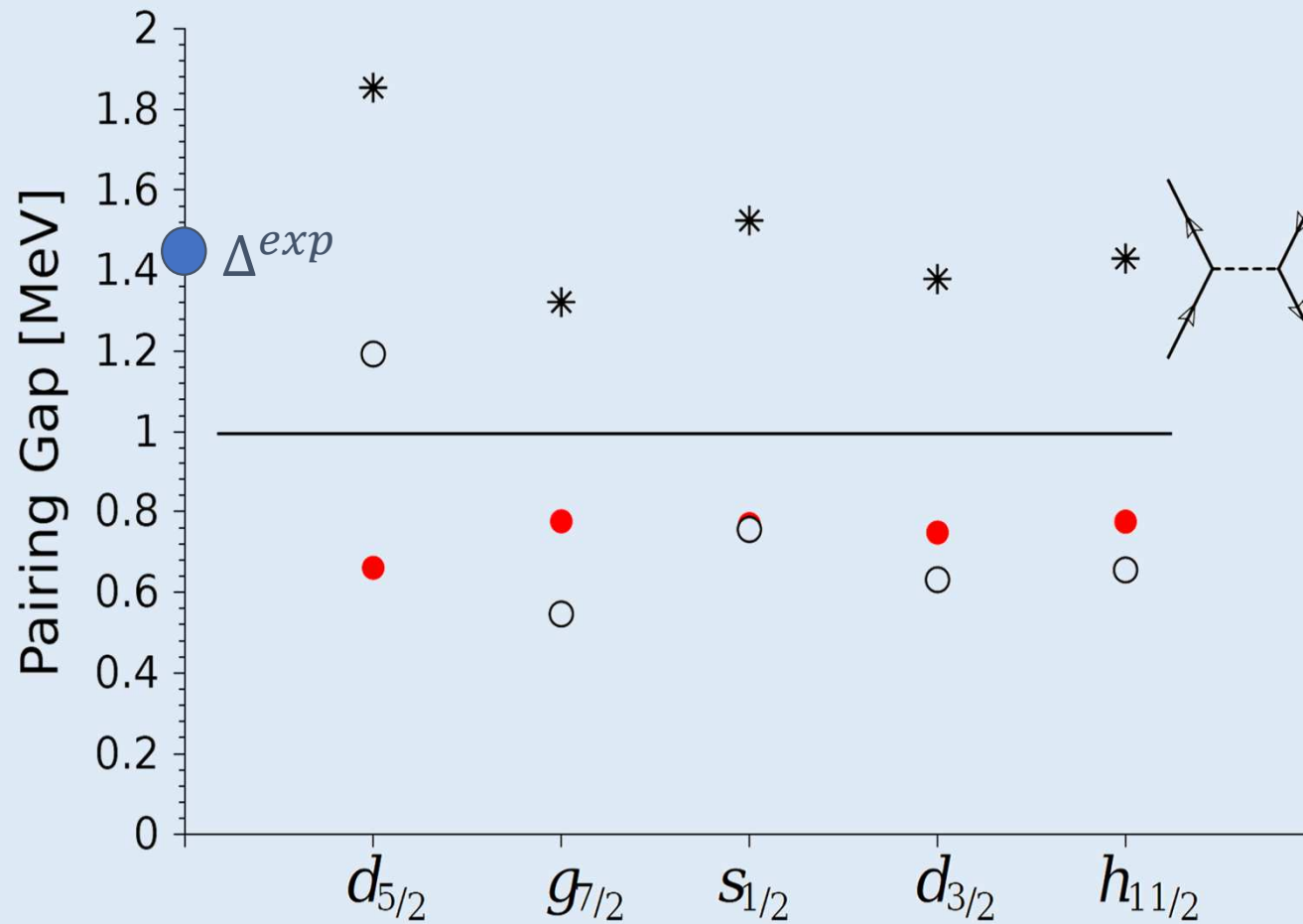
- Bare - BCS
- Bare – renorm.
- Induced

...but a novel contribution arises:
induced interaction (correlations)...



...getting the total value close to the experiment!

- Bare - BCS
- Bare – renorm.
- Induced
- * Total = Bare + Induced



We have a then consistent picture that explains

Independent particle **excitation energies**

$$\tilde{E}_j$$

Spectroscopic Factors

Pairing Gap

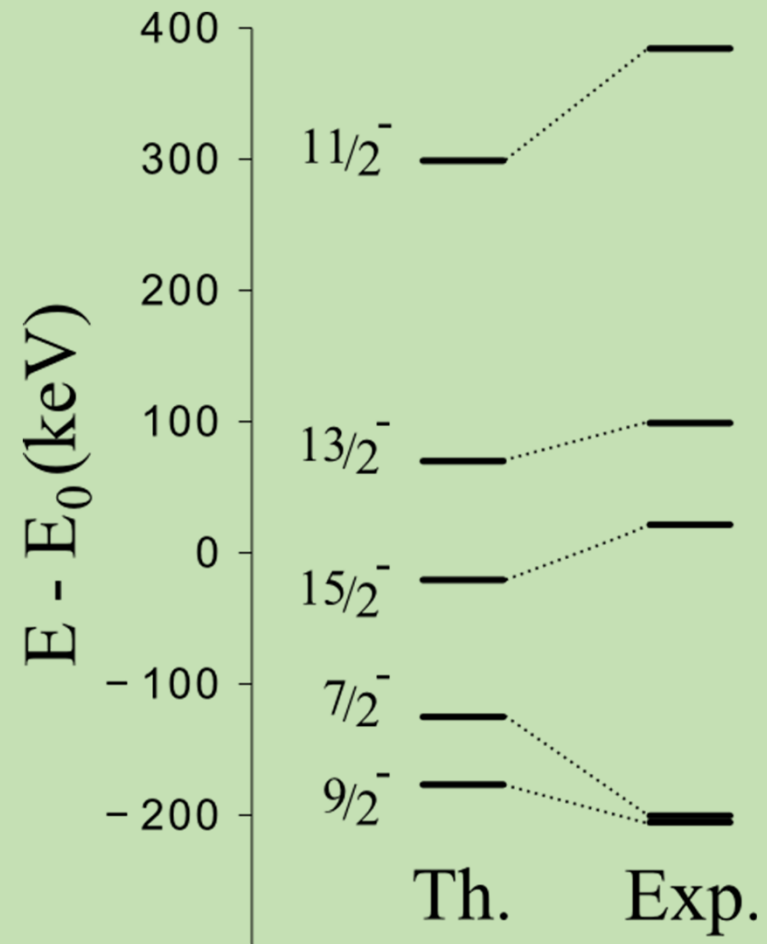
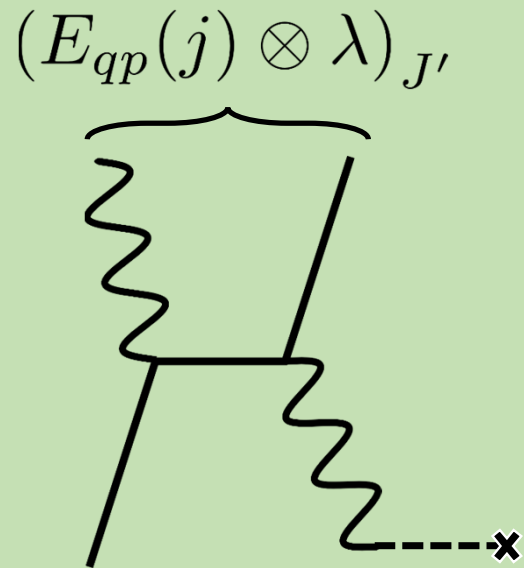
}

$$\tilde{u}_j \tilde{v}_j$$

These are inputs for...

Multiplet

Elastic excitation of a
quasiparticle state coupled
to the core vibrations



Considering PVC we thus have:

- ☑ Increased Hartree-Fock excitation spectrum density.
- ☑ Introduced fragmentation of quasiparticle strength and compared with experimental 1 particle transfer cross sections.
- ☑ Increased the pairing correlations and pairing gap energy of realistic bare interaction closer to the experimental value, and reproduced the 2-particle transfer cross sections.
- ☑ Opened other reaction channels, like coupling of core excitations and quasiparticles.

CONCLUSIONS (SUPERFLUIDITY part)

Basic Tool: The pp-RPA equations

$$|A+2, \tau\rangle = \left(\sum_{m < n} X_{mn}^{\tau} a_m^{\dagger} a_n^{\dagger} - \sum_{i < j} Y_{ij}^{\tau} a_j^{\dagger} a_i^{\dagger} \right) |A, 0\rangle$$

Pairing Interaction \rightarrow Coherent mix
 \rightarrow Collectivity \rightarrow Cooper pair like

$$\begin{pmatrix} A & B \\ B^{\dagger} & C \end{pmatrix} \begin{pmatrix} R_p^{\tau, \lambda} \\ R_h^{\tau, \lambda} \end{pmatrix} = \begin{pmatrix} 1 & 0 \\ 0 & -1 \end{pmatrix} \begin{pmatrix} R_p^{\tau, \lambda} \\ R_h^{\tau, \lambda} \end{pmatrix} \cdot \hbar \Omega_{\tau, \lambda},$$

$$A_{mnm'n'} = \delta_{mm'} \delta_{nn'} (\epsilon_m + \epsilon_n) + \bar{v}_{mnm'n'},$$

$$C_{ijij'} = -\delta_{ii'} \delta_{jj'} (\epsilon_i + \epsilon_j) + \bar{v}_{ijij'},$$

$$B_{mnij} = -\bar{v}_{mnij},$$

$$(R_p^{\tau})_{mn} = X_{mn}^{\tau}, \quad (R_p^{\lambda})_{mn} = Y_{mn}^{\lambda},$$

$$(R_h^{\tau})_{ij} = Y_{ij}^{\tau}, \quad (R_h^{\lambda})_{ij} = X_{ij}^{\lambda}.$$

From The Nuclear Many Body Problem by Ring and Schuck

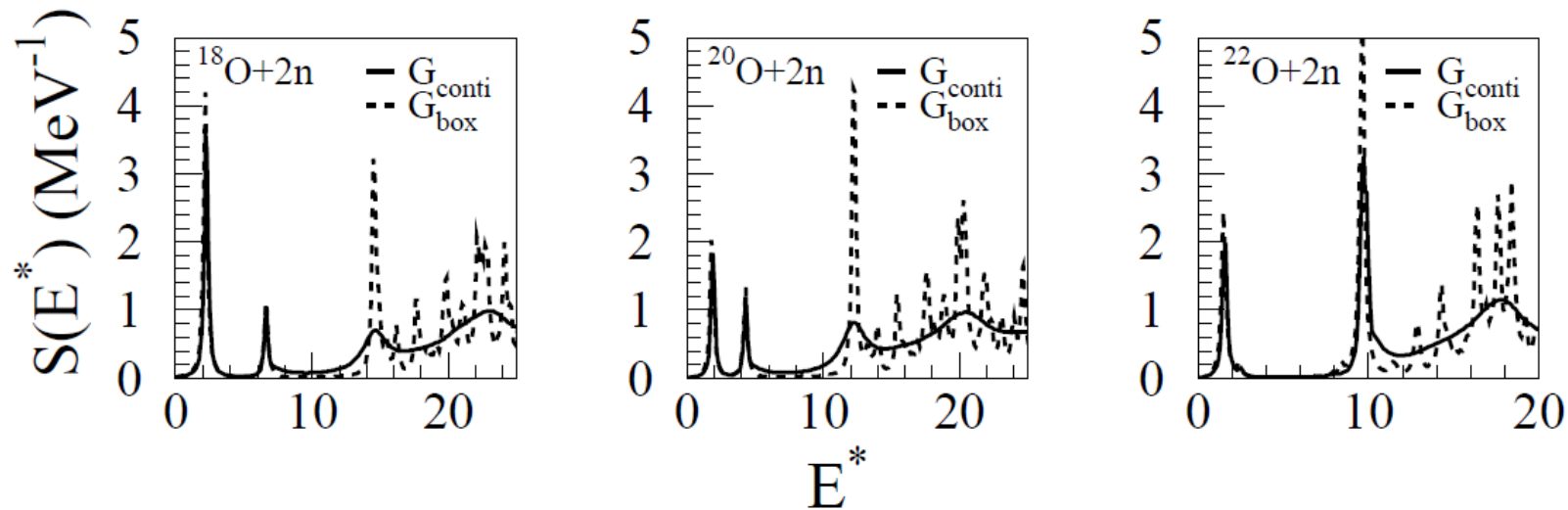
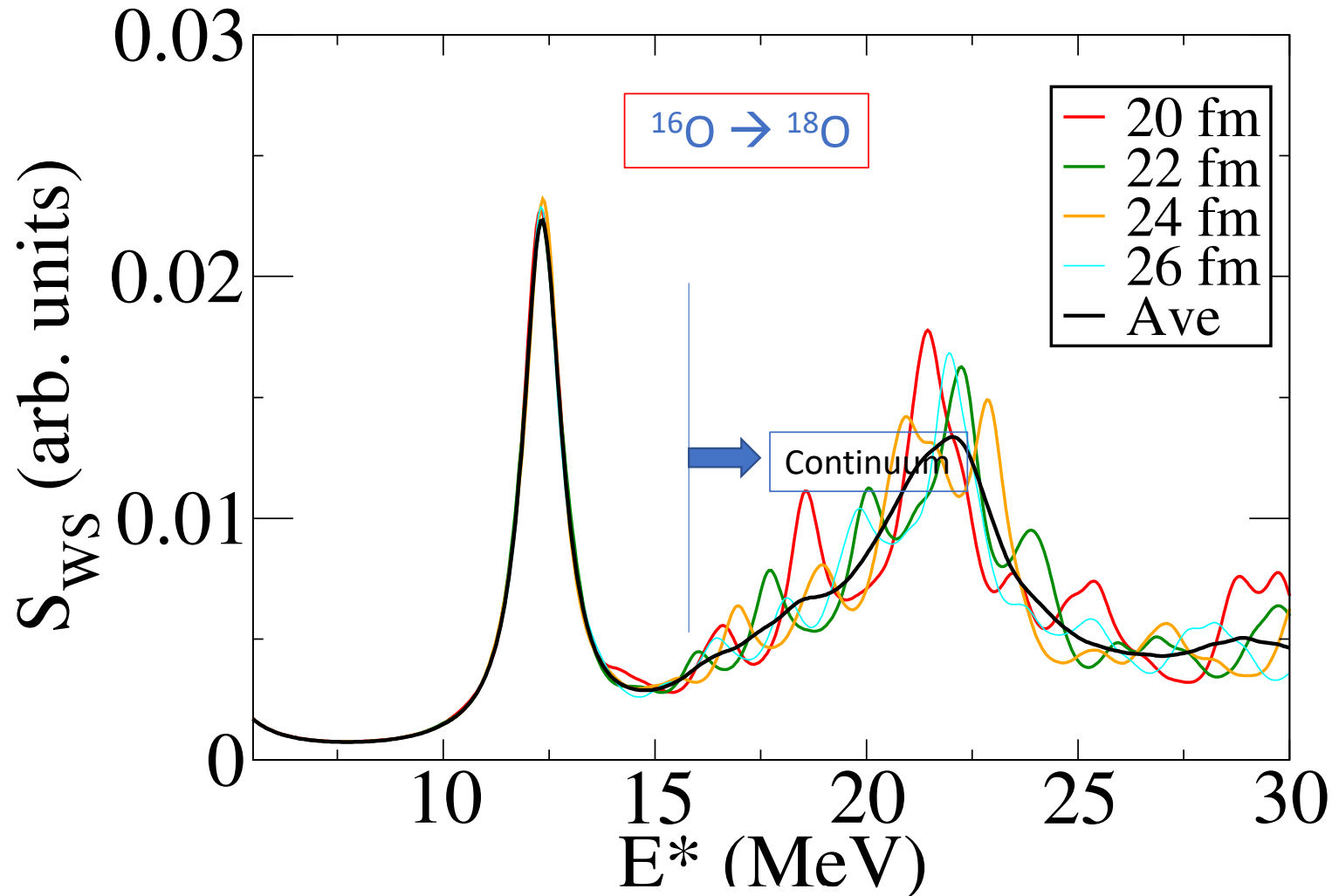


FIG. 1. The QRPA response for the two-neutron transfer on $^{18,20,22}\text{O}$. The exact continuum calculations are in solid lines whereas the calculations with box boundary conditions are in dashed lines. The results are displayed as functions of E^* , the excitation energy with respect to the parent nucleus ground state. $R_{\text{box}} = 22.5$ fm



pp-RPA with the Gogny(pairing) force.

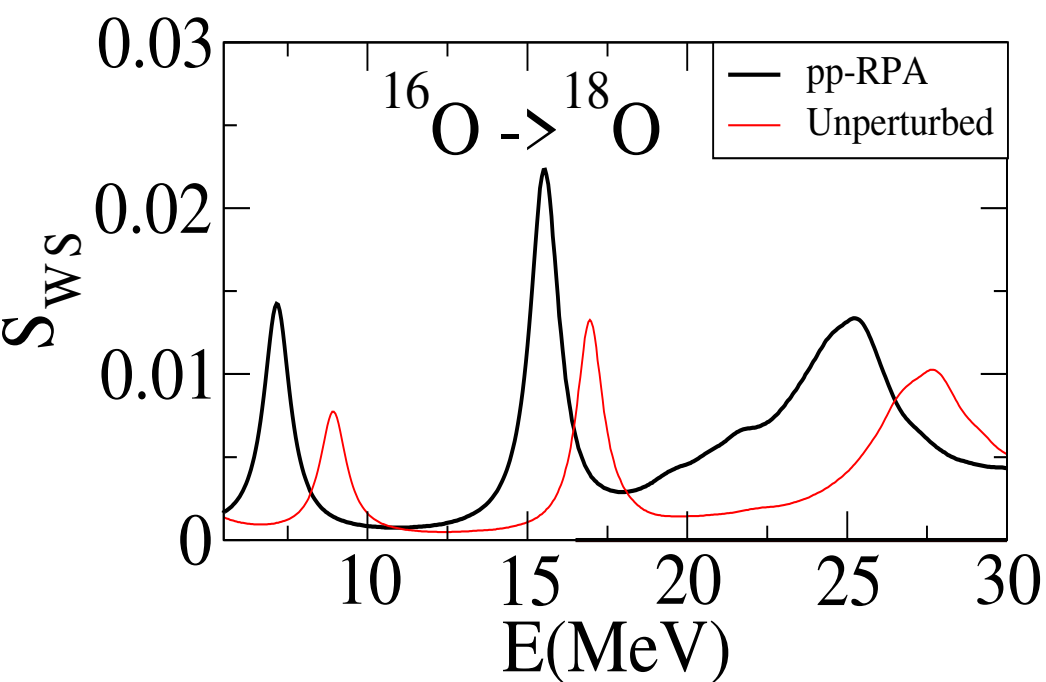
Averaging details:
1.Box sampling
2.Small Gaussian convolution.

$$S_{WS}^i = \sum_{nn'lj} [X_{nn'lj}^i + Y_{nn'lj}^i] \int dr G(r) \psi_{nlj}(r) \psi_{n'lj}(r).$$

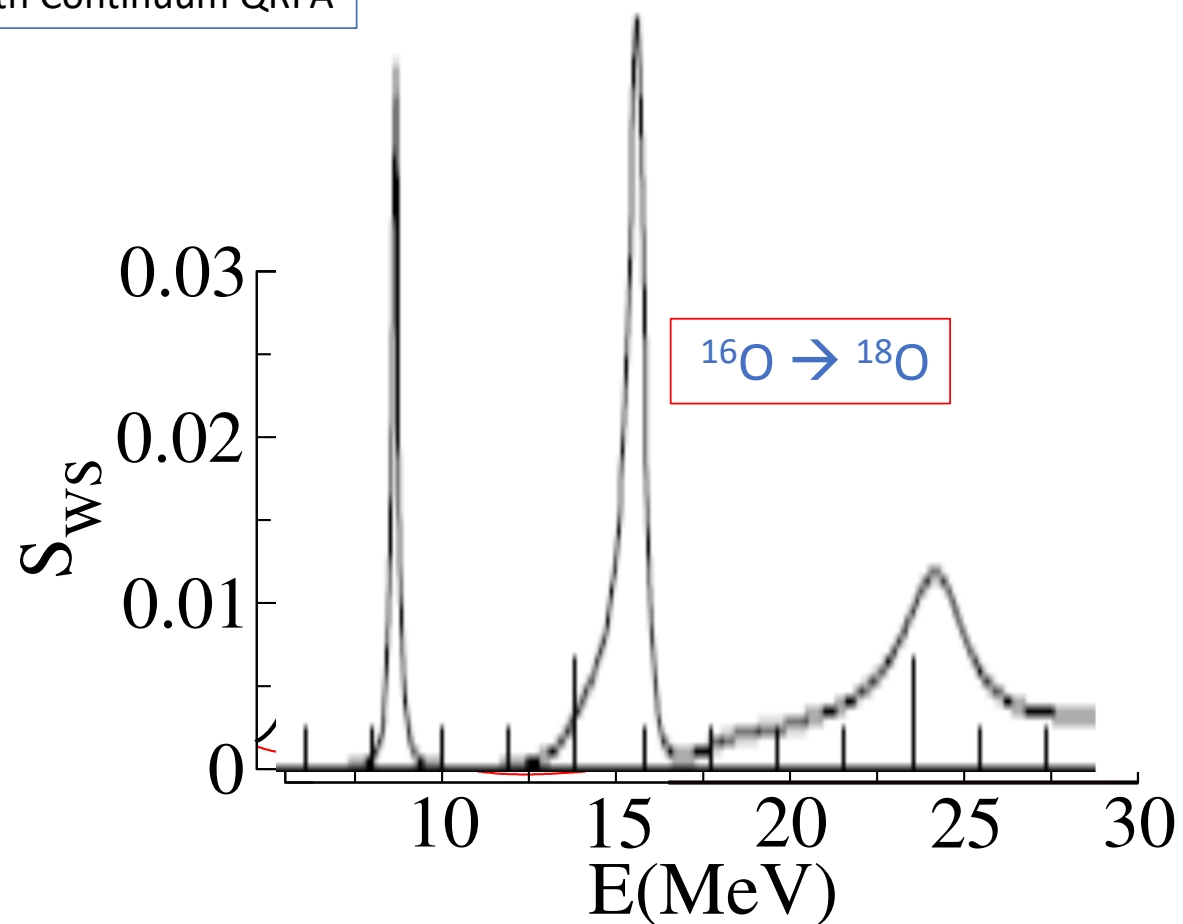
$$G(r) \equiv (1 + \exp[(r - R_S)/a_S])$$

ppRPA using BOX boundary conditions

Comparison with Continuum QRPA

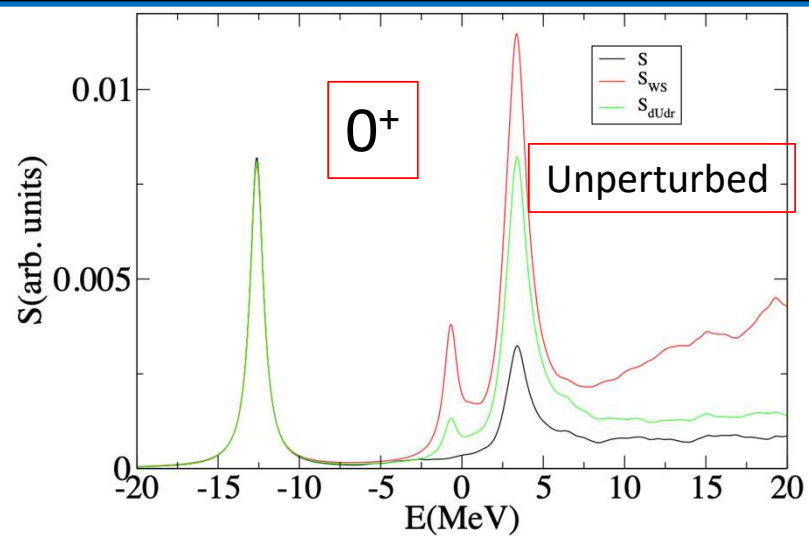


Using BOX boundary conditions. This work.



Continuum QRPA by Matsuo using Sly4 mean field plus DDDI pairing force (private communication)

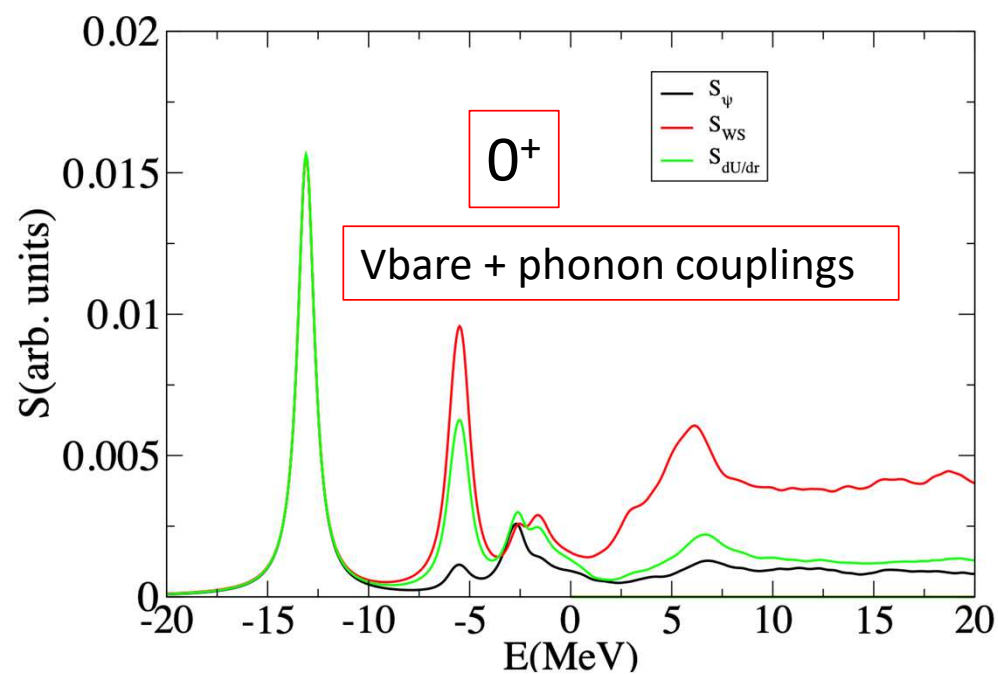
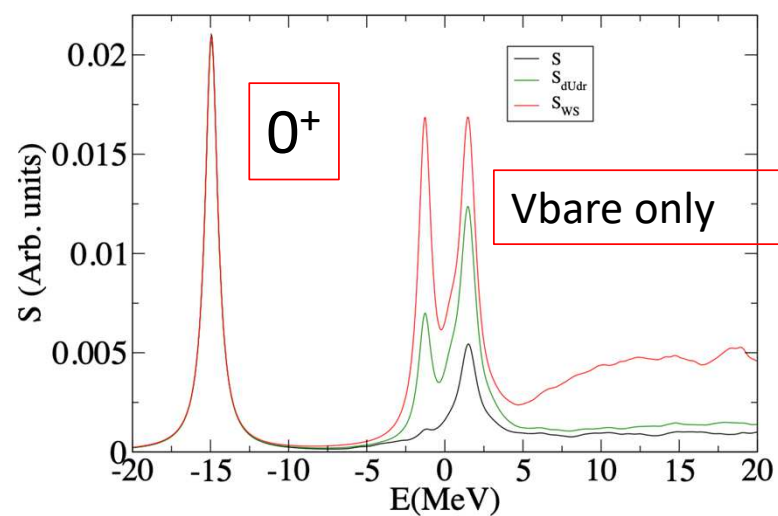
EXTENDED pp-RPA RESULTS



14C

Form factors:

- volume
- density
- surface



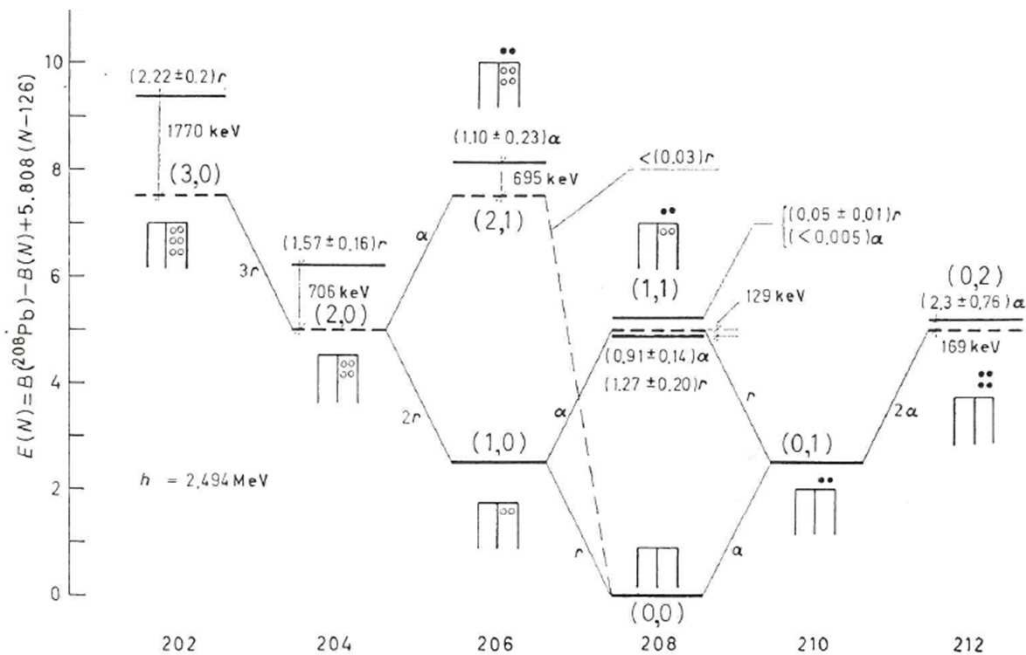


Fig. 6. – The many-phonon pairing spectrum around ^{208}Pb . The energies predicted by the pairing vibrational model are displayed as dashed horizontal lines, while the experimental values are drawn as continuous lines. The harmonic quantum numbers (n_r, n_a) are indicated for each level. A schematic representation of the many-particle many-hole structure of the state is also given. The transitions predicted by the model are indicated in units of r and a (cf. (3.11) and (3.12)). The corresponding experimental numbers are also given together with their errors, above each level. The dashed line between the states $(0,0)$ and $(2,1)$ indicates that the $^{208}\text{Pb}(p, t)^{208}\text{Pb}$ reaction to the three-phonon state in ^{206}Pb was carried out and an upper limit of $0.03r$ for the corresponding cross-section was determined. The (t, p) data are from ref. [27] and the (p, t) data from ref. [28].

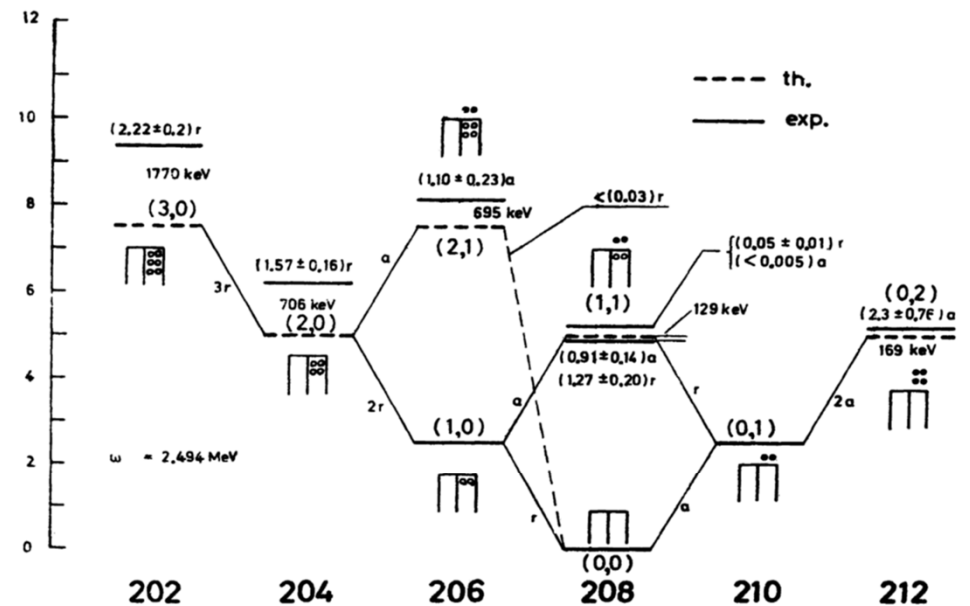


Fig. 1. The many-phonon neutron pairing spectrum around ^{208}Pb (Ref. 17)). The energies predicted by the pairing vibrational model are displayed as dotted horizontal lines while the experimental values are drawn as continuous lines. The harmonic quantum numbers (n_r, n_a) are indicated for each level. A schematic representation of the many-particle many-hole structure of the state is also given. The transitions predicted by the model are indicated in units of r and a . The corresponding experimental numbers are also given together with their errors above each level. The dotted line between the states $(0,0)$ and $(2,1)$ indicates that the $^{208}\text{Pb}(p, t)^{208}\text{Pb}$ reaction to the three-phonon states in ^{206}Pb was carried out and an upper limit of $0.03r$ for corresponding cross section was determined.

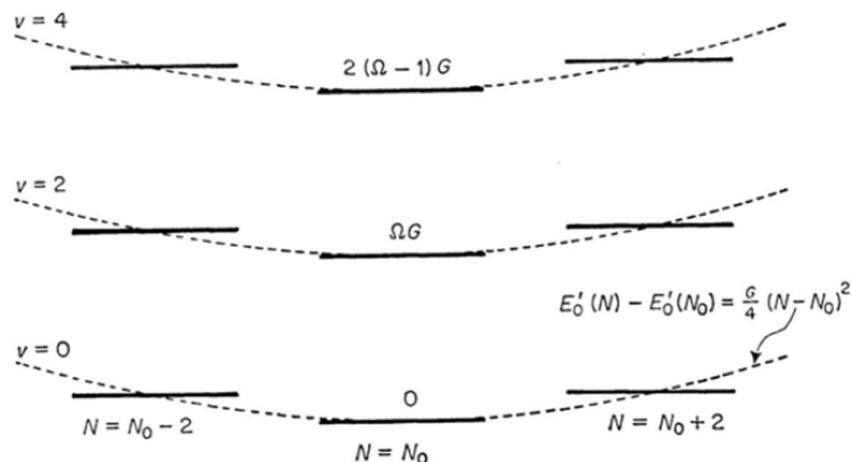


Figure 11.2. Exact energy spectrum for the Hamiltonian $H' = H - \lambda(N_0)n$.

BCS theory

$$|> = \prod_{\nu>0} (u_{\nu} + v_{\nu} a_{\nu}^{\dagger} a_{\nu}^{\dagger}) |0>$$

$$u_{\nu}^2 = \frac{1}{2} \left\{ 1 + \frac{\epsilon_{\nu} - \lambda}{[(\epsilon_{\nu} - \lambda)^2 + \Delta^2]^{\frac{1}{2}}} \right\} \quad \frac{G}{2} \sum_{\nu>0} \frac{1}{[(\epsilon_{\nu} - \lambda)^2 + \Delta^2]^{\frac{1}{2}}} = 1$$

$$v_{\nu}^2 = \frac{1}{2} \left\{ 1 - \frac{\epsilon_{\nu} - \lambda}{[(\epsilon_{\nu} - \lambda)^2 + \Delta^2]^{\frac{1}{2}}} \right\} \quad \sum_{\nu>0} \left\{ 1 - \frac{\epsilon_{\nu} - \lambda}{[(\epsilon_{\nu} - \lambda)^2 + \Delta^2]^{\frac{1}{2}}} \right\} = N$$

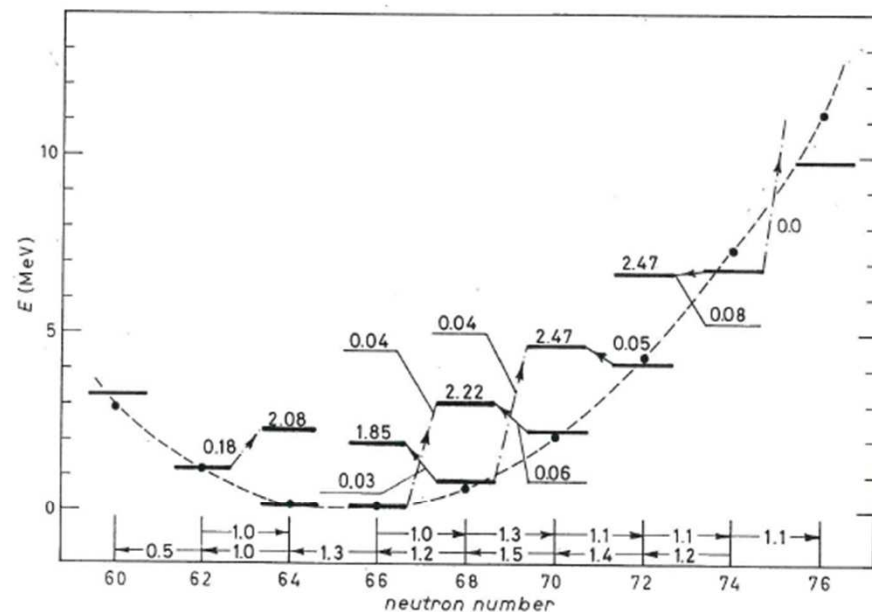


Fig. 3. - Experimental energies of the $J^{\pi} = 0^{+}$ states of the even Sn isotopes. The heavy drawn lines represent the values of the expression $E = -B(\text{Sn}) + E_{\text{exo}} + 8.50N + 45.3$ (MeV), where the binding energies $B(A)$ (in MeV) are taken from ref. [13]. The dashed line represents the parabola $0.10(A - 65.4)^2$, which corresponds to a rotational energy parameter $\hbar^2/2\mathcal{I} = 0.040$ MeV. Also displayed is the excited pairing vibrational mode. In all cases where more than one $J^{\pi} = 0^{+}$ state has been excited below 3 MeV in two-neutron transfer processes, the energy $\sum_i \sigma(0_i) E(0_i^{+}) / \sum_i \sigma(0_i^{+})$ of the centroid is quoted, as well as the corresponding cross-section $\sum_i \sigma(0_i^{+})$. The quantity $\sigma(0_i^{+})$ is the relative cross-sections with respect to the ground-state cross-sections. The numbers along the abscissa are the ground-state (p, t) and (t, p) cross-sections normalized to the $^{118}\text{Sn} \leftrightarrow ^{118}\text{Sn}(\text{gs})$ cross-section. The (t, p) and (p, t) data utilized in constructing this figure were taken from ref. [14-16].

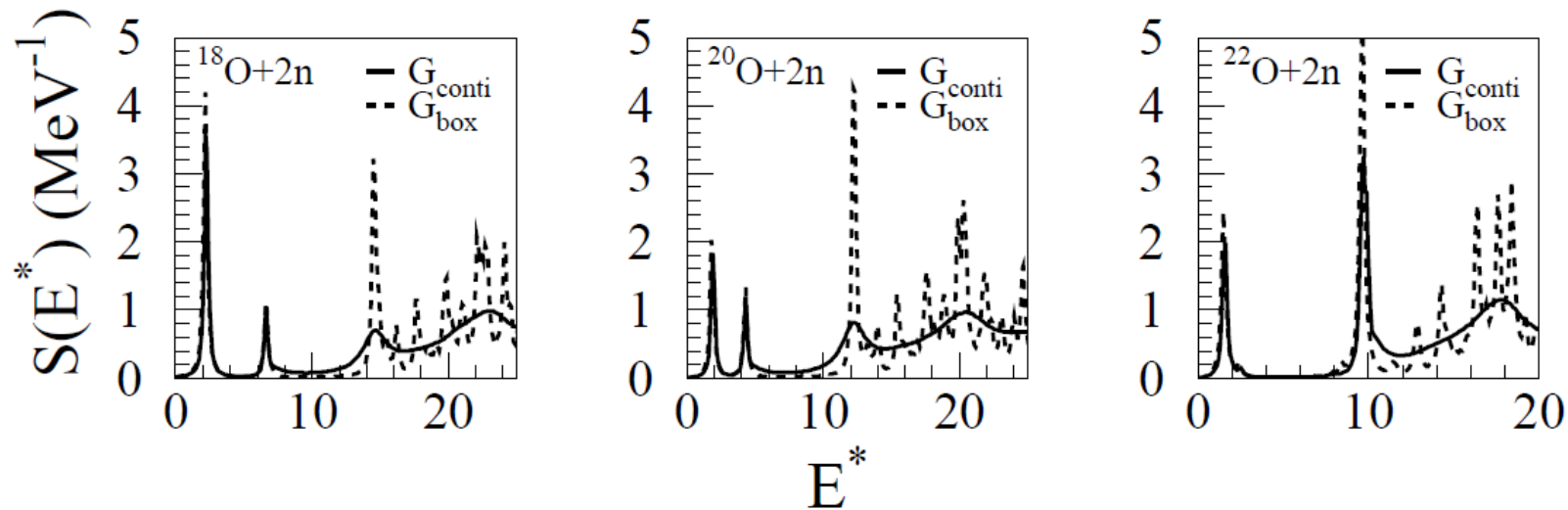
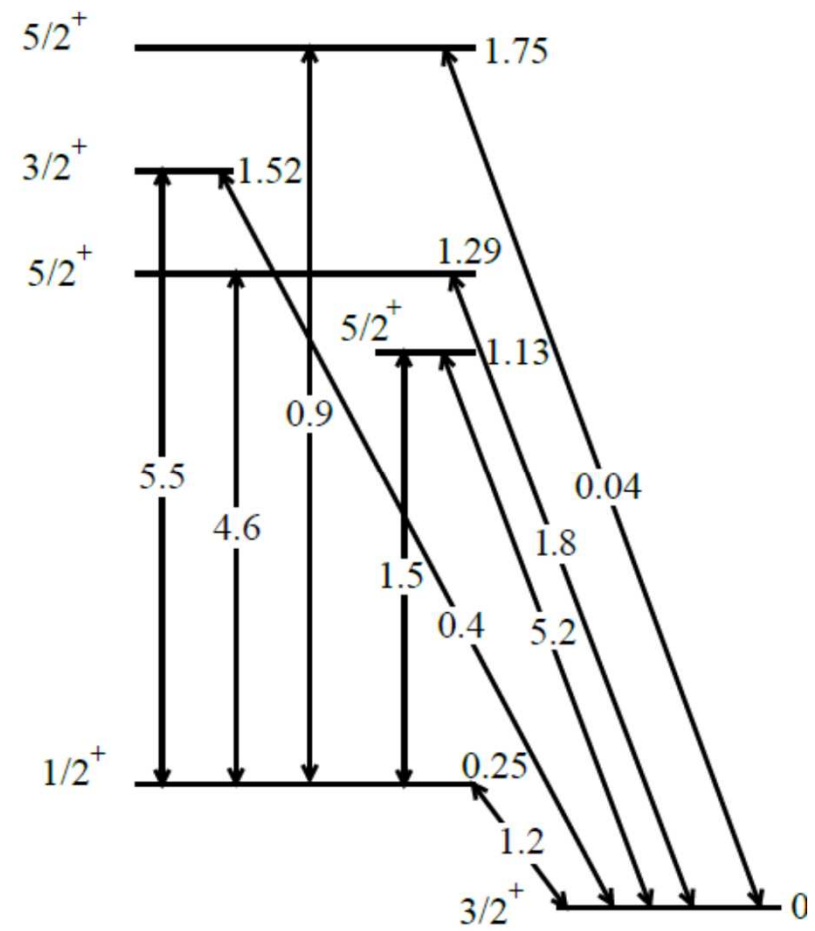
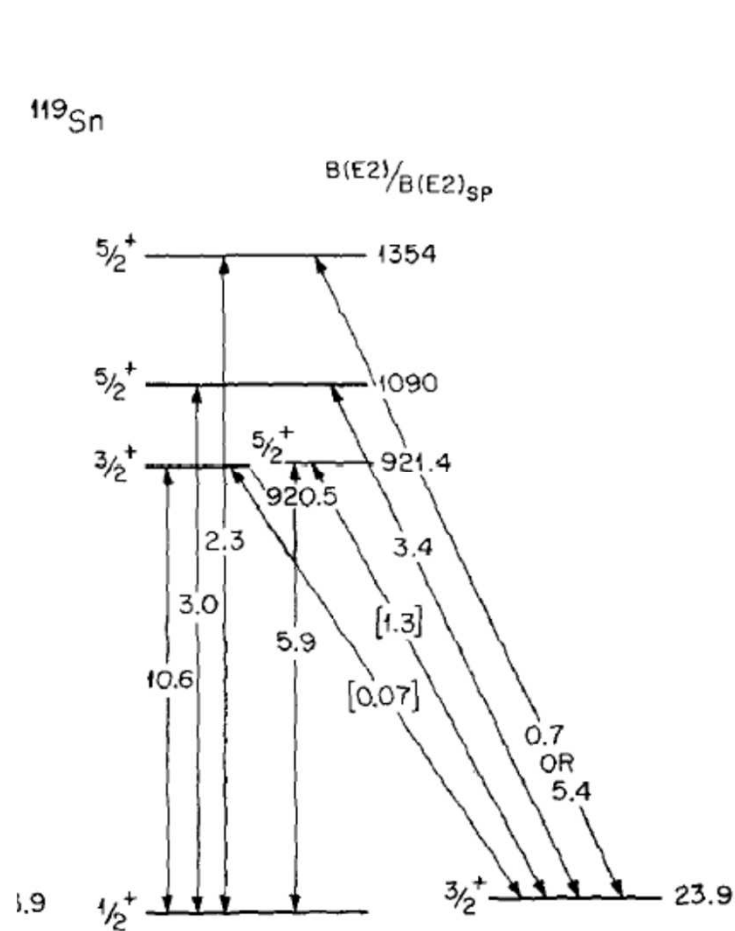


FIG. 1. The QRPA response for the two-neutron transfer on $^{18,20,22}\text{O}$. The exact continuum calculations are in solid lines whereas the calculations with box boundary conditions are in dashed lines. The results are displayed as functions of E^* , the excitation energy with respect to the parent nucleus ground state. $R_{\text{box}} = 22.5 \text{ fm}$

Comento per noi

Elab =84 sono $E_{cm}=40$ e quindi 2 MeV/n. Come e' possibile eccitare qualcosa a 20 MeV trasferendo solo 2 neutroni???

Electromagnetic Spectrum



Two particle transfer cross section

IInd order DWBA

$E_p = 21 \text{ MeV}$

.... 1375 μb

— 2190 μb

● $2250 \pm 352 \mu b$ Experimental

Only Bare

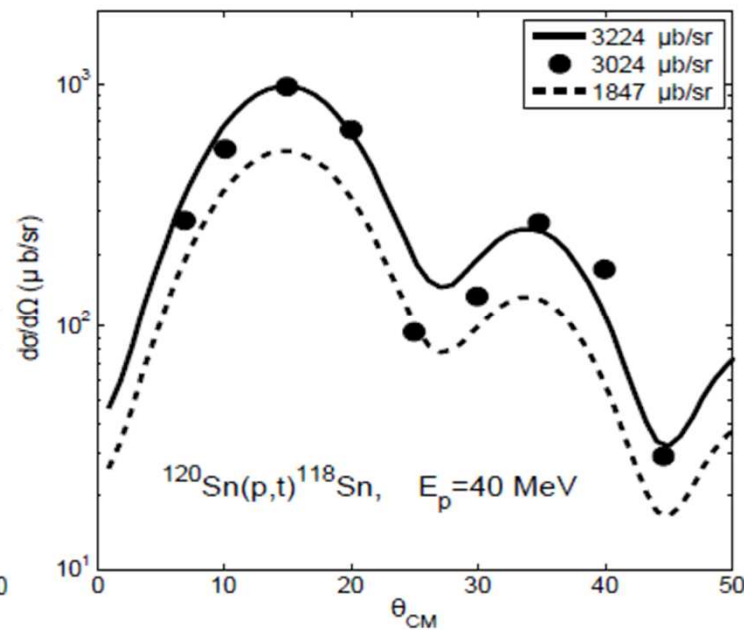
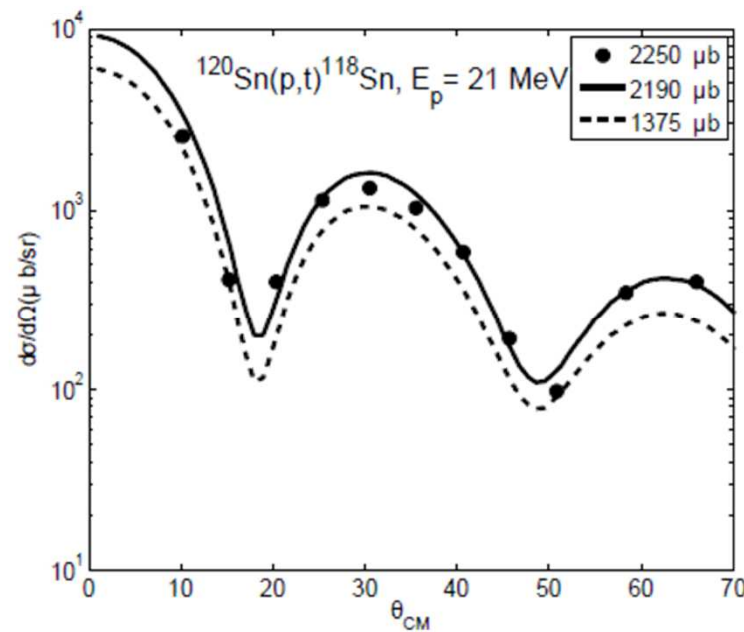
Total Pairing

$E_p = 40 \text{ MeV}$

1847 μb

3224 μb

$3024 \pm 907 \mu b$



$$\Sigma_{\gamma\delta}(\omega) = \sum_{pp'h'p''h''} V_{pp''h''\gamma} \sum_f \frac{X_{p'h'}^f X_{p''h''}^f}{\omega - \epsilon_p - \hbar\omega_f} V_{pp'h'\delta}$$

A close connection with

$$\Sigma^{RPA}(\alpha, \beta : E) = \frac{1}{2} \left\{ \sum_{\mu > F, n \neq 0} \frac{\Delta_{\alpha\mu}^{A+,n*} \Delta_{\beta\mu}^{A+,n}}{E - (\epsilon_\mu + (E_n^A - E_0^A)) + i\eta} + \sum_{\mu < F, m \neq 0} \frac{\Delta_{\alpha\mu}^{A-,m} \Delta_{\beta\mu}^{A-,m*}}{E - (\epsilon_\mu + (E_0^A - E_m^A)) - i\eta} \right\}$$

with

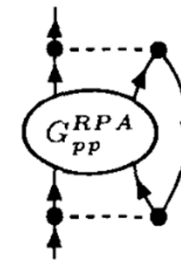
$$\Delta_{\alpha\mu}^{A+,n} = \sum_{\nu > F, \kappa < F; \nu < F, \kappa > F} \langle \alpha\kappa | G | \mu\nu \rangle R_{\nu\kappa}^{A+,n}$$

and

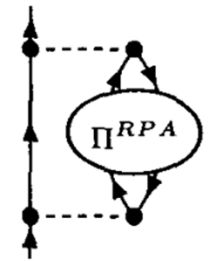
$$\Delta_{\alpha\mu}^{A-,m} = \sum_{\nu > F, \kappa < F; \nu < F, \kappa > F} \langle \alpha\kappa | G | \mu\nu \rangle R_{\kappa\nu}^{A-,m}.$$



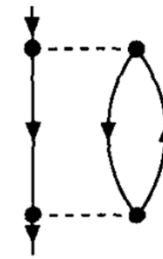
a)



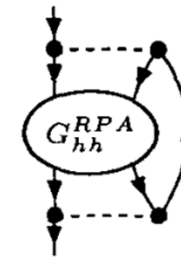
c)



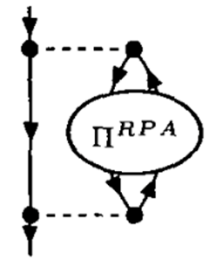
e)



b)

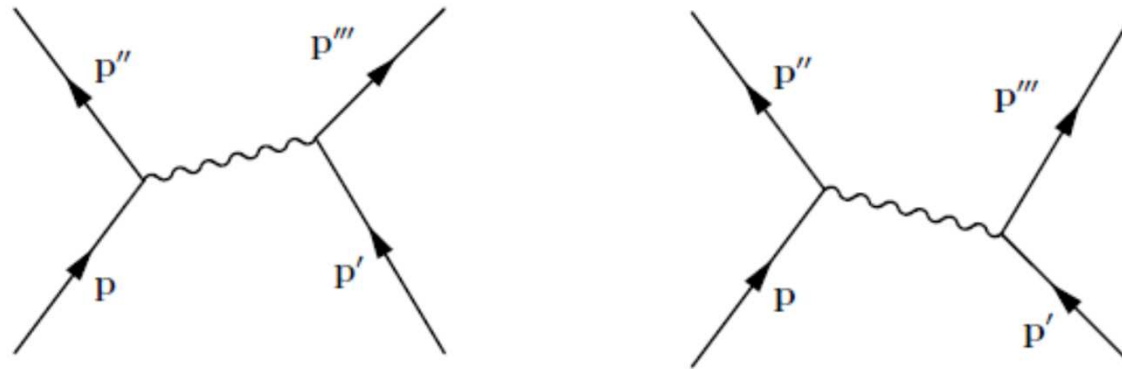


d)



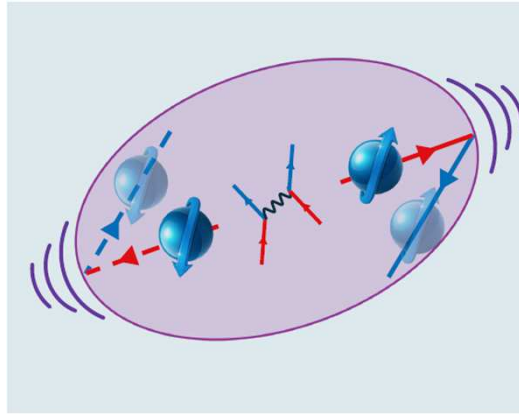
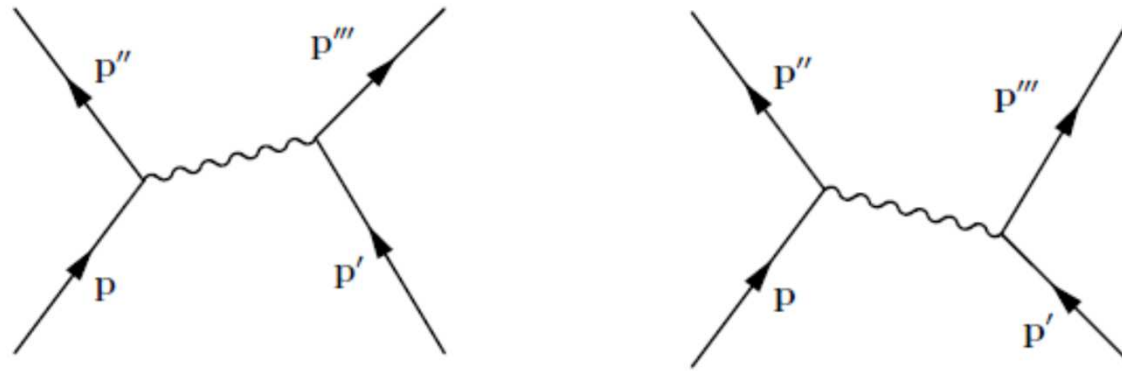
f)

Extended Role of Vibrations in the PV and GPV: The Phonon Exchange Induced Interaction, V_{ind}



In Spain we say:
"An image is better than thousand words"

Extended Role of Vibrations in the PV and GPV: The Phonon Exchange Induced Interaction, V_{ind}



Angular Momentum Decomposition

